Alma Mater Studiorum – Università di Bologna

DOTTORATO DI RICERCA IN

BIOINGEGNERIA

Ciclo XXVIII

Settore consersuale di afferenza: 09/G2

Settore scientifico disciplinare: ING-INF/06

GAZE STRATEGIES DURING OBSTACLE NEGOTIATION IN THE PRESENCE OF DISTRACTORS: A VIRTUAL REALITY BASED ASSESSMENT

Presentata da: **Valeria Serchi**

Coordinatore Dottorato

Prof. Elisa Magosso

Relatore

Prof. Ugo Della Croce

Co-relatore

Dott. Andrea Cereatti

Contro-relatori

Prof. Lorenzo Chiari

Prof. Mark Hollands

Esame finale anno 2017

Summary

The localization and the strategy used to avoid obstacles are important for a safe locomotion (Patla & Vickers, 1997). Vision actively influences the gait and, in particular, older adults show altered visual patterns compared to their younger counterpart when approaching challenges in the travel path (Chapman & Hollands, 2007) or have to cross obstacles (Cheng, Yang, Holloway, & Tyler, 2016). Attentional distractors significantly influence the motor strategies during obstacle crossing on a flat ground, and determine the toe-off clearance decrease over the obstacle (Lo, van Donkelaar, & Chou, 2015). In the scientific literature, there is a great focus on the combined assessment of the gait and gaze with the intent to gather new information from the coordination of gait and gaze (Stuart, Galna, Lord, & Rochester, 2015). In rehabilitation, treadmill and virtual reality (VR) are commonly used to train gait since VR allows for the setup of repeatable, safe and full variable control tasks with a positive motivational aspect for patients (Mirelman et al., 2013). Moreover, the gaze strategy when watching at videos of a first perspective walking is similar to that adopted in the real world (Stanley & Hollands, 2014). Therefore the insert of gaze monitoring in existing VR-based gait rehabilitation protocols could be feasible and give insights in the visuo-motor strategy adopted in challenging conditions. This research project aimed at assessing the effect of distractors on the gaze and gait strategies during obstacle avoidance tasks in a VR environment. The first part of the project assessed the reliability of a remote eye-tracker during treadmill walking and visual stimuli exposition (Serchi, Peruzzi, Cereatti, & Della Croce, 2016). The second part of the project aimed at studying the effect of distractors during obstacle avoidance in a purposely depicted VR (Serchi, Cereatti, Cinelli, & Croce, 2015).

The first study showed the quality of the gaze worsening for larger distances of the head from the eye-tracker and data loss occurring for large gaze angles. The gaze spatial accuracy, precision and trackability were not influenced by the stimulus location during neither standing nor walking. During walking, the head was within the remote eye-tracker workspace and the quality of the gaze was adequate. Walking and static tasks did not differ in the application of regions of interest analysis. The outcomes of this study foster the feasibility of the use of the tested remote eye-tracker for gaze analysis during walking in VR-based applications.

In the second study, young and older adults had to walk on a treadmill while navigating a VR world. The subjects had to step over obstacles with visual distractors trying to challenge their performance. The kinematics was not influenced by the presence of the distractors in both groups. The visual behaviour analysis highlighted differences between the groups. The older adults focused more on the obstacle when it was the only element of the scene and the young adults had a more variable visual behaviour. In contrast with the literature, in this study the kinematics was not influenced by the distractors neither in the young nor in the older adults. That was probably due to the nature of the distractors proposed. More cognitive involving distractors could have had a more pronounced influence on the kinematics parameters. This study highlights that young and older adults look at the scene differently. A possible explanation of this difference is that younger adults are more prone to react to unexpected elements of the scene and always have the whole scene under their control. These first results are promising and point out that this kind of test, once standardized for the clinics, could be easily used for the diagnose and the intervention against neuro-motor diseases and the improvement of the coordination between eyes and body movement.

References

Chapman, G. J., & Hollands, M. A. (2007). Evidence that older adult fallers prioritise the planning of future stepping actions over the accurate execution of ongoing steps during complex locomotor tasks. *Gait & Posture*, *26*, 59–67. http://doi.org/10.1016/j.gaitpost.2006.07.010.

Cheng, T.-J., Yang, B., Holloway, C., & Tyler, N. (2016). Effect of environmental factors on how older pedestrians detect an upcoming step, 1–11.

Lo, O.-Y., van Donkelaar, P., & Chou, L.-S. (2015). Distracting visuospatial attention while approaching an obstacle reduces the toe-obstacle clearance. *Experimental Brain Research*, *233*(4), 1137–1144. http://doi.org/10.1007/s00221-014-4189-1.

Mirelman, A., Rochester, L., Reelick, M., Nieuwhof, F., Pelosin, E., Abbruzzese, G., Dockx, K., Nieuwboer, A., and Hausdorff, J. M. (2013). V-TIME: a treadmill training program augmented by virtual reality to decrease fall risk in older adults: study design of a randomized controlled trial. *BMC Neurology*, *13*(1), 15. http://doi.org/10.1186/1471-2377-13-15. Patla, A. E., & Vickers, J. N. (1997). Where and when do we look as we approach and step over an obstacle in the travel path? *Neuroreport*, *8*(17), 3661–3665. http://doi.org/10.1097/00001756-199712010-00002.

Serchi, V., Cereatti, A., Cinelli, M. E., & DellaCroce, U. (2015). Gaze strategies while negotiating obstacles in a virtual environment with distractors. *Gait & Posture* (Vol. 42, p. S3). http://doi.org/10.1016/j.gaitpost.2015.07.018.

Serchi, V., Peruzzi, A., Cereatti, A., & Della Croce, U. (2016). Use of a remote eye-tracker for the analysis of gaze during treadmill walking and visual stimuli exposition. *BioMed Research International*, *2016*. http://doi.org/10.1155/2016/2696723.

Stanley, J., & Hollands, M. A. (2014). A novel video-based paradigm to study the mechanisms underlying age- and falls risk-related differences in gaze behaviour during walking. *Ophthalmic & Physiological Optics*, *34*(4), 459–69. http://doi.org/10.1111/opo.12137.

Stuart, S., Galna, B., Lord, S., & Rochester, L. (2015). A protocol to examine vision and gait in Parkinson's disease: impact of cognition and response to visual cues. *F1000Research*, (0), 1–15. http://doi.org/10.12688/f1000research.7320.1

Acknowledgments

I am really thankful to many people that during my PhD experience made me understanding how the world rules, specifically the difference between making good and bad research and the kind of researcher I want to become. I want to thank my supervisor Prof. Ugo Della Croce and my. co-supervisor Dr. Andrea Cereatti, my lab mates and my friends in Sassari. I want also to thank Prof. Mike Eric Cinelli and all the LPMB lab folk for all the support, example and friendship they showed me in Canada. Finally, I want to thank my family for supporting me in the everyday life.

List of Publications

International Peer-Reviewed Journals

1. Serchi V., Peruzzi A., Cereatti A., and Della Croce U., "Use of a Remote Eye-Tracker for the Analysis of Gaze during Treadmill Walking and Visual Stimuli Exposition." *BioMed research international* (2016).

2. Serchi V., Cereatti A., Cinelli M.E., and Della Croce U., "Assessment of distractors effect on vision and gait strategies during obstacle crossing: a virtual reality assessment." *In preparation.*

Conference Proceedings published on International Journals

1. Serchi V., Peruzzi A., Cereatti A., and Della Croce U., "Performance of a remote eye-tracker in measuring gaze during walking." *20th IMEKO TC4 International Symposium Benevento*, Italy, September 2014.

2. Serchi V., Peruzzi A., Cereatti A., and Della Croce U., "Tracking gaze while walking on a treadmill: spatial accuracy and limits of use of a stationary remote eye-tracker." *36th Annual International Conference of the IEEE Engineering in Medicine and Biology Society, IEEE*, 2014.

3. Serchi V., Cereatti A., Cinelli M.E., and Della Croce U., "Gaze strategies while negotiating obstacles in a virtual environment with distractors." *Gait & Posture*, 42 (2015): S3.

International Conference Proceedings

1. Serchi V., Peruzzi A., Cereatti A., and Della Croce U., “Validation of a remote eye-tracker: application to gait analysis.” *Proceedings of 25th SIAMOC-23th ESMAC 2014*, p.69, Rome, Italy, October 2014.

National Conference Proceedings

1. Serchi V., Cereatti A., Federighi P., Rufa A., and Della Croce U., "An experimental setup for the combined analysis of gaze and gait" *23th National Congress of SIAMOC*, Pisa, Italy, September 2013.

2. Serchi V., Peruzzi A., Cereatti A., and Della Croce U., "Tracking gaze while walking on a treadmill: limits of use of stationary remote eye-tracker" *Proceedings 4th Conference Gruppo Nazionale di Bioingegneria (GNB)*, Pavia, Italy, June 2014.

3. Serchi V., Cereatti A., Della Croce U., Cinelli M.E., "Gaze strategies during obstacle negotiation in presence of distractors: a virtual reality assessment of young and older adult populations" *Proceedings 12th annual Ontario Biomechanics Conference (OBC)*, Alliston, Canada (ON), March 2015.

Table of contents

Summary…….....i

Acknowledgements……iv

List of Publications…….…..….v

Table of contents……..…vii

List of Tables……...……ix

List of Figures…….....x

Glossary…….....xvi

1. Chapter I

Introduction

1.1. Motivation and general introduction…….. 1
1.1.1. Human gait analysis in the laboratory……...……..…… 1
1.1.2. Human vision analysis……..……..……... 2
1.1.3. Vision during gait……...…… 8
1.1.4. Vision and gait during obstacle crossing……. 9
1.1.5. Older adults and the risk of falling……..…… 9
1.1.5.1. Visuo-perturbation and visuo-spatial attention during obstacles crossing …
……..…… 10
1.1.6. Rehabilitation: gait, gaze and virtual reality…….……. 11
1.2. Overall goal and specific aims……. 11
1.3. Dissertation flow...…...…… 12
References……... 13

2. Chapter II

Use of a Remote Eye-Tracker for the Analysis of Gaze during Treadmill Walking and Visual Stimuli Exposition

2.1. Introduction…….. 20
2.2. Materials and Methods……. 22
2.2.1. Participants…… 22
2.2.2. Experimental set-up……... 22
2.2.3. Acquisition protocol…….. 25
2.2.4. Data analysis…….. 28

2.2.5. Statistical analysis…… 30
2.2.6. Results…… 30
2.2.7. Discussion…… 35
2.2.8. Conclusion…… 36
References…… 37

3. Chapter III

The effects of visual distractors on vision and gait strategies during obstacle negotiation: assessment in a virtual reality environment

3.1. Introduction…… 41
3.2. Materials and Methods…… 42
3.2.1. Participants…… 42
3.2.2. Experimental set-up…… 43
3.2.3. Experimental protocol…… 47
3.2.4. Acquisition protocol…… 48
3.2.5. Data analysis…… 49
3.2.6. Statistical analysis…… 54
3.2.7. Results…… 55
3.2.8. Discussion…… 65
3.2.9. Conclusion…… 67
References…… 68

4. Chapter IV

Conclusion and Future Perspectives

4.1. General results and main contributions…… 71
4.1.1. Validation of a remote eye-tracker for treadmill walking…… 71
4.1.2. Assessment of the visuo-motor strategies in the presence of distractors…… 73
4.2. Future perspectives and clinical applications …… 74
References…… 76

Annex 1…… 78
Annex 2…… 81
Annex 3…… 86
Annex 4…… 91
Annex 5…… 92

List of tables

Table 2.1 Accuracy ε, precision δ and index of trackability ϒ of the point of gaze measurements. The values are averaged over the 10 subjects and over the 13 dot-target locations.

Table 2.2 The percentage of *PoG* hitting the *RoI* defined around the 2D target moving on the screen with different patterns (*stat_r*: static at the center of the screen; *horiz_r*: moving horizontally, and vert_r: moving vertically). Percentages are reported for each motor task: *stRoI*: standing at 650 mm from the remote eye-tracker; *wslowRoI*: walking at 0.6 m/s and *wfastRoI*: walking at 1.1 m\s.

Table 3.1 Characteristics of the subjects participating to the study: age, ethnicity, color of the eyes, visual acuity for the left and the right eyes and if they used contact lenses during the study.

Table 3.2 Mean and standard deviation values of the failure rates of the young (**YA**) and older adults (**OA**) during the evaluation session. The values are reported divided by trials with distractors (**Dis**), trials with no distractors (**NoDis**) and global unsuccessful rate (**Total**).

Table 3.3 Mean and standard deviation values of the *CL* and *ΔP* parameters achieved by the young (**YA**) and the older (**OA**) adults for the successful trials occurred during the evaluation session. The values are reported divided by trials with (**Dis**) and with no (**NoDis**) distractors.

Table 3.4 Mean and standard deviation of the obstacle gaze hit percentages of young (**YA**) and older (**OA**) adults for the successful trials occurred during the evaluation session. The values are reported divided by trials with (**Dis**) and with no distractors (**NoDis**).

Table 3.5 Mean and standard deviation values of the horizontal (***horGaze***) and vertical (***verGaze***) variability of the gaze of the young (**YA**) and older (**OA**) adults for the successful trials occurred during the evaluation session. The values are reported divided by trials with (**Dis**) and with no (**NoDis**) distractors.

List of Figures

Figure 1.1 Representation of the four corneal reflexes generated by the reflexion and refraction of a luminous beam (**I**) by the ocular structures at different refraction indexes: **P1**, first corneal reflex generated with the anterior part of the cornea; **P2**, second corneal reflex generated with the posterior part of the cornea; **P3**, third corneal reflex generated with the anterior part of the lens and **P4**, the fourth corneal reflex generated with the posterior part of the lens (picture from (Babcock, Pelz, & Peak, 2003))

Figure 1.2 Image of the eye collected during a data collection session with a wearable eye-tracker (EyeTrac7, ASL). In the image the first corneal reflex (1) and the pupil (2) are pointed out.

Figure 1.3 Example of nine points calibration grid used for the calibration of a remote model of eye-tracker eyetribe (picture from http://theeyetribe.com/).

Figure 1.4 Example of high (left) and low (right) precision point of gaze data sample. In the case of low precision data an addition marginal (x_M, y_M) is added to the *RoI* in order to assign the *PoG* samples to that *RoI* (picture from (Holmqvist et al., 2011)).

Figure 2.1 A schematic representation of the experimental setup, which included a screen (1), a remote eye-tracker (2), a treadmill (3) and a stereo-photogrammetric system (4). Three retro-reflective markers were placed on the subject's head to track its movements. The inclination of the remote eye-tracker with respect to the horizontal plane (β) and its distance from the projecting surface (d) were respectively set to 18 deg and 690 mm. The head (H) reference frame and the remote eye-tracker (rET) reference frame are reported (AP, anterior-posterior; ML, medio-lateral; and V, vertical directions).

Figure 2.2 Image showing part of the experimental set-up used in this study: the projector over a purposely built adjustable platform. A similar adjustable platform was used also for the remote

eye-tracker. The adjustable platform was used in order to adjust both the projector and the remote eye-tracker in according to the height of the subject.

Figure 2.3 Picture of the synchronization cable built in order to connect the remote eye-tracking and the stereo-photogrammetric systems: 1) SMB female to male connector - jack male connector and 2) jack female connector - impedance adaptor - jack male connector. A 5-meter coaxial cable RF174 was used.

Figure 2.4 Schematic representation of the impedance adaptor used to gather a proper current to the remote eye-tracker sync port.

Figure 2.5 Picture showing the position of the markers over the subject during the anatomical calibration procedure.

Figure 2.6 Example of calibration feedback provided by the remote eye-tracker software for one of the participants to the study.

Figure 2.7 A schematic representation of: (a) the visual stimulus used for the identification of the remote eye-tracker workspace; (b) the 13 dot-target locations of the visual stimulus on the screen used for the determination of the remote eye-tracker accuracy and precision; (c) the 2D target used to test the remote eye-tracker applicability for *RoI* analysis.

Figure 2.8 The head *mRoTs* (green) and *mRoMs* (magenta) along the AP^{rET} (*tAP*: A, anterior; P: posterior), ML^{rET} (*tML*: L, left; R, right) and V^{rET} (*tV*: U, up; D, down) direction and around the V^{H} (*rV*: L, left; R, right) and ML^{H} (*rML*: U, up; D, down) directions.

Figure 2.9 A graphical representation of ε_i and δ_i values found for each dot-target location during the trials *st550*, *st650*, *st750* (a) and *wslow*, *wfast* (b). Each dot-target location on the image is a black dot. The circles center positions (colored dots) reflect the accuracy of the *PoG* measurements (ε_i) while their radius reflects the precision of the *PoG* measurements (small radius, $\delta_i < 4$ mm; average radius, 4 mm$< \delta_i <$ 8 mm; large radius, $\delta_i > 8$ mm).

Figure 2.10 The intervals between the minimum and the maximum values of the head *RoMs* (green) obtained during the trials *wslow* (violet) and *wfast* (light blue) across the subjects:

translations along the AP^{rET} (A, anterior; P, posterior), ML^{rET} (L, left; R, right) and V^{rET} (U, up; D, down) directions and rotations around the ML^{H} (U, up; D, down) and V^{H} (L; R left; R, right) directions. The green band represents the remote eye-tracker workspace.

Figure 3.1 Representation of the experimental set-up adopted for this study: 1) 3 blocks of optoelectronics cameras, 2) a treadmill, 3) a wearable eye-tracker and 4) a blank surface onto which a projected virtual reality was projected. The treadmill had lateral bars to which the subject was allowed to hold.

Figure 3.2 Screen shot of a scene of the virtual reality-based task. All of the elements of the task are shown: 1) avatar shoes, 2) tree trunk -obstacle- and 3) crossing deer -distractor-.

Figure 3.3 Representation of the marker-set adopted for this study. In blue, the cluster of markers placed on the head, upper and lower trunk, and on the back part of the feet are reported, whereas the single markers placed directly on the left and right greater trochanters, left and right lateral epicondyles and left and right malleoli are reported in green. In red is reported the position of the virtual markers digitized with respect to the clusters of markers and then reconstruct in post-processing: left and right ears, left and right shoulders, T10, left and right ASIS and PSIS, left and right 1^{st} and 5^{th} metatarsals and heels.

Figure 3.4 Schematic representation of the experimental set-up with the detail of the position and orientation of the technical reference frames of the optoelectronic system and of the wearable eye-tracker system. The stereo-photogrammetric system reference frame had the x-axis (anterior-posterior –AP– direction) parallel to the ground and pointing accordingly to the direction of progression, the z-axis (vertical –V– direction) perpendicular to the ground and pointing down and the y-axis (medio-lateral –ML– direction) perpendicular to the xz plan and pointing toward the right. The eye-tracker reference frame had its origin coinciding with the centre of the calibration grid and was parallel to the stereo-photogrammetric system reference frame.

Figure 3.5 Representation of the steps followed in order to align the signals gathered from the eye-tracker, stereo-photogrammetric and VR systems. The head coordinates were streamed from the stereo-photogrammetric system to the other two systems. Therefore the same signal was

saved in the output of the three systems with a different time-stamp proper of the specific device. The operator pointed out a point for each signal (a) and computed a translation factor to be used in order to align the time-stamp of the three systems (b) and therefore to get a synchronization between the recordings.

Figure 3.6 A schematic representation of the steps followed to compute the *CL* and *ΔP* parameters. In black the trailing (dotted) and leading (full) feet AP (a) and V (b) coordinates are reported along with the AP and V coordinates of the obstacle (red) in the virtual scene. The toe-offs (TO) and heel-strikes (HS) of the leading foot are reported. The leading foot was the more advanced foot in the AP direction during the obstacle crossing. The clearance index (CL_i) was identified as the time with the minimum vertical heel-obstacle distance when the obstacle and the foot had the same AP coordinates (a). The maximum peak index (P_i) of the leading foot was identified as the time with the maximum heel V coordinates during the obstacle crossing (a). Afterwards the obstacle clearance (*CL*) was defined as the V heel-obstacle distance at CL_i and the delay of the maximum peak (*ΔP*) was defined as the absolute value of the difference between CL_i and P_i (b).

Figure 3.7 Example of the *PoG* hit assignment to the regions of interest defined around the obstacle and the distractor during a trial. The horizontal (dotted lines) and vertical (plain line) coordinates of the gaze (blue), obstacle (green) and distractor (yellow) with respect to the calibration grid frame of reference are reported. The assignment of the *PoG* to the regions of interest of the obstacle and of the distractor is reported in black and in red respectively.

Figure 3.8-3.11 Kinematics and visual behavior output computation for a successful and an unsuccessful trial performed by one of the participants belonging to the young adults group and one belonging to the older adults group. From the top to the bottom the trunk and pelvis rotation angles (AP: black; ML: gray and V: red), the left (green) and right (blue) angles of the joints (hip flexion-extention, hip ab-adduction, knee flexion-extention and ankle plantar-dorsiflexion), the elevation of the left (green) and right (blue) heels and the *PoG* hit over the areas of interest defined in the scene are reported. The vertical lines stand for the left (green) and right (blue) heel-strikes (plain line) and toe-offs (dotted lines). A vertical dashed line is reported in correspondence

to the clearance time stamp of the leading foot (the color of the line corresponds to the leading foot side). Green and red stars are reported over the signal if at the specific time of the trial the heel quote was above or under the height of the obstacle. The *PoG* hit is reported in blue if no assignment occurred, in black if the assignment of the hit was for the obstacle area of interest and in red if it was for the distractor area of interest.

Figure 3.12 Mean and standard error of the values of failure rate of the young (**Young**) and older (**Old**) adults for the trials of the evaluation session. The values are reported divided by the trials with (**Dis**) and with no (**NoDis**) distractors and global unsuccessful rate (**All**).

Figure 3.13 Mean and standard error values of the *CL* (a) and ΔP (b) parameters achieved by the young (**Young**) and the older (**Old**) adults for the successful trials occurred during the evaluation session. The values are reported divided by trials with (**Dis**) and with no distractors (**NoDis**).

Figure 3.14 Mean and standard error of the obstacle gaze hit percentages of young (**Young**) and older (**Old**) adults for the successful trials occurred during the evaluation session. The values are reported divided by trials with (**Dis**) and with no distractors (**NoDis**). The significant differences are reported.

Figure 3.15 Mean and standard error values of the horizontal (a: **Horz Gaze**) and vertical variability (b: **Vert Gaze**) of the *PoG* of the young (**Young**) and older (**Old**) adults for the successful trials occurred during the evaluation session. The values are reported divided by trials with (**Dis**) and with no (**NoDis**) distractors. The significant differences are reported.

Figure A1.1 The head *RoTs* (green) and *RoMs* (magenta) along the V^{rET} (+, up; -, down) direction.

Figure A1.2 The head *RoTs* (green) and *RoMs* (magenta) along the ML^{rET} (-, left; +, right) direction. The median values of the minimum and maximal limits of the *RoTs* and of the *RoMs* across the subjects are reported (vertical bars).

Figure A1.3 The head *RoTs* (green) and *RoMs* (magenta) along the AP^{rET} direction. The median values of the minimum and maximal limits of the *RoTs* and of the *RoMs* across the subjects are reported (vertical bars).

Figure A1.4 The head *RoTs* (green) and *RoMs* (magenta) around the V^{H} direction (-, down; +, up). The median values of the minimum and maximal limits of the *RoTs* and of the *RoMs* across the subjects are reported (vertical bars).

Figure A1.5 The head *RoTs* (green) and *RoMs* (magenta) around the ML^{H} direction (-, left; +, right). The median values of the minimum and maximal limits of the *RoTs* and of the *RoMs* across the subjects are reported (vertical bars).

Figure A2.1-10 A graphical representation of ε_i and δ_i values for subject 1-10 found for each dot-target location during the trials *st550* (blue), *st650* (green), *st750* (red). Each dot-target location on the image is a black dot. The circles center positions (colored dots) reflect the accuracy of the *PoG* measurements (ε_i) while their radius reflects the precision of the *PoG* measurements (small radius, $\delta i < 4$ mm; average radius, 4 mm$< \delta_i <$ 8 mm; large radius, $\delta_i >$ 8 mm).

Figure A3.1-10 A graphical representation of ε_i and δ_i values for subject 1-10 found for each dot-target location during the trials *wslow* (magenta) and *walkfast* (light blue). Each dot-target location on the image is a black dot. The circles center positions (colored dots) reflect the accuracy of the *PoG* measurements (ε_i) while their radius reflects the precision of the *PoG* measurements (small radius, $\delta_i < 4$ mm; average radius, 4 mm$< \delta_i <$ 8 mm; large radius, $\delta_i >$ 8 mm).

Glossary

VOG = Video-OculoGraphy

PC-CR = Pupil Center – Corneal Reflex

RoI = Region of Interest

CNS = Central Nervous System

VR = Virtual Reality

PoG = Point of Gaze

H = Head

rET = Remote Eye-Tracker

AP = Anterior-Posterior

ML = Medio-Lateral

V = Vertical

RoT = Range of Trackability

RoM = Range of Motion

REB = Research Ethical Board

ASIS = Anterior Superior Iliac Spines

PSIS = Posterior Superior Iliac Spines

YA = Young Adult

OA = Old Adult

HS = Heel-Strike

TO = Toe-Off

CL = Clearance

2D = Bidimensional

3D = Tridimensional

Chapter 1

Introduction

1.1. Motivation and general introduction

Gait is visually influenced and that is more evident in older adults and particularly in those at high risk of falling. The falls and the way older adults move and interact with the surrounding environment are critical. In fact, the consequences of falls on older adults determine a great expense for our society. Generally older adults are more prone to adopt risky behaviors and show a deficit in the distractors suppression. Young adults show a decrease in the motor performances when distractors are presented during obstacles crossing. Understanding better the visuo-motor coordination of older adults during obstacles crossing with distractors is important in order to address better the gait rehabilitation interventions. The laboratory environment and the related evaluation tools are important to determine gait issues and to train it to be effective and safe in the everyday life. In this contest adding the gaze monitoring to already existing rehabilitation protocols could improve the rehabilitation effectiveness and give insights in how the visuo-motor systems interact in challenging conditions. A contact-less gaze tracking paradigm should be preferable for applications with young and older adults because it is more tolerable and usable for a greater lapse of time, but this technology allows only for a limited range of motion of the head. Therefore it is necessary to assess the feasibility of this technology for its use during walking.

1.1.1. Human gait analysis in the laboratory

The term gait referred to humans refers to the most common type of locomotion achieved through the movement of the limbs (Perry, 1992). The laboratory setting allows for a safe and reproducible analysis of the patterns of the gait through *ad hoc* instrumentations for motion capture allowing for accurate, reliable and objective measurements. Nowadays, the gold standard for gait analysis is the stereo-photogrammetric technology that combined to force platforms allows for the assessment of the joints kinematics and kinetics. This technology is based on the

use of a set of cameras sensitive to the light in the infrared spectrum and either passive or active markers. The stereo-photogrammetric systems allow for the 3D reconstruction of a moving point in the laboratory reference frame. The reconstruction of a rigid body segment is then possible having at least three non-collinear markers lying on the segment (Cappozzo, 1984, 1991; Cappozzo, Della Croce, Leardini, & Chiari, 2005). From the information about the pose of the body segments the joints kinematics and kinetics is then reconstructed (A. Cappozzo, Catani, Della Croce, & Leardini, 1995).

1.1.2. Human vision analysis

The eyes represent a complex system of lens and holes through which the light passes to reach the retina in the back part of the ocular camera. The retina is composed of photoreceptors (cones and rods) sensitive to the light that transduce the luminous signal into electric pulses to be sent to the optic nerve. The point of the retina with the highest density of cones and rods is called fovea and his surface has an extension of about 2 degrees of visual angle. When the light arrives directly to this point we are able to see sharply the details of what we are looking at (Openstax College, 2013). Therefore, the eyes move continuously with the intent to focus on the fovea the details of the object we are observing. Understanding how, what, why and when people look at has always been really interesting. Through the eyes we have the idea to be capable of reading the behavior of people. For that reason in the last decades many technologies were developed aiming to track the motion of the eyes (eye-tracking technology). Between these the most widespread for their easy set-up and mini-invasiveness are the eye-trackers based on the video-oculography (VOG) technique (L. Young & Sheena, 1975). The VOG technique consists in light sources pointed toward the eye and in sensitive elements capturing the image of the eye. From the image of the eye the ocular structures are then segmented based on the chromatic contrast highlighted by the illumination in the visible or in the infrared spectrum (L. R. Young & Sheena, 1975). The eye-trackers working in the infrared spectrum are the most common. The most popular functioning principle they are based on is called PC-CR, pupil center – corneal reflex (Holmqvist et al., 2011). The corneal reflexes (up to four) are little light spots generated by the reflection and refraction of the light over the ocular lenses (Figure 1.1) (Duchowski, 2007).

Figure 1.1 Representation of the four corneal reflexes generated by the reflexion and refraction of a luminous beam (**I**) by the ocular structures at different refraction indexes: **P1**, first corneal reflex generated with the anterior part of the cornea; **P2**, second corneal reflex generated with the posterior part of the cornea; **P3**, third corneal reflex generated with the anterior part of the lens and **P4**, the fourth corneal reflex generated with the posterior part of the lens (picture from (Babcock, Pelz, & Peak, 2003)).

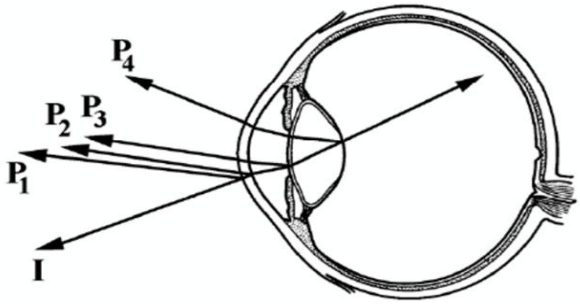

The most commercial eye-trackers work with the detection of the first corneal reflex that in the image of the eye looks like a light spot in the proximity of the pupil looking like a wider black circle (Figure 1.2).

Figure 1.2 Image of the eye collected during a data collection session with a wearable eye-tracker (EyeTrac7, ASL). In the image, the first corneal reflex (1) and the pupil (2) are pointed out together with their segmentation made by the proprietary software.

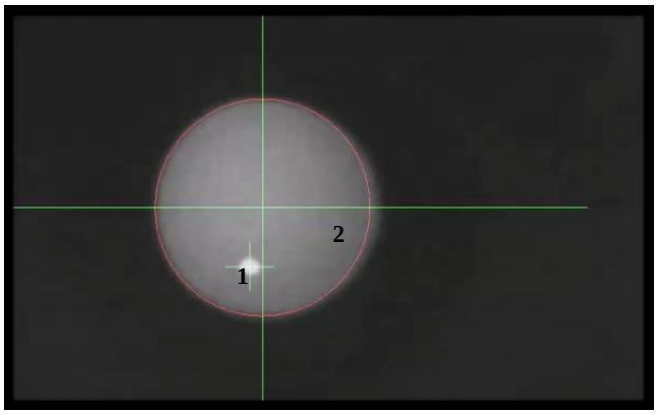

For assumption of perfect spherical cornea, if the light source has a stable position with respect to the ocular bulb, the corneal reflex will appear almost always on the same position on the cornea

while the eye rotates in the orbit. Therefore, the center of the pupil will vary its position according to the eye rotation and consequently, the distance between the corneal reflex and the center of the pupil will be function of the point of gaze (Babcock et al., 2003; Duchowski, 2007; Guestrin & Eizenman, 2006). According to the number of light sources and sensitive elements, a subject-specific calibration is necessary to estimate the point of gaze. The calibration of the point of gaze consists in the subject looking at known points on a screen or on a scene, where the stimuli will be presented (Guestrin & Eizenman, 2006) (Figure 1.3).

Figure 1.3 Example of a nine points calibration grid used for the calibration of a remote model of eye-tracker –eyetribe– on a monitor screen (picture from http://theeyetribe.com/).

During the calibration procedure, for each calibration point, the eye-tracker software acquires a lot of image of the eye in order to estimate the parameters characteristic of the eye of the person being tested. The more the acquired images of the eye are similar, the most accurate the estimation of the physiological parameters and therefore the calibration will be. To this end, during the calibration procedure the subject is required to keep the head still and sometimes experimenters recur to chinrests or bitebars (Guestrin & Eizenman, 2006).

The video eye-trackers can be grouped by wearable and remote eye-trackers (Duchowski, 2002; Poole & Ball, 2005). The wearable eye-trackers have both the light sources and the sensitive elements attached to the head of the subjects through supports such as glasses or caps. A recent model of wearable eye-tracker includes the integration with motion analysis systems to get the point of gaze coordinates with respect to a calibrated plan (Duchowski, 2007; Laboratories Applied Science, 2014). The remote eye-trackers have the light sources and the sensitive

elements on a certain distance from the subject; usually on a desk in front of him/her. This is critical for the accuracy and precision of the measures we gather and based on the specific application (clinics) it is preferable to have the head immobilized to avoid bias due to the deviation of the head from the calibration position (Morimoto & Mimica, 2005). The quality of the point of gaze can be affected also by other inaccuracy factors to which attention should be paid. A list of the main inaccuracy factors affecting the reconstruction of the point of gaze is reported (Holmqvist, Nyström, & Mulvey, 2012; Nyström, Andersson, Holmqvist, & van de Weijer, 2013).

- ✓ *Deviations of the head from the calibration pose* could introduce bias in the estimation of the point of gaze.
- ✓ *Glasses or lenses* could distort the image of the corneal reflex on the eye image or create other light spots that could be wrongly recognized by the segmentation software.
- ✓ *Other light sources* in the environment could create other spot lights on the image of the eye different from the corneal reflex.
- ✓ *Large gaze angles* could induce an excessive rotation of the eye and therefore a distorted image of the pupil in the image of the eye.
- ✓ *Droopy eye-lids* could cover the pupil (even partially) so that errors are introduced in the location of the center of the pupil.

The manufacturer always gives reference values for the accuracy and precision of the point of gaze estimated for a specific device. Nevertheless, prior to run an experiment it is best practice always to test the device in the specific experimental set-up of use and with the specific population of interest (Morgante, Zolfaghari, & Johnson, 2012; S. Stuart, Alcock, Galna, Lord, & Rochester, 2014; Wass, Forssman, & Leppänen, 2014).

The point of gaze is mainly analyzed in terms of gaze saccades (duration: 30-80 ms; speed: 50-500 deg/s) and fixations. A saccade is a fast voluntary movement aiming at orientating the fovea on a target of interest. A fixation is a stationary state of the eye occurring between a saccade and another (Duchowski, 2007; Holmqvist et al., 2011). There exist also other movements analyzed as indexes of cognitive load or cognitive deficit (*e.g. blinks, microsaccades, intrusions, nystagmus, etc…*) (Kowler, 2011) that will not be discussed in this contest. To analyze the

interaction of the subject with certain parts of the stimulus or for interactive applications in which the gaze is used as input to a communication device, regions of interest (*RoI*) are defined over the stimulus according to the specific hypothesis of a study or to the specific needs of an interaction application. A *RoI* is a region of the screen defined in size and position by the researcher. This region is defined according to the hypothesis of the study around parts of the stimulus the investigator wants to assess the interaction of the subject with. The metrics usually used with the *RoI* are related to the fixations or to the gaze samples falling within the defined *RoI* during a specific visual task (*e.g.* time of first fixation, percentage of gaze falling over the *RoI*, *etc…*). In order to avoid any erroneous assignment of the point of gaze to a *RoI*, it is important to be aware of the accuracy and precision of the device we are using. In the case of multiple *RoIs* a really inaccurate point of gaze could determine the assignment to the wrong *RoI* in the scene. In the case of a point of gaze not precise, if the subject is looking at the boundaries of the *RoI*, the point of gaze could fall outside the *RoI* even if it is within the boundaries and vice versa. In order to well design one or multiple *RoIs* on a scene the user should choose appropriately their size. The size of a *RoI* should not be less than the accuracy of the *PoG* measurements and two *RoI* should not be closer than the accuracy of the *PoG* measurements. Moreover, around an element of interest in the scene a *RoI* should we drawn considering an adding margin equal to the precision gathered with the device (Holmqvist et al., 2011) (Figure 1.4).

Figure 1.4 Example of high (left) and low (right) precision point of gaze data sample. In the case of low precision data an addition marginal (x_M, y_M) is added to the *RoI* in order to assign the *PoG* samples to that *RoI* (picture from (Holmqvist et al., 2011)).

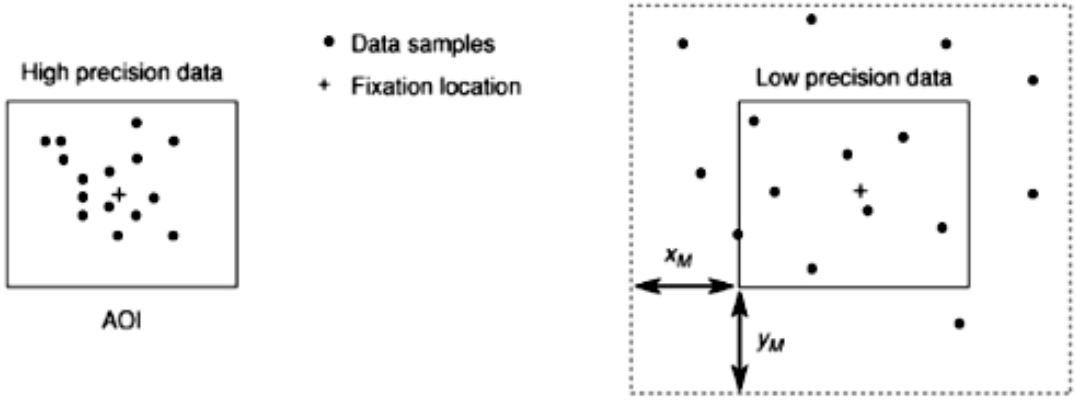

Overlapping *RoIs* should not occur if the stimulus design has followed the previously mentioned rules, but it is not always the case. For instance in the case of dynamic stimuli, dynamic *RoIs* could be generated (moving and changing in size and form) (Holmqvist et al., 2011). A possible example is a scene of a car crossing a road. In this case if we want to investigate how many times a subject looks at the car and at the road, we should define two *RoIs*, one for the car and one for the road. The *RoI* associated with the car will be a dynamic one. In this case at least for a certain lapse of time the two *RoIs* will overlap. The assignment of the *PoG* to one of the two *RoIs* in the overlapped phase is complex. What we can do is to accept that by assuming that the participant fully perceives both *RoIs* or to assign the *PoG* to one of the *RoIs* following a criterion. For example we could compute the distance between the *PoG* coordinates and the barycenter of the *RoIs*. The *PoG* will be then assigned to the *RoI* having the smallest distance from the *PoG* coordinates (Holmqvist et al., 2011).

Having under control the quality of the point of gaze is important in order to perform studies answering to the scientific questions we pose. To improve the quality of the point of gaze we can recur to filters and denoisers to pre-process the signal prior the data analysis. In the following, a brief description of the main causes of noise in the gaze signal along with a description of simple methods to manage them is reported (Holmqvist et al., 2011, 2012; Nyström et al., 2013).

Blinks are physiological movements occurring in terms of closure of the eye-lids. The closure of the eye-lids causes first a deformation of the image of the pupil in the image of the eye and then, a complete loss of the pupil image. Usually the commercial eye-trackers give information about the pupil size. A general approach to deal with blinks is to find the consecutive frames of the signal having a value of the pupil size equal to zero for at least 100 ms. Such parts of the signal are than flagged as blinks and either analyzed for cognitive load assessments or discarded (Holmqvist et al., 2011; Onorati, 2016).

Optic artifacts and *spikes* in the signal are caused by the bad recognition of the features of the eye. The corneal reflex, for instance could be wrongly recognized in another part of the image of the eye. In these cases the signal shows outliers (optic artifacts) or at high speed signal frames. One of the possible approaches to deal with the presence of outliers in the signal is to window the signal and to remove everything deviating more than 1.5*variance of the signal contained in the

window. The spikes at high speed can be removed by setting a velocity threshold above which a part of the signal is discarded because having a speed not compatible with any physiological eye movements (Holmqvist et al., 2011).

Other filters: the gaze signal is characterized by a characteristic noise due the physiology of the visual system itself (oculomotor noise). To further improve the quality of the signal the application of a filter to remove the high frequency noise could be necessary (Špakov, 2012; Veneri, Federighi, Rosini, Federico, & Rufa, 2010).

1.1.3 Vision during gait

The visual system is uniquely positioned to provide information on the static and dynamic features of the near and far environment in which animals live and move in order to negotiate the constraints and to plan the locomotor path (*visual sampling*, (Patla, 1997)). In 1958 the importance of the visual input in modifying the gait patterns had been already underlined (Gibson & Gibson, 1958). Eyes and stepping movements are strongly coordinated (M. A. Hollands & Marple-Horvat, 2001) to accomplish the locomotor tasks. Researchers have shown that environmental information provided by vision is used in a feed-forward mode, and intermittent sampling of the environment is sufficient for a safe locomotion (Patla, Adkin, Martin, Holden, & Prentice, 1996; Patla & Vickers, 2003), even when, in adaptive locomotion, stepping onto targets accurately requires visual guidance (M. A. Hollands & Marple-Horvat, 1996). When the travel path is relatively sterile with none or few objects to be avoided or stepped on, eyes are not usually actively moved to a specific location, but rather they are focused often on the ground ahead and carried along with the locomotor apparatus (whole body) (*travel fixation*) (Patla & Vickers, 1997). The *travel fixation* is evident also when people are required to step onto targets suggesting that during this phase this behaviour provides enough information about the environment and the motion of the body thanks to the optic flux generated (Patla & Vickers, 2003). When the travel path is more complex, fixations are made toward the regions at maximal informative content with a frequency of the visual sampling dictated by the terrain characteristics in a sequential online manner in order to guarantee stability to unexpected changes in the terrain (Marigold & Patla, 2007; Patla et al., 1996).

1.1.4 Vision and gait during obstacle crossing

Obstacles avoidance is a challenging task for a safe locomotion and young and older adults show different strategies in performing it (Caetano et al., 2016; H. C. Chen, Ashton-Miller, Alexander, & Schultz, 1991; Hui-Fen Pan, Horng-Chaung Hsu, Wei-Ning Chang, Jenn-Huei Renn, 2016). Obstacles avoidance is usually planned in the steps before the crossing (~ three steps) often without fixating the obstacle while stepping over it (Patla, 1997). During the avoidance of expected obstacles on a flat ground the visual behavior is split between *travel gaze* and *obstacle sampling*. Obstacle sampling refers to the visual inspection of the obstacle to gather the information necessary for a successful avoidance (Patla, 1997; Patla & Vickers, 2003).

1.1.5 Older adults and the risk of falling

Falls in older adults have a pronounced social impact. Numerous studies assessed the effects of the age-related neuro-sensory decline and the issues affecting the mobility of older pedestrians (Reed-Jones et al., 2013; Tournier, Dommes, & Cavallo, 2016) in order to create effective rehabilitation programs to prevent the risk of falls (Mirelman et al., 2013). As mentioned before young and older adults (in particular those at high risk of falling) show different strategies while approaching and negotiating challenges or obstacles in the travel path. In particular, the elderly appear to adopt a more cautious strategy by slowing down the obstacle crossing phase, but in the mean time, they also adopt shorter landing distances and a reduced base of support that could potentially put them at risk of imbalance (Caetano et al., 2016; H.-C. Chen, Ashton-Miller, Alexander, & Schultz, 1994; H. C. Chen et al., 1991; Galna, Peters, Murphy, & Morris, 2009; Hui-Fen Pan, Horng-Chaung Hsu, Wei-Ning Chang, Jenn-Huei Renn, 2016; Lowrey, Watson, & Vallis, 2007).

Vision significantly influences the performance of the older adults. In fact, when compared to young adults, older adults generally need a longer gaze fixation time on challenges in the travel path (Bock, Brustio, & Borisova, 2016; Chapman & Hollands, 2006). Moreover, when asked to face with multiple stepping constraints, fallers appear to prioritize visual information regarding future constraints in a travel path. The young adults in the same situation usually maintain gaze on a stepping target until after heel contact inside it, while the elderly transfer their gaze away from the target significantly earlier in order to fixate a second target in the travel path (Chapman

& Hollands, 2007). Therefore, the elderly adopt a visual risky behavior that could expose them to the risk of falling. This behavior may be driven by deficits in visual information processing within the central nervous system (CNS), decline in visuomotor processing ability, increased anxiety and cognitive impairment (Chapman & Hollands, 2007; Greany & Di Fabio, 2008; Hackney, Ann Vallis, & Cinelli, 2012; W. R. Young, Wing, & Hollands, 2012; William R. Young & Mark Williams, 2015).

1.1.5.1 Visuo-perturbation and visuo-spatial attention during obstacle crossing

The increase of the cognitive demand while crossing obstacles has a worsening effect on the motor performances of the older adults (Harley, Wilkie, & Wann, 2009). The elderly appear to rely on the visual feedback provided by the scene and by the environment and their motor performance is affected by the visual information they can gather more than their younger counterpart (Cheng, Yang, Holloway, & Tyler, 2016; Franz, Francis, Allen, O'Connor, & Thelen, 2015). Recent researches aimed at investigating the effect of visuo-attentional distractors on the motor performance over obstacles (Lo & Chou, 2015; Lo, van Donkelaar, & Chou, 2015, Brown, McKenzie, & Doan, 2005). The most attentionally demanding phase for the elderly is the pre-crossing phase (Brown, McKenzie, & Doan, 2005). Young adults show a reduced toe-off clearance when visuo-spatial distractors are presented prior the position of the obstacle (Lo et al., 2015). During other kinds of motor tasks, both young and older adults show a correlation between the visuo-motor performances and the ability to suppress the distractors and, in the specific, the elderly show a deficit in the suppression of the distractors (Mevorach, Spaniol, Soden, & Galea, 2016). The elderly are more prone to allocate their attention on factors different from the task itself (Healey, Campbell, & Hasher, 2008) together with a lack in the coordination between the environment navigation and a visually demanding task (Beurskens & Bock, 2012, 2013). This suggests that in complex tasks as the one of avoiding obstacles, if distractors are present, the elderly could show visuo-motor patterns different and possibly worse than the younger adults. Therefore understanding better the relationships between the visuo-spatial attention distraction and the motor performances during obstacles crossing is important in order to investigate and address better the rehabilitation of the gait in the elderly.

1.1.6. Rehabilitation: gait, gaze and virtual reality

The rehabilitation of gait for the elderly with reduced mobility following falls or other pathologies has a primary role for our society. Recent literature showed that the administration of obstacle avoidance trainings is effective to avoid further fallings and to enhance the gait (K. L. Hollands, Pelton, Tyson, Hollands, & van Vliet, 2012; Jaffe, Brown, Pierson-Carey, Buckley, & Lew, 2004; Yamada et al., 2012). Virtual reality based rehabilitation interventions have the potential to become effective tools for the rehabilitation of gait (Darekar, McFadyen, Lamontagne, & Fung, 2015) even in conditions of increasing cognitive demanding (Kizony, Levin, Hughey, Perez, & Fung, 2010). Virtual reality and video-games are already employed in gait rehabilitation protocols involving walking on treadmills with visual context or walking on a treadmill while navigating a projected virtual reality environment challenging obstacles avoidance (Mirelman et al., 2013; van Ooijen et al., 2013). Virtual reality is well accepted by the patients (Peruzzi, Cereatti, Della Croce, & Mirelman, 2016) and allows for a flexible protocol design.

In these kinds of protocols no attention is paid to the rehabilitation of the visual behavior yet, but the previous discussion highlighted how the motor performance and the visual input are correlated one to the other. Recent researches showed how simple trainings are effective to enhance visuo-motor strategies (Reed-Jones, Dorgo, Hitchings, & Bader, 2012; W. R. Young & Hollands, 2010). Moreover recent protocols proposing a combined analysis of the gait and gaze performances are proposed (Samuel Stuart, Galna, Lord, & Rochester, 2015). Therefore the idea to integrate a visual training to the already existing virtual reality based gait rehabilitation protocols seem to be the logic following step.

1.2 Overall goal and specific aims

The general purpose of the current work was to assess the visuo-motor performances of young and older adults during virtual reality-based obstacle crossing tasks in the presence of visual distractors. The hypothesis was that the young and older adults would show a decrease in the obstacle negotiation task motor performance, and that such a worsening would be more evident in the elderly also looking at their visual behavior. As secondary aim this study wanted to set-up

and to test an easy experimental set-up for an unobtrusive tracking of the gaze for the use in such an experimental design.

1.4 Dissertation flow

The thesis is organized as follows:

Chapter 1 (current chapter) introduces the topic of this thesis through the presentation of the characteristics of vision and gait in young and older adults. Characteristics of the gaze signal are presented along with an overview of the technology and its criticalities. An overview of the literature on the coordination of vision and gait during the environment navigation along with the influence of the visual perturbation on gait is provided with a specific focus on obstacles crossing. Finally recent achievements in the rehabilitation domain for both gait and vision are briefly described, along with the potential of a set-up proposing a combined tracking of both gaze and gait could pose. The motivations and the specific aims of the research work are then described together with an outline of the content of the thesis.

Chapter 2 describes a validation study aiming at assessing the performances of a remote eye-tracker while treadmill walking during the exposition to large stimuli. The validation is performed in terms of determination of the workspace of the remote eye-tracker within the specific experimental set-up and in terms of accuracy and precision of the point of gaze measurements for large gaze angles, at different distances from the device and during walking. A simple demonstration of the use of the region of interests in such an experimental set-up is also presented.

Chapter 3 describes a study performed in a virtual reality environment on young and older adults. This study aimed at assessing the effect of visual distractors on the visuo-motor strategies of these populations during obstacle avoidance tasks in a virtual reality environment.

Chapter 4 discusses the main results achieved and highlights the main achievements of this thesis.

References

Babcock, J. S., Pelz, J. B., & Peak, J. (2003). The Wearable Eyetracker : A Tool for the Study of High-level Visual Tasks. *Proceedings of the Military Sensing Symposia Specialty Group on Camouflage Concealment and Deception Tucson Arizona*, (February), 13. http://citeseerx.ist.psu.edu/viewdoc/download?doi=10.1.1.63.9833&rep=rep1&type=pdf.

Beurskens, R., & Bock, O. (2012). Age-related Deficits of dual-task walking: A review. *Neural Plasticity*, 2012. http://doi.org/10.1155/2012/131608.

Beurskens, R., & Bock, O. (2013). Does the walking task matter? Influence of different walking conditions on dual-task performances in young and older persons. *Human Movement Science*, 32(6), 1456–1466. http://doi.org/10.1016/j.humov.2013.07.013.

Bock, O., Brustio, P. R., & Borisova, S. (2016). Age Differences of Gaze Distribution during Pedestrian Walking in a Virtual-Reality Environment, *International Journal of Applied Psychology*, 6(3), 64–69. http://doi.org/10.5923/ j.ijap.20160603.03.

Brown, L. a, McKenzie, N. C., & Doan, J. B. (2005). Age-dependent differences in the attentional demands of obstacle negotiation. *The Journals of Gerontology. Series A: Biological Sciences and Medical Sciences*, 60(7), 924–927. http://doi.org/10.1093/gerona/60.7.924.

Caetano, M. J. D., Lord, S. R., Schoene, D., Pelicioni, P. H. S., Sturnieks, D. L., & Menant, J. C. (2016). Age-related changes in gait adaptability in response to unpredictable obstacles and stepping targets. *Gait & Posture*, 46, 35–41. http://doi.org/10.1016/j.gaitpost.2016.02.003.

Cappozzo, A. (1984). Gait analysis methodology. *Human Movement Science*, 3(1–2), 27–50. http://doi.org/10.1016/0167-9457(84)90004-6.

Cappozzo, A. (1991). Three-dimensional analysis of human walking: Experimental methods and associated artifacts. *Human Movement Science*, 10(5), 589–602. http://doi.org/10.1016/0167-9457(91)90047-2.

Cappozzo, A., Catani, F., Della Croce, U., & Leardini, A. (1995). Position and orientation in space of bones during movement: Anatomical frame definition and determination. *Clinical Biomechanics*, 10(4), 171–178. http://doi.org/10.1016/0268-0033(95)91394-T.

Cappozzo, A., Della Croce, U., Leardini, A., & Chiari, L. (2005). Human movement analysis using stereophotogrammetry. Part 1: theoretical background. *Gait & Posture*, 21(2), 186–96. http://doi.org/10.1016/j.gaitpost.2004.01.010.

Chapman, G. J., & Hollands, M. A. (2006). Age-related differences in stepping performance during step cycle-related removal of vision. *Experimental Brain Research*, 174(4), 613–621.

http://doi.org/10.1007/s00221-006-0507-6.

Chapman, G. J., & Hollands, M. A. (2007). Evidence that older adult fallers prioritise the planning of future stepping actions over the accurate execution of ongoing steps during complex locomotor tasks. *Gait & Posture*, 26, 59–67. http://doi.org/10.1016/j.gaitpost.2006.07.010.

Chen, H.-C., Ashton-Miller, J., Alexander, N., & Schultz, A. (1994). Age effects on strategies used to avoid obstacles. *Gait & Posture*, 2(3), 139–146. http://doi.org/10.1016/0966-6362(94)90001-9.

Chen, H. C., Ashton-Miller, J. a, Alexander, N. B., & Schultz, A. B. (1991). Stepping over obstacles: gait patterns of healthy young and old adults. *Journal of Gerontology*, 46(6), M196-203. Retrieved from http://www.ncbi.nlm.nih.gov/pubmed/1940078.

Cheng, T.-J., Yang, B., Holloway, C., & Tyler, N. (2016). Effect of environmental factors on how older pedestrians detect an upcoming step, *Lighting Research & Technology*, 1–11.

Darekar, A., McFadyen, B. J., Lamontagne, A., & Fung, J. (2015). Efficacy of virtual reality-based intervention on balance and mobility disorders post-stroke: a scoping review. *Journal of Neuroengineering and Rehabilitation*, 12(1), 46. http://doi.org/10.1186/s12984-015-0035-3.

Duchowski, A. T. (2002). A breadth-first survey of eye-tracking applications. *Behavior Research Methods, Instruments, & Computers : A Journal of the Psychonomic Society*, 34(4), 455–470. http://doi.org/10.3758/BF03195475.

Duchowski, A. T. (2007). Eye Tracking Methodology: Theory and Practice. Book (Second, Vol. 55). London: Springer London. http://doi.org/10.1007/978-1-84628-609-4.

Franz, J. R., Francis, C. a., Allen, M. S., O'Connor, S. M., & Thelen, D. G. (2015). Advanced age brings a greater reliance on visual feedback to maintain balance during walking. *Human Movement Science*, 40, 381–392. http://doi.org/10.1016/j.humov.2015.01.012.

Galna, B., Peters, A., Murphy, A. T., & Morris, M. E. (2009). Obstacle crossing deficits in older adults: A systematic review. *Gait & Posture*, 30(3), 270–275. http://doi.org/10.1016/j.gaitpost.2009.05.022.

Gibson, B. Y. J. J., & Gibson, J. (1958). Visually Controlled Locomotion and Visual Orientation in Animals, *British journal of psychology*, 49.3 , 182–194.

Greany, J. F., & Di Fabio, R. P. (2008). Saccade to stepping delays in elders at high risk for falling. *Aging Clinical and Experimental Research*.

Guestrin, E. D., & Eizenman, M. (2006). General theory of remote gaze estimation using the pupil center and corneal reflections. *IEEE Transactions on Biomedical Engineering*, 53(6),

1124–33. http://doi.org/10.1109/TBME.2005.863952.

Hackney, A. L., Ann Vallis, L., & Cinelli, M. E. (2012). Action strategies of individuals during aperture crossing in non-confined space. *The Quarterly Journal of Experimental Psychology*, (October), 1–20. http://doi.org/10.1080/17470218.2012.730532.

Harley, C., Wilkie, R. M., & Wann, J. P. (2009). Stepping over obstacles: Attention demands and aging. *Gait & Posture*, 29(3), 428–432. http://doi.org/10.1016/j.gaitpost.2008.10.063.

Healey, M. K., Campbell, K. L., & Hasher, L. (2008). Chapter 22 Cognitive aging and increased distractibility: Costs and potential benefits. *Progress in Brain Research* (Vol. 169). Elsevier. http://doi.org/10.1016/S0079-6123(07)00022-2.

Hollands, K. L., Pelton, T. a., Tyson, S. F., Hollands, M. A., & van Vliet, P. M. (2012). Interventions for coordination of walking following stroke: Systematic review. *Gait & Posture*, 35(3), 349–359. http://doi.org/10.1016/j.gaitpost.2011.10.355.

Hollands, M. A., & Marple-Horvat, D. E. (1996). Visually guided stepping under conditions of step cycle-related denial of visual information. *Experimental Brain Research. Experimentelle Hirnforschung. Experimentation Cerebrale*, 109(2), 343–356. http://doi.org/10.1007/BF00231792.

Hollands, M. A., & Marple-Horvat, D. E. (2001). Coordination of Eye and Leg Movements During Visually Guided Stepping. *Journal of Motor Behavior*, 33(2), 205–216. http://doi.org/10.1080/00222890109603151.

Holmqvist, K., Nyström, M., Andersson, R., Dewhurst, R., Jarodzka, H., & Van de Weijer, J. (2011). Eye Tracking: A comprehensive guide to methods and measures. *OXFORD University*.

Holmqvist, K., Nyström, M., & Mulvey, F. (2012). Eye tracker data quality: what it is and how to measure it. *In ETRA '2012 Proceedings of the Symposium on Eye Tracking Research and Applications* (pp. 45–52).

Hui-Fen Pan, Horng-Chaung Hsu, Wei-Ning Chang, Jenn-Huei Renn, H.-W. W. (2016). Strategies for obstacle crossing in older adults with high and low risk of falling. *Physical Therapy Science*, 28, 1614–1620.

Jaffe, D. L., Brown, D. a, Pierson-Carey, C. D., Buckley, E. L., & Lew, H. L. (2004). Stepping over obstacles to improve walking in individuals with poststroke hemiplegia. *Journal of Rehabilitation Research and Development*, 41(3A), 283–292. http://doi.org/10.1682/JRRD.2004.03.0283.

Kizony, R., Levin, M. F., Hughey, L., Perez, C., & Fung, J. (2010). Cognitive load and dual-task performance during locomotion poststroke: a feasibility study using a functional virtual environment. *Physical Therapy*, 90(2), 252–260. http://doi.org/10.2522/ptj.20090061.

Kowler, E. (2011). Eye movements : The past 25 years. *Vision Research*, 51(13), 1457–1483. http://doi.org/10.1016/j.visres.2010.12.014.

Laboratories Applied Science. (2014). Eye Tracker Systems Manual ASL EYE-TRAC 7 Head Mounted Optics.

Lo, O.-Y., & Chou, L.-S. (2015). Effects of Different Visual Attention Tasks on Obstacle Crossing in Healthy Young Adults. *Biomedical Engineering: Applications, Basis and Communications*, 27(6), 1550059. http://doi.org/10.4015/S1016237215500593.

Lo, O.-Y., van Donkelaar, P., & Chou, L.-S. (2015). Distracting visuospatial attention while approaching an obstacle reduces the toe-obstacle clearance. *Experimental Brain Research*, 233(4), 1137–1144. http://doi.org/10.1007/s00221-014-4189-1.

Lowrey, C. R., Watson, A., & Vallis, L. A. (2007). Age-related changes in avoidance strategies when negotiating single and multiple obstacles. *Experimental Brain Research*, 182(3), 289–299. http://doi.org/10.1007/s00221-007-0986-0.

Marigold, D. S., & Patla, A. E. (2007). Gaze fixation patterns for negotiating complex ground terrain. *Neuroscience*, 144(1), 302–313. http://doi.org/10.1016/j.neuroscience.2006.09.006.

Mevorach, C., Spaniol, M. M., Soden, M., & Galea, J. M. (2016). Age-dependent distractor suppression across the vision and motor domain. *Journal of Vision*, 16(11), 27. http:// doi.org/10.1167/16.11.27.

Mirelman, A., Rochester, L., Reelick, M., Nieuwhof, F., Pelosin, E., Abbruzzese, G., Hausdorff, J. M. (2013). V-TIME: a treadmill training program augmented by virtual reality to decrease fall risk in older adults: study design of a randomized controlled trial. *BMC Neurology*, 13(1), 15. http://doi.org/10.1186/1471-2377-13-15.

Morgante, J. D., Zolfaghari, R., & Johnson, S. P. (2012). A critical test of temporal and spatial accuracy of the Tobii T60XL eye tracker. *Infancy*, 17(1), 9–32. http://doi.org/10.1111/ j.1532-7078.2011.00089.x.

Morimoto, C. H., & Mimica, M. R. M. (2005). Eye gaze tracking techniques for interactive applications. *Computer Vision and Image Understanding*, 98(1), 4–24. http://doi.org /10.1016/ j.cviu.2004.07.010.

Nyström, M., Andersson, R., Holmqvist, K., & van de Weijer, J. (2013). The influence of calibration method and eye physiology on eyetracking data quality. *Behavior Research Methods*, 45(1), 272–88. http://doi.org/10.3758/s13428-012-0247-4.

Onorati, F. (2016). Reconstruction and analysis of the pupil dilation signal : Application to a psychophysiological affective protocol. *In Engineering in Medicine and Biology Society (EMBC), 2013 35th Annual International Conference of the IEEE* (pp.5-8), http:// doi.org/10.1109/ EMBC.2013.6609423.

Openstax College, R. U. (2013). Anatomy & Physiology. OpenStax College. Retrieved from http://cnx.org/content/col11496/latest/.

Patla, A. E. (1997). Understanding the roles of vision in the control of human locomotion. *Gait & Posture*, 5(1), 54–69. http://doi.org/10.1016/S0966-6362(96)01109-5.

Patla, A. E., Adkin, A., Martin, C., Holden, R., & Prentice, S. (1996). Characteristics of voluntary visual sampling of the environment for safe locomotion over different terrains. Experimental Brain Research. Experimentelle Hirnforschung. *Experimentation Cerebrale*, 112(3), 513–522. http://doi.org/10.1007/BF00227957.

Patla, A. E., & Vickers, J. N. (1997). Where and when do we look as we approach and step over an obstacle in the travel path? *Neuroreport*, 8(17), 3661–5.

Patla, A. E., & Vickers, J. N. (2003). How far ahead do we look when required to step on specific locations in the travel path during locomotion? *Experimental Brain Research*, 148(1), 133–138. http://doi.org/10.1007/s00221-002-1246-y.

Perry, J. (1992). Gait Analysis Normal and Pathological Function. *SLACKIncorporated*.

Peruzzi, A., Cereatti, A., Della Croce, U., & Mirelman, A. (2016). Effects of a virtual reality and treadmill training on gait of subjects with multiple sclerosis: a pilot study. *Multiple Sclerosis and Related Disorders*, 5, 91–96. http://doi.org/10.1016/j.msard.2015.11.002.

Poole, A., & Ball, L. J. (2005). Eye Tracking in Human-Computer Interaction and Usability Research: Current Status and Future Prospects. In C. Ghaoui (Ed.), *Encyclopedia of Human-Computer Interaction* (211–219). Idea Group. http://doi.org/10.4018/978-1-59140-562-7.

Reed-Jones, R. J., Dorgo, S., Hitchings, M. K., & Bader, J. O. (2012). Vision and agility training in community dwelling older adults: Incorporating visual training into programs for fall prevention. *Gait & Posture*, 35(4), 585–589. http://doi.org/10.1016/j.gaitpost.2011.11.029.

Reed-Jones, R. J., Solis, G. R., Lawson, K. a., Loya, A. M., Cude-Islas, D., & Berger, C. S. (2013). Vision and falls: A multidisciplinary review of the contributions of visual impairment to falls among older adults. *Maturitas*, 75(1), 22–28. http://doi.org/ 10.1016/j.maturitas.2013.01.019.

Špakov, O. (2012). Comparison of eye movement filters used in HCI. *Proceedings of the Symposium on Eye Tracking Research and Applications - ETRA '12*, 281. http://doi.org /10.1145/ 2168556.2168616.

Stuart, S., Alcock, L., Galna, B., Lord, S., & Rochester, L. (2014). Visual sampling in Parkinson's disease: current methodological issues, *Posture and Gait Research World Congress*, Vancouver, Canada, 2014.

Stuart, S., Galna, B., Lord, S., & Rochester, L. (2015). A protocol to examine vision and gait in

Parkinson's disease: impact of cognition and response to visual cues. *F1000Research*, (0), 1–15. http://doi.org/10.12688/f1000research.7320.1.

Tournier, I., Dommes, A., & Cavallo, V. (2016). Review of safety and mobility issues among older pedestrians. *Accident Analysis and Prevention*, 91, 24–35. http://doi.org/10.1016/j.aap.2016.02.031.

Van Ooijen, M. W., Roerdink, M., Trekop, M., Visschedijk, J., Janssen, T. W., & Beek, P. J. (2013). Functional gait rehabilitation in elderly people following a fall-related hip fracture using a treadmill with visual context: design of a randomized controlled trial. *BMC Geriatrics*, 13, 34. http://doi.org/10.1186/1471-2318-13-34.

Veneri, G., Federighi, P., Rosini, F., Federico, A., & Rufa, A. (2010). Influences of data filtering on human-computer interaction by gaze-contingent display and eye-tracking applications. *Computers in Human Behavior*, 26(6), 1555–1563. http://doi.org/10.1016/j.chb. 2010. 05.030.

Wass, S. V., Forssman, L., & Leppänen, J. (2014). Robustness and precision: How data quality may influence key dependent variables in infant eye-tracker analyses. *Infancy*, 19(5), 427–460. http://doi.org/10.1111/infa.12055.

Yamada, M., Aoyama, T., Arai, H., Nagai, K., Tanaka, B., Uemura, K., Mori, S., & Ichihashi, N. (2012). Complex obstacle negotiation exercise can prevent falls in community-dwelling elderly Japanese aged 75years and older. *Geriatrics and Gerontology International*, 12(3), 461–467. http://doi.org/10.1111/j.1447-0594.2011.00794.x.

Young, L. R., & Sheena, D. (1975). Survey of eye movement recording methods. *Behavior Research Methods & Instrumentation*, 7(5), 397–429. http://doi.org/10.3758/BF03201553

Young, L., & Sheena, D. (1975). Survey of eye movement recording methods. *Behavior Research Methods & Instrumentation*, 7(5), 397–429.

Young, W. R., & Hollands, M. A. (2010). Can telling older adults where to look reduce falls? Evidence for a causal link between inappropriate visual sampling and suboptimal stepping performance. *Experimental Brain Research*, 204(1), 103–113. http://doi.org/10.1007/s00221-010-2300-9.

Young, W. R., & Mark Williams, A. (2015). How fear of falling can increase fall-risk in older adults: Applying psychological theory to practical observations. *Gait & Posture*, 41(1), 7–12. http://doi.org/10.1016/j.gaitpost.2014.09.006.

Young, W. R., Wing, A. M., & Hollands, M. A. (2012). Influences of state anxiety on gaze behavior and stepping accuracy in older adults during adaptive locomotion. *The Journals of Gerontology Series B: Psychological Sciences and Social Sciences*, 67 B(1), 43–51. http://doi.org/10.1093/geronb/gbr074.

Chapter 2

*Use of a Remote Eye-Tracker for the Analysis of Gaze during Treadmill Walking and Visual Stimuli Exposition**

***** This chapter is based on

Serchi V., Peruzzi A., Cereatti A., and Della Croce U., "**Use of a Remote Eye-Tracker for the Analysis of Gaze during Treadmill Walking and Visual Stimuli Exposition.**" *BioMed research international* (2016).

Serchi V., Peruzzi A., Cereatti A., and Della Croce U., "**Performance of a remote eye-tracker in measuring gaze during walking.**" 20th IMEKO TC4 International Symposium Benevento, Italy, September 2014, ACTA IMEKO.

Serchi V., Peruzzi A., Cereatti A., and Della Croce U., "**Tracking gaze while walking on a treadmill: spatial accuracy and limits of use of a stationary remote eye-tracker.**" *2014 36th Annual International Conference of the IEEE Engineering in Medicine and Biology Society*. IEEE, 2014.

Serchi V., Cereatti A., Federighi P., Rufa A., and Della Croce U., "**An experimental setup for the combined analysis of gaze and gait.**" 23th National Congress of SIAMOC, Pisa, Italy, September 2013.

Serchi V., Peruzzi A., Cereatti A., and Della Croce U., "**Tracking gaze while walking on a treadmill: limits of use of stationary remote eye-tracker.**" *Proceedings 4th Conference Gruppo Nazionale di Bioingegneria (GNB)*, Pavia, Italy, June 2014.

Serchi V., Peruzzi A., Cereatti A., and Della Croce U., "**Validation of a remote eye-tracker: application to gait analysis.**" *Proceedings of 25th SIAMOC-23th ESMAC 2014*, p.69, Rome, Italy, October 2014.

Introduction

Visual sampling plays a crucial role during challenging locomotor tasks (Reed-Jones et al., 2013) and previous studies involving obstacle avoidance showed that effective visual behavior is important for safe locomotion (Chapman & Hollands, 2006, 2007; Patla, 1997). Rehabilitation programs including motor and cognitive aspects (*e.g.* obstacle negotiation exercises (Mirelman et al., 2011, 2013; Peruzzi, Cereatti, Mirelman, & Della Croce, 2013) should assess both motor and visual strategies (Reed-Jones, Dorgo, Hitchings, & Bader, 2012; Young & Hollands, 2010). However, this is rarely the case, most probably due to the complexity of the experimental set-up that is required. In fact, the validity of an experimental study aiming at measuring gait and gaze while moving in a complex environment recreated in a laboratory setting may be challenged by the difficulty of designing tasks similar to those performed in real life (Stanley & Hollands, 2014).

The use of virtual reality (VR) environments allows for the most part to overcome such limitations, and to create safe, repeatable and controlled experimental set-ups. Furthermore, the integration of VR, gait analysis and eye-tracking allows for a full control of the environmental variables while evaluating the subject's performance in terms of visual and locomotion variables. In this context, projected VR environments have been successfully used to elicit visual behavior similar to those observed in a real environment (Stanley & Hollands, 2014). Moreover monitor-based projected VR has been successfully employed in several gait rehabilitation protocols and its feasibility and acceptance have been tested for several pathologic populations (Mirelman et al., 2006, 2013; Peruzzi, Cereatti, Della Croce, & Mirelman, 2016; Peruzzi et al., 2013).

The point of gaze (*PoG*) can be measured either using wearable and remote eye-trackers (Holmqvist et al., 2011; Morimoto & Mimica, 2005). Recent literature evidenced that remote eye-trackers should be preferred to wearable eye-trackers, since they allow for unobtrusive tracking of the gaze and, hence, for more natural head movements and longer periods of data collection (Holmqvist et al., 2011; Weigle & Banks, 2008). Modern remote eye-trackers permit to record gaze within a limited volume of operation even if the head is not completely stationary (Guestrin & Eizenman, 2006; Holmqvist et al., 2011). The use of a treadmill and a projected VR environment represents a convenient technological solution to analyze gait kinematics while recording the *PoG*. In fact, this set-up allows to limit the volume in which the head motion is

measured and to maintain the relative distances and angles between the subject, the remote eye-tracker and the visual stimulus source within predefined ranges.

In general, the quality of the *PoG* measurements depends on the specific remote eye-tracker characteristics (*i.e.* camera resolution, sampling frequency, pupil illumination mode, binocular or monocular vision mode). The reliability of the *PoG* measurements is also influenced by several factors independent from the remote eye-tracker characteristics. Some of them are subject specific (the morphology and physiology of the subject's eyes), others depend on the experimental conditions (the operator's expertise in calibrating the remote eye-tracker, changes in the environmental light and in the brightness of the stimulus, environmental interferences and the range of motion of the subject's head) (Holmqvist et al., 2011; Holmqvist, Nyström, & Mulvey, 2012). Moreover, accuracy and precision of the *PoG* are crucial for interpreting the collected data, particularly when regions of interest are defined in order to analyze the interaction of the subject with specific parts of the stimulus (regions of interest - *RoI*) (Blignaut & Wium, 2014; Holmqvist et al., 2011).

Unfortunately, while few studies have investigated the influence of some of the above-mentioned critical factors on the *PoG* quality (Blignaut & Wium, 2014; Hessels, Cornelissen, Kemner, & Hooge, 2014; Morgante, Zolfaghari, & Johnson, 2012; Niehorster, Cornelissen, Holmqvist, Hooge, & Hessels, 2017; Wass, Forssman, & Leppänen, 2014), to the authors' knowledge none of them have explored the use of remote eye-trackers during a dynamic motor task such as walking. The goal of this study was to evaluate the reliability of the measures of a remote eye-tracker (Tobii TX300), in an experimental set-up requiring the subject to walk on a treadmill while looking at projected visual stimuli. Good practice guidelines, which can be extended to more complex experimental conditions and visuo-motor rehabilitation protocols, are also provided. The following critical factors were investigated: (a) definition of the remote eye-tracker workspace; (b) evaluation of the spatial accuracy, precision and trackability of the *PoG* measurements for different locations of the stimuli while either walking or standing and (c) applicability of *RoI* analysis to remote eye-tracker *PoG* measurements while walking.

Materials and methods

Participants

Ten healthy subjects (Caucasian, 5 m., 5 f., height: 1.7±0.1 m; age: 36.3±9.5 y. o.) volunteered to the study. The participants were not allowed to wear glasses nor contact lenses and therefore, the participants not able to see the screen clearly were excluded from the study. The Tobii TX300 allows for the eye tracking when lenses are used, but in this study the use of lenses was excluded since it was considered as a possible source of inaccuracy in the *PoG* measurements estimation.

Experimental setup

The experimental setup consisted of a treadmill, a remote eye-tracker (Tobii TX300, sampling at 300 frames/s), a projector (Epson, WXGA), a screen and a marker-based 6-camera stereo-photogrammetric system (Vicon T20, sampling at 300 frames/s). The treadmill, the remote eye-tracker and the projecting surface were arranged as shown in Figure 2.1.

Figure 2.1 A schematic representation of the experimental set-up, which included a screen (1), a remote eye-tracker (2), a treadmill (3) and a stereo-photogrammetric system (4). Three retro-reflective markers were placed on the subject's head to track its movements. The inclination of the remote eye-tracker with respect to the horizontal plane (β) and its distance from the projecting surface (d) were respectively set to 18 deg and 690 mm. The head (H) reference frame and the remote eye-tracker (rET) reference frame are reported (AP, anterior-posterior; ML, medio-lateral; and V, vertical axes).

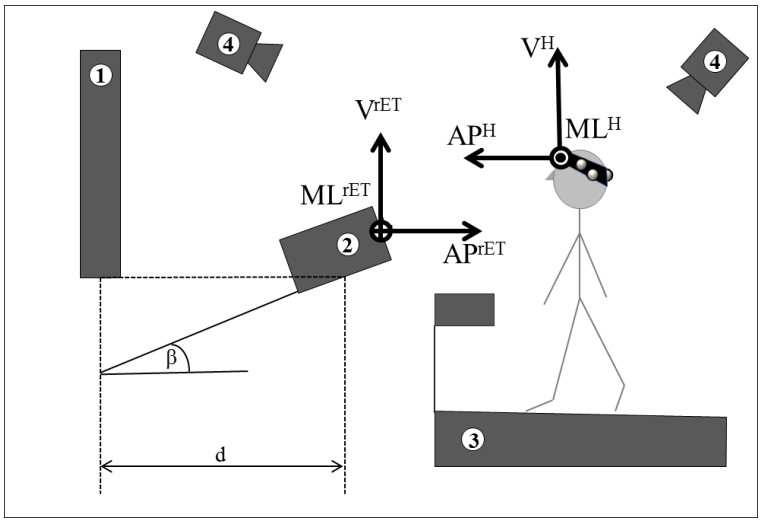

In order to limit any interference between the two devices, both working in the infrared light spectrum, care was paid in positioning the cameras of the stereo-photogrammetric system so that the infrared light interference with the remote eye-tracker was limited (Holmqvist et al., 2011; Tobii Technology AB, 2004). Specifically, none of the stereo-photogrammetric cameras faced neither the subject's eyes nor directly the remote eye-tracker sensor. This was made in order to prevent errors in the reconstruction of the *PoG* due to a bad recognition of the corneal reflex in the image of the eye gathered by the remote eye-tracker sensor.

The image on the screen was of 1040 mm × 580 mm (1280 px × 1024 px). The remote eye-tracker and the projector were placed over adjustable platforms that allowed regulating the height of both the remote eye-tracker and of the projector based on the height of the subject (Figure 2.2). Specifically, the center of the image was set at the same height of the subject's eyes, whereas the remote eye-tracker was placed at the same height of the lower edge of the image.

Figure 2.2 Image showing part of the experimental set-up used in this study: the projector over a purposely built adjustable platform. A similar adjustable platform was used also for the remote eye-tracker. The adjustable platform was used in order to adjust both the projector and the remote eye-tracker in according to the height of the subject.

Five retro-reflective markers were placed on the front of the remote eye-tracker to locate the device in the space to be able to measure accurately the configuration parameters of the remote eye-tracker. In particular four markers were on in each corner and one over a point indicated in

the user manual as the point to which all the configuration measurements are referred to (Tobii Technology AB, 2004). Four additional markers were placed over the corners of the image projected so that image position and orientation could be determined with respect to the remote eye-tracker. Finally, three retro-reflective markers were attached on a headband worn by the subject. The headband was adjusted so that one marker was over the inion and another above the left ear of the subject.

With the assistance of the Tobii and Vicon technical supports a cable was built in order to connect the remote eye-tracker (sync port, SMB female to male connector) and the stereo-photogrammetric systems (Giganet sync output, jack male connector) through the Tobii Studio software (Figure 2.3) (Tobii Technology AB, 2012b, 2012c; Vicon Motion Systems, 2011).

Figure 2.3 Picture of the synchronization cable built in order to connect the remote eye-tracker and the stereo-photogrammetric systems: 1) SMB female to male connector - jack male connector and 2) jack female connector - impedance adaptor - jack male connector. A 5-meter coaxial cable RF174 was used.

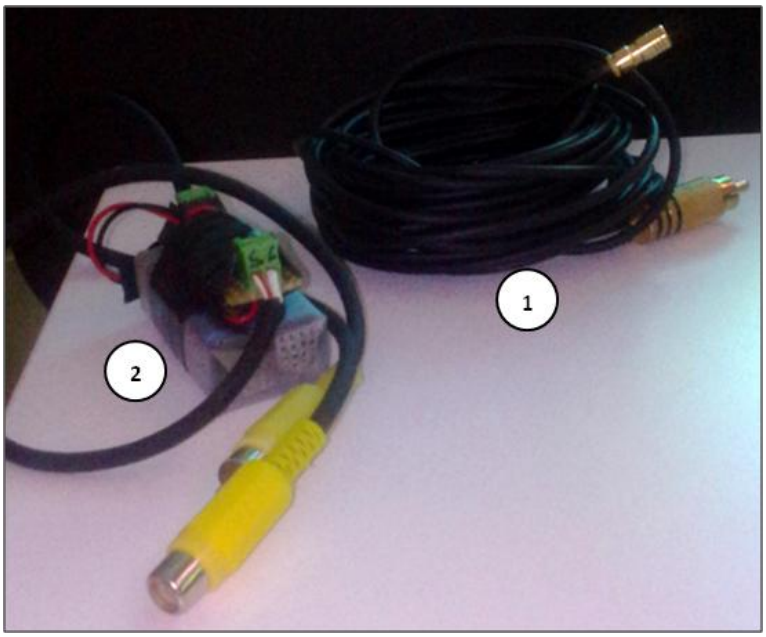

The cable connected the two systems through an impedance adapter in order to gather a proper current to the remote eye-tracker sync input (Figure 2.4). The Tobii Studio configuration was set in order to listen and record an external stimulus (LightView Enable). In this way, once the

recording of the stereo-photogrammetric system started, a 5 V pulse was sent to the remote eye-tracker hardware device. A trigger event was stored as a flag within the remote eye-tracker recordings and used in post-processing to align the gaze to the head motion signal.

Figure 2.4 Schematic representation of the impedance adaptor used to gather a proper current to the remote eye-tracker (Tobii TX300) sync port.

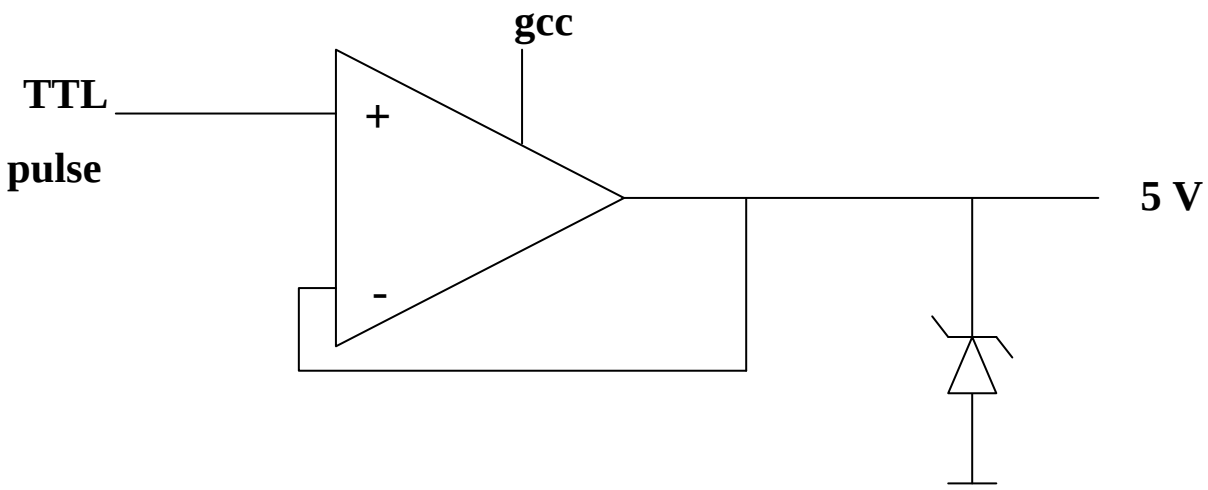

Acquisition protocol

A reference frame embedded with the remote eye-tracker was defined using the retro-reflective markers attached to it. The origin of the reference frame of the remote eye-tracker was made to coincide with the center of the remote eye-tracker sensor, the vertical (V^{rET}) axis pointing upwards, the anterior-posterior (AP^{rET}) axis parallel to the floor and pointing toward the subject and the medio-lateral (ML^{rET}) axis orthogonal to both V^{rET} and AP^{rET} (Figure 2.1).

A static stereo-photogrammetric acquisition was performed to locate the image in the remote eye-tracker reference frame. The markers on the image corners and on the remote eye-tracker were then removed.

To define an anatomical head reference frame, an *ad hoc* calibration procedure was carried out while the subject was standing on the treadmill, with the eyes closed, while wearing both the headband and a marker attached on each eye-lid (Cappozzo, Della Croce, Leardini, & Chiari, 2005) (Figure 2.5). In the static acquisition, the markers placed over the eye-lids were anatomically calibrated with respect to the technical frame of reference defined above the three markers of the head-band. The markers on the eye-lids were then removed. Afterwards, in the

dynamic acquisition, the position of the removed markers was reconstructed in order to define the anatomical head reference of frame.

Figure 2.5 Picture showing the position of the markers over the subject during the anatomical calibration procedure.

The anatomical head reference frame origin was positioned in the midpoint between the two eyes, the medio-lateral (ML^H) axis was the line passing through the eyes, the vertical (V^H) axis was orthogonal to the plane identified by the position of the two eyes and the inion and pointing upwards and the anterior-posterior (AP^H) axis was orthogonal to both V^H and AP^H (Figure 2.1).

The use of the remote eye-tracker requires a preliminary subject-specific calibration of the *PoG* on a user defined calibration plan. The calibration procedure was performed once for each subject at the beginning of the acquisition protocol via the remote eye-tracker proprietary software (nine-point procedure; Tobii Studio, firmware 3.2). During the calibration the distance between the subject and the subject's eyes was set at 650 mm as suggested in the user manual. The subject was asked to upright stand with the head toward the screen and to keep the head still and to look at nine calibration points appearing on the screen. A calibration check was performed through the remote eye-tracker proprietary software which consisted in the generation of a circle around each calibration point within which a green dot was displayed in the case of a good calibration (Tobii Technology AB, 2012c) (Figure 2.6).

Figure 2.6 Example of calibration feedback provided by the Tobii Studio software for one of the participants to the study.

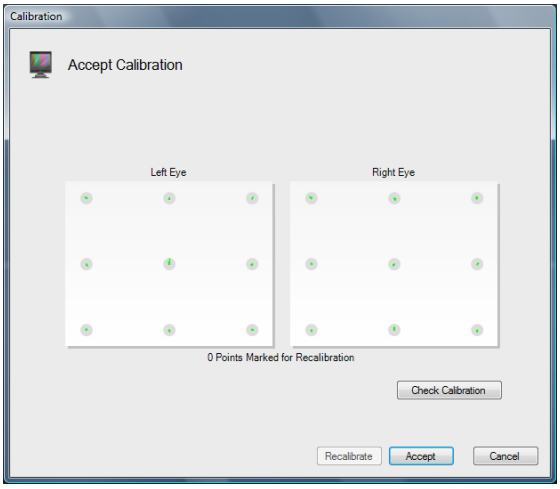

A validation of the calibration was also performed to check the quality of the calibration. The subject was asked to look at each point of the calibration grid while the operator checked the estimation of the *PoG* made by the remote eye-tracker. The calibration was repeated in the case of an unsatisfactory result for one or more points of the calibration grid.

To characterize the performance of the remote eye-tracker, three different experimental sessions were carried out in a dark room.

Workspace identification

The subject initially stood on the treadmill facing the screen at a distance of 650 mm from the remote eye-tracker. The subject was asked to look at a dot-target located at the center of the image on the screen (Figure 2.7a), while translating anterior-posteriorly (*tAP*,~±200 mm), medio-laterally (*tML*, ~±100 mm) and vertically (*tV*, ~±100 mm) (Tobii Technology AB, 2012a) and rotating the head around both ML^H (*rML*, ~±50 deg) and V^H (*rV*, ~±50 deg) axes. This task was performed to define the range within which the head of the subject could move without eye tracking interruption.

Accuracy and precision determination

The subject was asked to look at a dot-target displayed sequentially in 13 fix locations of the image on the screen (Figure 2.7b). The dot-target persisted in each location for two seconds. Recordings were first performed with the subject standing still at 550 mm (*st550*), 650 mm

(*st650*) and 750 mm (*st750*) from the rET. Then, the subject was asked to perform the same gaze task while walking at two different speeds (*wslow*: 0.6 m/s, and *wfast*: 1.1 m/s). The subject was free to hold the treadmill bar for safety.

Remote eye-tracker *applicability for RoI analysis*

The subject was asked to look at a 2D target used as visual stimulus (a rectangular shape - Figure 2.7c, 230 mm × 80 mm) initially located at the center of the image (*stat_r*). After five seconds, the 2D target moved along a horizontal line at constant speed (80 pixels/s) from the right to the left (*horiz_r*), and along a vertical line from the top to the bottom (*vert_r*). The subject performed the task while standing at 650 mm from the remote eye-tracker (*stRoI*) and while walking on the treadmill at 0.6 m/s (*wslowRoI*) and 1.1 m/s (*wfastRoI*). The subject was free to hold the treadmill bar for safety.

Figure 2.7 A schematic representation of: (a) the visual stimulus used for the identification of the remote eye-tracker workspace; (b) the 13 dot-target locations of the visual stimulus on the screen used for the determination of the remote eye-tracker accuracy and precision and (c) the 2D target used to test the remote eye-tracker applicability for RoI analysis.

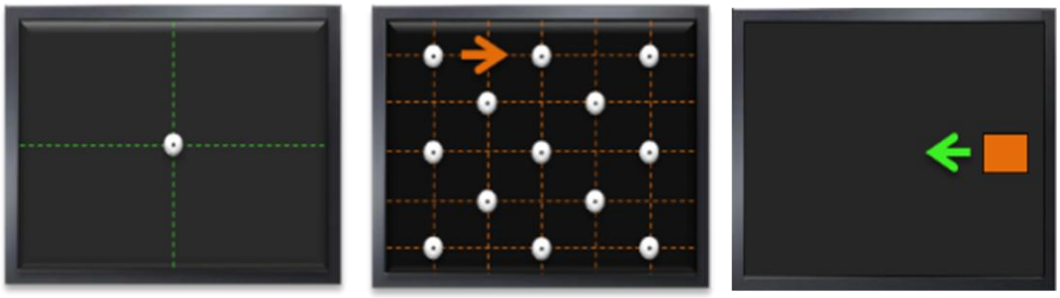

Data analysis

Blinks, saccades, short gaze deviations and signal flickering instances were extracted from the *PoG* horizontal and vertical components. A validity score, provided by the remote eye-tracker proprietary software, is associated to each sampled *PoG* (0: eye found with high confidence; 4: eye not found). *PoG* time series scoring 4 for both eyes and longer than 100 ms, were marked as blinks (Bekele et al., 2013; Holmqvist et al., 2011, 2012).

Saccades were identified as those *PoG* time series with velocity greater than 300 deg/s, amplitude greater than 7 deg and duration higher than 20 ms (Holmqvist et al., 2011). The *PoG* outliers were removed according to (Holmqvist et al., 2011). Moreover, *PoG* time series with a velocity greater than 1000 deg/s, being not compatible with any physiological eye movement, were classified as flickering (Holmqvist et al., 2011). The first 800 ms of the stimulus presentation time were not considered in the data processing to take into account the physiological delay between the stimulus appearance and the transfer of gaze on it (Tobii Technology, 2011)

The data processing for each experimental acquisition is described below.

Workspace identification

For each subject, the minimum and maximum linear and angular values of the head position reached during the head movements (*tAP*, *tML*, *tV*, *rML*, *rV*) were estimated and the relevant ranges of motion (*RoM*) computed. Similarly, for each subject, the minimum and maximum linear and angular values of the head position within which the remote eye-tracker was able to track both eyes, were computed and referred to as ranges of trackability (*RoTs*). To each head movement, the median values of both *RoMs (mRoM)* and *RoTs (mRoT)*, computed across subjects, were obtained. The remote eye-tracker workspace was defined as the combination of the *mRoTs* along the different directions.

Accuracy and precision determination

For each trial (*st550*, *st650*, *st750*, *wslow*, *wfast*), the *PoG* accuracy was computed as the estimated *PoG* distance from the known position of the *i-th* stimulus (i = 1, …, 13) averaged over the stimulus presentation time and subjects (ε_i). Similarly, the *PoG* precision was computed as the standard deviation of the estimated *PoG* averaged over the *i-th* stimulus presentation time and the subjects (δ_i). For each analyzed trial, the overall *PoG* accuracy and precision (ε, δ) were computed as the average values of ε_i and δ_i over all dot-target locations.

For each trial (*st550*, *st650*, *st750*, *wslow*, *wfast*), the overall index of trackability of the *PoG* was computed as the percentage ratio between the valid and the expected samples during the *i-th* stimulus presentation time averaged over the subjects and the dot target locations (γ). For *wslow*

and *wfast* trials, the head *RoMs* were computed for each subject to verify that the head moved within the remote eye-tracker workspace.

Remote eye-tracker applicability for RoI analysis

A *RoI* was defined by adding a margin, equal to the δ value obtained in the *wfast* trial, to the 2D target. The percentage of the *PoG* hitting the *RoI* was computed over the 2D target presentation time (*%stat_r, %horiz_r* and *%vert_r*).

Statistical analysis

Accuracy and precision determination

A Friedman test for non-normal distribution was used to assess a) if ε_i and δ_i were statistically different among the dot-target locations, b) if ε and δ were significantly different among the trials *st550, st650, st750, wslow* and *wfast,* and c) if ς was statistically different among the trials *st550, st650, st750, wslow* and *wfast.*

rET applicability for RoI analysis

A Friedman test for non-normal distribution was performed to assess a) if *%stat_r, %horiz_r* and *%vert_r* obtained for each 2D target motion (*stat_r, horiz_r* and *vert_r*) were significantly different and b) if *%stat_r, %horiz_r* and *%vert_r* obtained for each motor task (*stRoI*, *wslowRoI* and *wfastRoI*) were significantly different.

The level of significance was set to 0.05 for all statistical analyses. Pairwise comparisons were performed using a Wilcoxon signed-ranked test with a Holm-Bonferroni correction (α=0.05) for the significant findings. The effect size *r* was computed for the significantly different pairs.

Results

Workspace identification

The *RoTs* of the remote eye-tracker for each subject along and around the tested directions are reported in Annex 1. The *mRoTs* of the remote eye-tracker along and around the tested directions are shown in Figure 2.8 (translations: AP^{rET} *-tAP-*, 484 to 765 mm; ML^{rET} *-tML-*, -98 to 86 mm; V^{rET} *-tV-*, -78 to 61 mm; rotations: ML^{H} *-rML-*, -26 to 38 deg; V^{H} *-rV-*, -29 to 26 deg). No gaze tracking interruptions occurred for the positive translation along the ML direction.

Figure 2.8 The head *mRoTs* (green) and *mRoMs* (magenta) along the AP^{rET} (*tAP*: A, anterior; P: posterior), ML^{rET} (*tML*: L, left; R, right) and V^{rET} (*tV*: U, up; D, down) direction and around the V^{H} (*rV*: L, left; R, right) and ML^{H} (*rML*: U, up; D, down) directions.

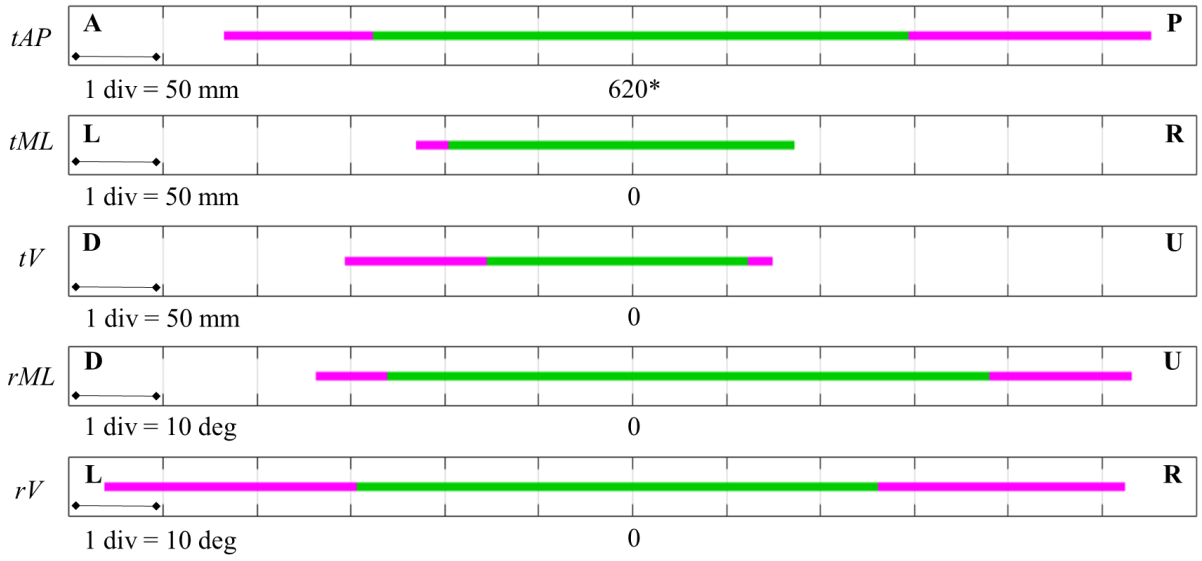

(*) The *tAP* values are centered at 620 mm, which is the projection of the original distance from the sensor on the AP^{rET} axis (650 mm).

Accuracy and precision determination

A graphical representation of ε_i and δ_i values found for each dot-target location during the static and dynamics trials *st550*, *st650*, *st750* and *wslow* and *wfast* for each subject is reported in Annex 2 and Annex 3 respectively. A graphical representation of ε_i and δ_i values found for each dot-target location (averaged over the subjects) during the trials *st550*, *st650*, *st750* is reported in Figure 2.9a. A similar graphical representation for the trials *wslow* and *wfast* is reported in Figure 2.9b.

Figure 2.9 A graphical representation of ε_i and δ_i values found for each dot-target location during the trials *st550*, *st650*, *st750* (a) and *wslow*, *wfast* (b). Each dot-target location on the image is a black dot. The circles center positions (colored dots) reflect the accuracy of the *PoG* measurements (ε_i) while their radius reflects the precision of the *PoG* measurements (small radius, δ_i < 4 mm; average radius, 4 mm< δ_i < 8 mm; large radius, δ_i > 8 mm).

(a)

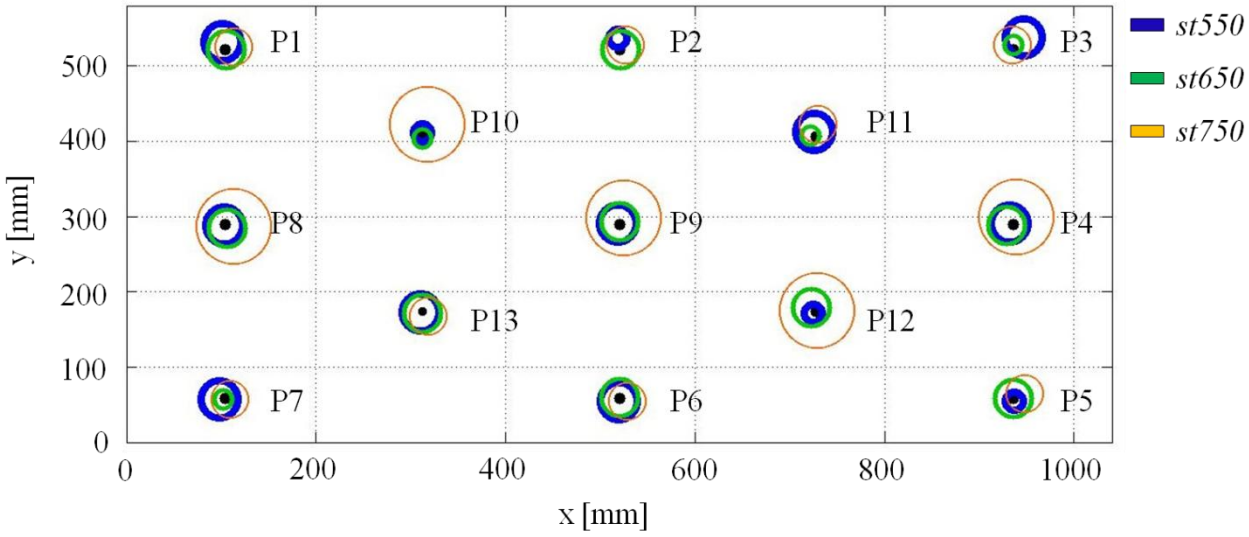

(b)

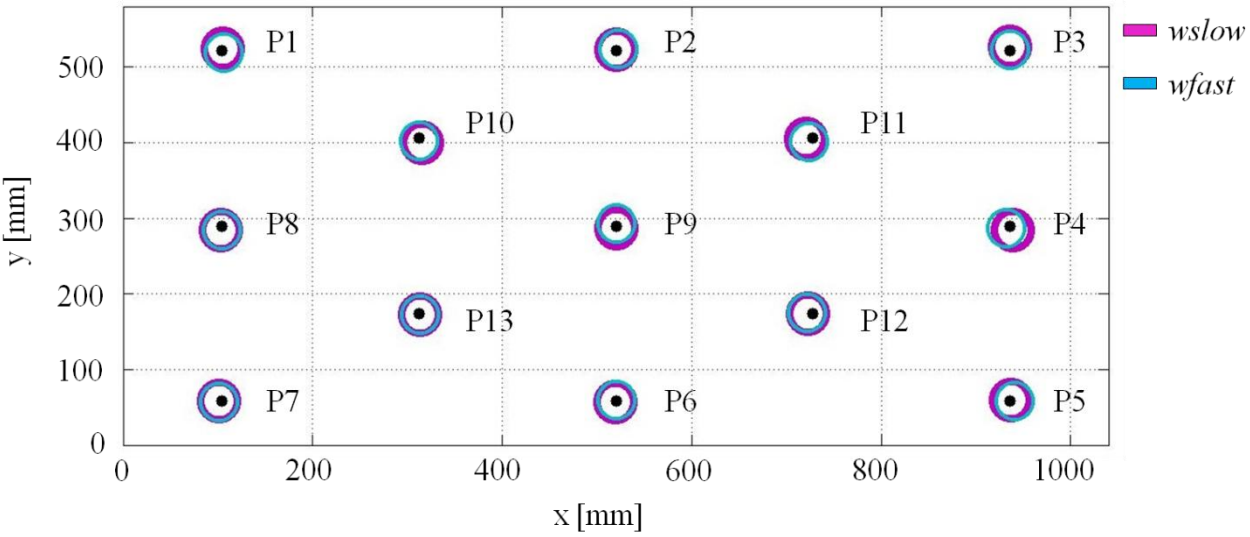

During the trial *st550*, the *PoG* was lost in one of the top corners (P1 or P3) for three subjects. The values relative to these points in the trial *st550* were excluded from the computation of the relevant following parameters. For ε_i and δ_i no significant differences were found among the 13 dot-target locations in any of the trials *st550*, *st650*, *st750*, *wslow* and *wfast*.

The ε, δ and τ values for *st550*, *st650*, *st750*, *wslow* and *wfast* are reported in Table I.

Table I. *PoG* measurements accuracy ε, precision δ and index of trackability τ. The values are averaged over the 10 subjects and over the 13 dot-target locations.

	st550	*st650*	*st750*	*wslow*	*wfast*
ε *[mm]*	13	10	17	12	13
δ *[mm]*	4	4	8	5	6
τ *[%]*	77	90	90	88	87

No significant differences were found among the ε and τ values of the trials *st550*, *st650*, *st750*, *wslow* and *wfast*. A significant difference was found among their δ values ($p < 0.001$). The value of δ computed for *st750* resulted significantly larger than those computed for *st550* ($p = 0.040$), *st650* ($p = 0.045$) and *wslow* ($p = 0.045$) with a large effect size ($r = 0.64$, 0.63 and 0.64, respectively).

The intervals between the minimum and the maximum values of the head *RoMs* across subjects obtained during the trials *wslow* and *wfast* are reported in Figure 2.10. The head motion remained always within the rET workspace.

Figure 2.10 The intervals between the minimum and the maximum values of the head *RoMs* (green) obtained during the trials *wslow* (violet) and *wfast* (light blue) across the subjects: translations along the AP^{rET} (A, anterior; P, posterior), ML^{rET} (L, left; R, right) and V^{rET} (U, up; D, down) directions and rotations around the ML^{H} (U, up; D, down) and V^{H} (L; R left; R, right) directions. The green band represents the remote eye-tracker workspace.

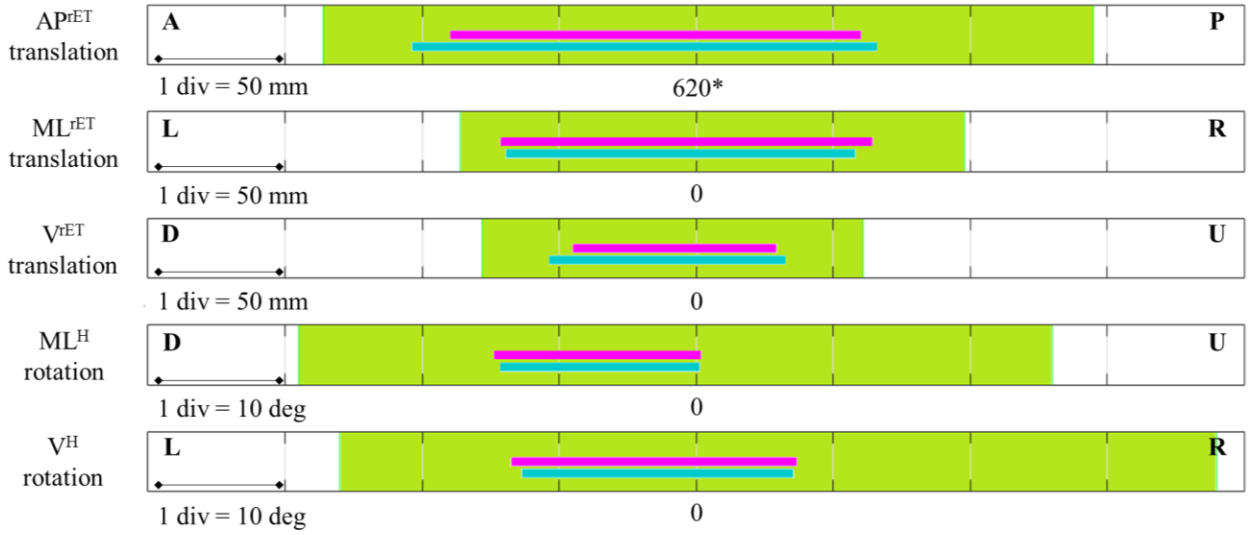

(*) The values of the translations along the AP^{rET} direction are centered at 620 mm, which is the projection of the original distance from the sensor on the AP^{rET} axis (650 mm)

rET applicability for RoI analysis

The values of *%stat_r*, *%horiz_r* and *%vert_r* are reported in Table II.

Table II. The percentage of PoG hitting the RoI defined around the 2D target moving on the screen with different patterns (stat_r: static at the center of the screen; horiz_r: moving horizontally, and vert_r: moving vertically). Percentages are reported for each motor task: *stRoI*: standing at 650 mm from the rET; *wslowRoI*: walking at 0.6 m/s and *wfastRoI*: walking at 1.1 m\s.

	%stat_r	*%horiz_r*	*%vert_r*
stRoI [%]	96±3	98±2	97±4
wslowRoI [%]	96±5	98±2	94±7
wfastRoI [%]	97±3	98±1	95±6

Neither the motion of the 2D target (*stat_r*, *horiz_r*, and *vert_r*) nor the motor task (*stRoI*, *wslowRoI* and *wfastRoI*) significantly influenced the percentage of *PoG* (*%stat_r*, *%horiz_r* and *%vert_r*) hitting the *RoI*.

Discussion

The main goal of the present study was to evaluate the suitability of the use of remote eye-tracking technology (Tobii TX300) during treadmill walking. This analysis can be relevant when developing projected VR-based applications aiming at investigating the visual behavior during walking in controlled environments. In particular, we aimed at defining the ranges of trackability, at providing a detailed description of *PoG* data quality during standing and walking (accuracy, precision and trackability) and at testing the remote eye-tracker feasibility for dynamic *RoI* analysis. While previous studies (Blignaut & Wium, 2014; Hessels et al., 2014) limited the assessment of the *PoG* quality during various static head orientations and positions, we extended the remote eye-tracker testing under dynamic exercises such as gait.

The workspace identified in this study set-up is in accordance with the datasheet of the device for what concerns the anterior-posterior head motion (500-800 mm distance from the remote eye-tracker), whereas the range of trackability along the medio-lateral and vertical directions was slightly smaller than the nominal range declared by the manufacturer (medio-lateral: ±100 mm; vertical: ±80 mm). In agreement with Blignaut and colleagues (Blignaut & Wium, 2014), we found a general decline of the quality of the *PoG* measurements for larger distances from the remote eye-tracker (750 mm) and a few gaze losses for large gaze angles corresponding to the closest distance tested (in trial *st550*, a loss of *PoG* occurred on two dot-target locations located at the grid top corners). In another study, Hessel et al. (Hessels et al., 2014) concluded that the quality of the *PoG* measurements is jeopardized at extreme head rotations around the V axis; however, no information about the amplitude of the angular head rotations were reported. Similarly to (Hessels et al., 2014), we found some loss of *PoG* data during the head rotation around the vertical direction limiting the range of trackability to -29 to 26 deg.

The statistical analysis revealed that the position of the stimulus on the image does not influence the *PoG* accuracy, precision and trackability both while standing and walking. In particular, head displacements were within the ranges of trackability during walking trials (speeds

up to 1.1 m/s), confirming that the Tobii TX300 can be conveniently used for the determination of the *PoG* during gait.

Furthermore, neither the motion of the 2D target (static, vertical, horizontal) nor the motor task (static, slow and fast gait) significantly influenced the percentage of the *PoG* samples hitting the *RoI* thus supporting the use of dynamic *RoIs* during the analysis of walking tasks. This finding fosters the usability of the remote eye-tracker TX300 for the gaze analysis during treadmill gait in projected VR-based applications. To the authors' knowledge, this study provides the first characterization of a remote eye-tracker used for tracking gaze while walking. This study represents also a fundamental preliminary step for a correct, unobtrusive assessment of the interactions between motor and visual strategies occurring during gait rehabilitation protocols requiring VR environments.

Conclusion

This study demonstrated that the remote eye-tracker Tobii TX300 can be used to analyze gaze during walking on a treadmill, since the performance of the remote eye-tracker and the quality of the measurements did not significantly differ from those obtained during static tasks. The outcomes of this study may provide elements for the design and implementation of analytical and experimental procedures for the combined analysis of gaze and human locomotion in VR-based applications.

References

Bekele, E., Zheng, Z., Swanson, A., Crittendon, J., Warren, Z., & Sarkar, N. (2013). Understanding How Adolescents with Autism Respond to Facial Expressions in Virtual Reality Environments. *IEEE Transactions on Visualization and Computer Graphics*, *19*(4), 711–720. http://doi.org/10.1109/TVCG.2013.42.

Blignaut, P., & Wium, D. (2014). Eye-tracking data quality as affected by ethnicity and experimental design. *Behavior Research Methods*, *46*, 67–80. http://doi.org/ 10.3758/ s13428-013-0343-0.

Cappozzo, A., Della Croce, U., Leardini, A., & Chiari, L. (2005). Human movement analysis using stereophotogrammetry. Part 1: theoretical background. *Gait & Posture*, *21*(2), 186–96. http://doi.org/10.1016/j.gaitpost.2004.01.010.

Chapman, G. J., & Hollands, M. A. (2006). Evidence for a link between changes to gaze behaviour and risk of falling in older adults during adaptive locomotion. *Gait & Posture*, *24*, 288–94. http://doi.org/10.1016/j.gaitpost.2005.10.002.

Chapman, G. J., & Hollands, M. A. (2007). Evidence that older adult fallers prioritise the planning of future stepping actions over the accurate execution of ongoing steps during complex locomotor tasks. *Gait & Posture*, *26*, 59–67. http://doi.org/10.1016/j.gaitpost .2006.07.010.

Guestrin, E. D., & Eizenman, M. (2006). General theory of remote gaze estimation using the pupil center and corneal reflections. *IEEE Transactions on Biomedical Engineering*, *53*(6), 1124–33. http://doi.org/10.1109/TBME.2005.863952.

Hessels, R. S., Cornelissen, T. H. W., Kemner, C., & Hooge, I. T. C. (2014). Qualitative tests of remote eyetracker recovery and performance during head rotation. *Behavior Research Methods*. http://doi.org/10.3758/s13428-014-0507-6.

Holmqvist, K., Nyström, M., Andersson, R., Dewhurst, R., Jarodzka, H., & Van de Weijer, J. (2011). *Eye Tracking: A comprehensive guide to methods and measures*. OXFORD University.

Holmqvist, K., Nyström, M., & Mulvey, F. (2012). Eye tracker data quality: what it is and how to measure it. In *ETRA '2012 Proceedings of the Symposium on Eye Tracking Research and Applications* (pp. 45–52).

Mirelman, A., Maidan, I., Herman, T., Deutsch, J. E., Giladi, N., & Hausdorff, J. M. (2011). Virtual reality for gait training: Can it induce motor learning to enhance complex walking and reduce fall risk in patients with Parkinson's disease? *Journals of Gerontology - Series A Biological Sciences and Medical Sciences*, *66 A*(2), 234–240. http://doi.org/10.1093/ gerona/glq201.

Mirelman, A., Rochester, L., Maidan, I., Din, S. Del, Alcock, L., Nieuwhof, F., Rikkert, M. O., Bloem, B. R., Pelosin, E., Avanzino, L., Abbruzzese, G., Dockx, K., Bekkers, E., Giladi, N., Nieuwboer, A., and Hausdorff, J. M., (2006). Addition of a non-immersive virtual reality component to treadmill training to reduce fall risk in older adults (V-TIME): a randomised controlled trial. *The Lancet*, *0*(0), 807–824. http://doi.org/10.1016/s0140-6736(16)31325-3.

Mirelman, A., Rochester, L., Reelick, M., Nieuwhof, F., Pelosin, E., Abbruzzese, G., Dockx, K., Nieuwboer, A., and Hausdorff, J. M. (2013). V-TIME: a treadmill training program augmented by virtual reality to decrease fall risk in older adults: study design of a randomized controlled trial. *BMC Neurology*, *13*(1), 15. http://doi.org/10.1186/1471-2377-13-15.

Morgante, J. D., Zolfaghari, R., & Johnson, S. P. (2012). A critical test of temporal and spatial accuracy of the Tobii T60XL eye tracker. *Infancy*, *17*(1), 9–32. http://doi.org/10.1111/j.1532-7078.2011.00089.x

Morimoto, C. H., & Mimica, M. R. M. (2005). Eye gaze tracking techniques for interactive applications. *Computer Vision and Image Understanding*, *98*, 4–24. http://doi.org/10.1016/j.cviu.2004.07.010.

Niehorster, D. C., Cornelissen, T. H., Holmqvist, K., Hooge, I. T., & Hessels, R. S. (2017). What to expect from your remote eye-tracker when participants are unrestrained. Behavior Research Methods, 1-15.

Patla, A. E. (1997). Understanding the roles of vision in the control of human locomotion. *Gait & Posture*, *5*(1), 54–69. http://doi.org/10.1016/S0966-6362(96)01109-5.

Peruzzi, A., Cereatti, A., Della Croce, U., & Mirelman, A. (2016). Effects of a virtual reality and treadmill training on gait of subjects with multiple sclerosis: a pilot study. *Multiple Sclerosis and Related Disorders*, *5* (NOVEMBER), 91–96. http://doi.org/10.1016/j.msard.2015.11.002.

Peruzzi, A., Cereatti, A., Mirelman, A., & Della Croce, U. (2013). Feasibility and Acceptance of a Virtual Reality System for Gait Training of Individuals with Multiple Sclerosis. *European International Journal of Science and Technology*, *2*(6), 171–181.

Reed-Jones, R. J., Dorgo, S., Hitchings, M. K., & Bader, J. O. (2012). Vision and agility training in community dwelling older adults: Incorporating visual training into programs for fall prevention. *Gait & Posture*, *35*(4), 585–589. http://doi.org/10.1016/j.gaitpost.2011.11.029.

Reed-Jones, R. J., Solis, G. R., Lawson, K. a., Loya, A. M., Cude-Islas, D., & Berger, C. S. (2013). Vision and falls: A multidisciplinary review of the contributions of visual impairment to falls among older adults. *Maturitas*, *75*(1), 22–28. http://doi.org/10.1016/j.maturitas.2013.01.019.

Stanley, J., & Hollands, M. A. (2014). A novel video-based paradigm to study the mechanisms

underlying age- and falls risk-related differences in gaze behaviour during walking. *Ophthalmic & Physiological Optics*, *34*(4), 459–69. http://doi.org/10.1111/opo.12137.

Tobii Technology. (2011). *Accuracy and precision test method for remote eye trackers*. *Technology*.

Tobii Technology AB. (2004). Tobii TX300 Eye Tracker User MAnual. *Technology*.

Tobii Technology AB. (2012). *Accuracy and precision Test report TX300 fw 1.0.7 RC*.

Tobii Technology AB. (2012). *Stim Tracker for Tobii TX300 Eye Tracker Product Description User Guide*.

Tobii Technology AB. (2012). *User Manual — Tobii Studio* (Ver 3.2).

Vicon Motion Systems. (2011). *Go Further with Vicon MX T-Series*.

Wass, S. V., Forssman, L., & Leppänen, J. (2014). Robustness and precision: How data quality may influence key dependent variables in infant eye-tracker analyses. *Infancy*, *19*(5), 427–460. http://doi.org/10.1111/infa.12055.

Weigle, C., & Banks, D. C. (2008). Analysis of eye-tracking experiments performed on a Tobii T60. *Proceedings of SPIE*, *6809*, 680903-680903–12. http://doi.org/10.1117/12.768424.

Young, W. R., & Hollands, M. A. (2010). Can telling older adults where to look reduce falls? Evidence for a causal link between inappropriate visual sampling and suboptimal stepping performance. *Experimental Brain Research*, *204*(1), 103–113. http://doi.org/10.1007/s00221-010-2300-9.

Chapter 3

The effects of visual distractors on vision and gait strategies during obstacle negotiation: assessment in a virtual reality environment

---

***** This chapter is based on

Serchi V., Cereatti A., Cinelli M.E., and Della Croce U., "**Assessment of the distractors effect on vision and gait strategies during obstacle crossing: a virtual reality assessment.**" *In preparation.*

Serchi V., Cereatti A., Cinelli M.E., and Della Croce U., "**Gaze strategies while negotiating obstacles in a virtual environment with distractors.**" *Gait & Posture* 42 (2015): S3.

Serchi V., Cereatti A., Della Croce U., Cinelli M.E., "**Gaze strategies during obstacle negotiation in presence of distractors: a virtual reality assessment of young and older adult populations.**" *Proceedings 12th annual Ontario Biomechanics Conference (OBC)*, Alliston, Canada (ON), March 2015.

Introduction

The environment navigation is a complex task during which the sensory input from the surroundings is crucial in order to safely plan the next locomotion actions. Vision is important to gather the information from the environment (*visual sampling*, (Patla, 1997)). When facing a complex travel path, fixations are made toward the regions at maximal informative content in a sequential online manner to guarantee stability to unexpected changes in the terrain in a number reflecting the condition of the terrain (Marigold & Patla, 2007; Patla et al., 1996). Gait accuracy when facing constrains and challenging in the travel path is visually influenced and that is more evident in the elderly population (Chapman & Hollands, 2006, 2007, 2010). During the locomotor task, obstacles could challenge the safety and expose to the risk of loss of balance. The avoidance of expected obstacles on smooth grounds is usually planned in the steps before (*obstacle sampling*) the crossing (~ three steps) often without fixating the obstacle while stepping over it (*travel gaze*) (Patla, 1997; Patla & Vickers, 2003). The visual attention is important in order to cross in a safe manner the obstacles in the travel path but distractors are frequent in the everyday life and potentially challenge the attention already allocated to the locomotor task. The increase of the cognitive load has a worsening effect on the motor performances of the older adults (Harley, Wilkie, & Wann, 2009). The elderly appear to rely on the visual feedback provided by the scene and by the environment and their motor performance is affected by the visual information they can gather more than their younger counterpart (Cheng, Yang, Holloway, & Tyler, 2016; Franz, Francis, Allen, O'Connor, & Thelen, 2015). Recent researches aimed at investigating the effect of visuo-attentional distractors on the motor performance over obstacles (Lo & Chou, 2015; Lo, van Donkelaar, & Chou, 2015, Brown, McKenzie, & Doan, 2005). Young adults show a reduced toe-off clearance when visuo-spatial distractors are presented prior the negotiation of the obstacle (Lo et al., 2015), while preparing the negotiation is highly demanding for the elderly (Brown, McKenzie, & Doan, 2005). During other motor tasks, both young and older adults show a correlation between the visuo-motor performances and the ability to suppress the distractors; specifically the elderly show a deficit in the suppression of the distractors (Mevorach, Spaniol, Soden, & Galea, 2016). The elderly are more prone to allocate their attention on factors different from the task (Healey, Campbell, & Hasher, 2008) together with a lack in the coordination between the environment navigation and a visually demanding

task (Beurskens & Bock, 2012, 2013). This suggests that, in complex tasks as the one of avoiding obstacles, if distractors are present, the elderly could show visuo-motor patterns different and possibly worse than younger adults. Therefore understanding better the relationships between the visuo-spatial attention distraction and the motor performances during obstacle crossing is important to better address the rehabilitation intervention on the gait of the elderly. The primary aim of this work is to assess such relationship through a paradigm used in recent rehabilitation programs for the enhancement of gait (Mirelman et al., 2006). Therefore, the general purpose of the current work is to analyze the visuo-motor performances of both young and older adults during a virtual reality based navigation challenging obstacles crossing and visual distractors. The hypothesis is that the young and older adults would show a decrease in the obstacle negotiation task motor performance with the presence of distractors and that such a worsening would be more evident in the elderly also looking at their visual behavior. As secondary aim this study wants to highlight the potentiality of such an experimental set-up for the combined training and/or analysis of the gait and of the gaze.

Materials and Methods

Participants

Seven healthy young adults (females, age: 23±2.6 y.o.) and five healthy older adults (females, age: 67±1.7 y.o.) participated in the study. Young adults were recruited from the undergraduate program in Kinesiology at the Wilfrid Laurier University (Ontario, Canada). The older adults were recruited from a fitness program for older adults. They were in excellent health and without motor or cognitive impairments. They had normal or corrected to normal (contact lenses) sight. For each participant the visual acuity was measured in 20/100 through a standard Snellen Chart. The participants had to stand upright 20 feet from the visual acuity board and had to read loud the letters displayed with one eye at the time. The visual acuity was tested in the condition in which the test was performed (*i.e.* those subjects wearing contact lenses during the acquisition protocol had to wear them also during the visual acuity test). The visual acuity scores of the young and older adult participants are reported in Table 3.1. This study was approved by the Laurier Ethics Board (REB 4396&2399). The recruitment was performed through approved fliers (Annex 4), e-mails and phone-calls. As advertised, the older adults received a 5 $/hour compensations to take

part to the study. Prior to take part to the study the participants were thoroughly informed about the upcoming task and if agreed with the experimental protocol had to sign an inform consent (Annex 5).

Table 3.1 Characteristics of the subjects participating to the study: age, ethnicity, color of the eyes, visual acuity for the left and the right eyes and if they used contact lenses during the study.

Subject's ID	Age	Ethnicity	Eyes color	Visual acuity		Lenses
				Left eye	*Right eye*	
SBJ1	69	Caucasian	Brown	20/100	20/20	Yes
SBJ2	69	Caucasian	Brown	20/30	20/50	No
SBJ3	65	Caucasian	Brown	20/25	20/15	No
SBJ4	67	Caucasian	Blue	20/30	20/40	No
SBJ5	68	Caucasian	Brown	20/30	20/30	No
SBJ6	26	Caucasian	Blue	20/20	20/20	No
SBJ7	22	Caucasian	Brown	20/16	20/20	No
SBJ8	23	Caucasian	Blue	20/20	20/20	No
SBJ9	23	Caucasian	Green	20/16	20/12.5	No
SBJ10	27	Asian	Brown	20/30	20/30	No
SBJ11	19	African	Brown	20/16	20/25	No
SBJ12	23	Asian	Brown	20/25	20/25	Yes

Experimental set-up

The experimental set-up was composed by a treadmill, an active optoelectronic system (OptoTrak Certus, NDI; 120 Hz), a projector projecting a virtual reality (VR) environment onto a blank surface (3×3 m) positioned three meters away, and a wearable eye-tracker (ET7, Applied Science Laboratories; 120 Hz). The treadmill was placed in the center of the capture volume of the stereo-photogrammetric system (3 blocks of cameras). The treadmill was put facing the blank surface onto which the VR environment was projected (Figure 3.1).

The VR environment was purposely devised for this study (WorldViz Vizard 5.0 Enterprise). The VR environment consisted in a tree-lined country road and three main elements: avatar shoes, obstacles and distractors (Figure 3.2). The avatar shoes were virtual shoes representing the position and the motion of the subjects' feet within the virtual scene. The obstacles were tree logs lying across the walking path. The distractors were avatar deers appearing on the left or on the right side of the road and then crossing it to reach the opposite side.

Figure 3.1 Representation of the experimental set-up adopted for this study: 1) 3 blocks of optoelectronics cameras, 2) a treadmill, 3) a wearable eye-tracker and 4) a blank surface onto which a projected virtual reality was projected. The treadmill had lateral bars to which the subject was allowed to hold.

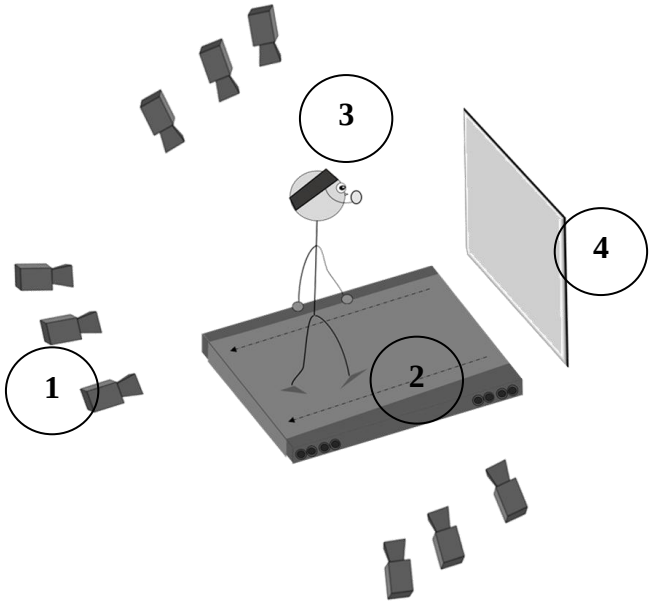

Figure 3.2 Screen shot of a scene of the virtual reality-based task. All of the elements of the task are shown: 1) avatar shoes, 2) tree log -obstacle- and 3) crossing deer -distractor-.

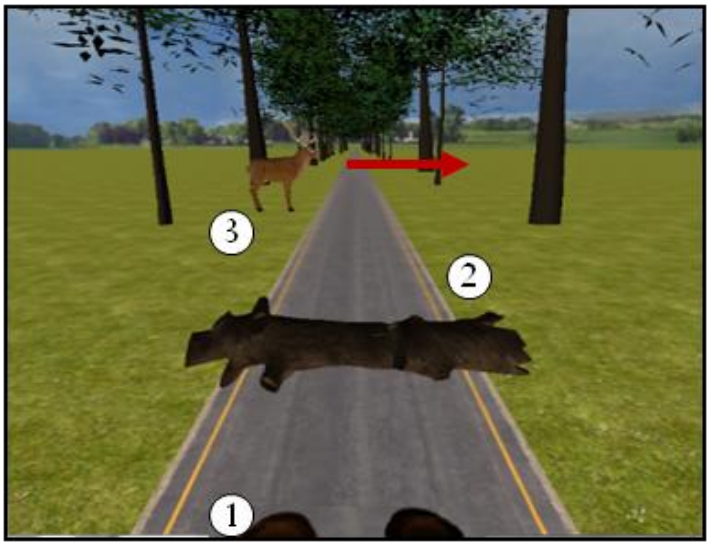

The distractors appearance and animation was timed according to the distance of the feet from the obstacle. The distractors appeared in the scene when the subject was 5 steps away from the obstacle (1 step= ~75 cm) and their animation was triggered when the participant was at 4, 3, 2 or 1 steps far from the obstacle.

The avatar shoes had a double purpose. The avatar shoes moved as the feet of the subject moved in the laboratory and were used both to tune the translation of the virtual reality toward the subject (stop of the motion of the virtual scene if the subject stopped) and to onset a negative feedback in the case of a collision between the shoe and the obstacle. The feedback was a sudden change of the point of view of the subject in the visual scene, suggesting a fall. The VR environment was guided by the stereo-photogrammetric system signal to simulate the subject moving in the virtual world according to his/her real motion in the laboratory (WorldViz LLC).

In order to track the limb kinematics, the participants were instrumented with clusters of markers placed on the head, upper and lower trunk, and on the feet (Northen Digital, 2010). Single markers were placed directly on the left and right greater trochanters, left and right lateral epicondyles and left and right malleoli to compute the joint kinematics in the sagittal plan (Figure 3.3).

The stereo-photogrammetric system was integrated with the wearable eye-tracker system to compute the point of gaze (*PoG*) of the subject relative to a calibrated plane (Applied Science Laboratories, 2014a; Northen Digital, 2010) (EyeHead integration procedure). During the EyeHead integration procedure the eye-tracker system was connected to the stereo-photogrammetric one via Ethernet. The systems were set in communication by pointing out the coordinates of three non collinear points lying on the blank 3x3 m surface through a wand provided by the stereo-photogrammetric manufacturer (points 9, 7, and 1, Figure 3.4). Once the eye-tracker system had the information of these three points, it was possible to define the frame of reference of the calibration plane and therefore to refer the gaze to that plane. The calibration plane was defined through a purposely built nine-points calibration grid placed on the projection surface with the centre set to be coinciding with the centre of projection screen (Applied Science Laboratories, 2014b).

Figure 3.3 Representation of the marker-set adopted for this study. In blue the clusters of markers placed on the head, upper and lower trunk, and on the back part of the feet are reported, whereas the single markers placed directly on the left and right greater trochanters, left and right lateral epicondyles and left and right malleoli are reported in green. In red is reported the position of the virtual markers digitized with respect to the clusters of markers and then reconstructed in post-processing: left and right ears, left and right shoulders, T10, left and right ASIS and PSIS, left and right 1st and 5th metatarsals and heels.

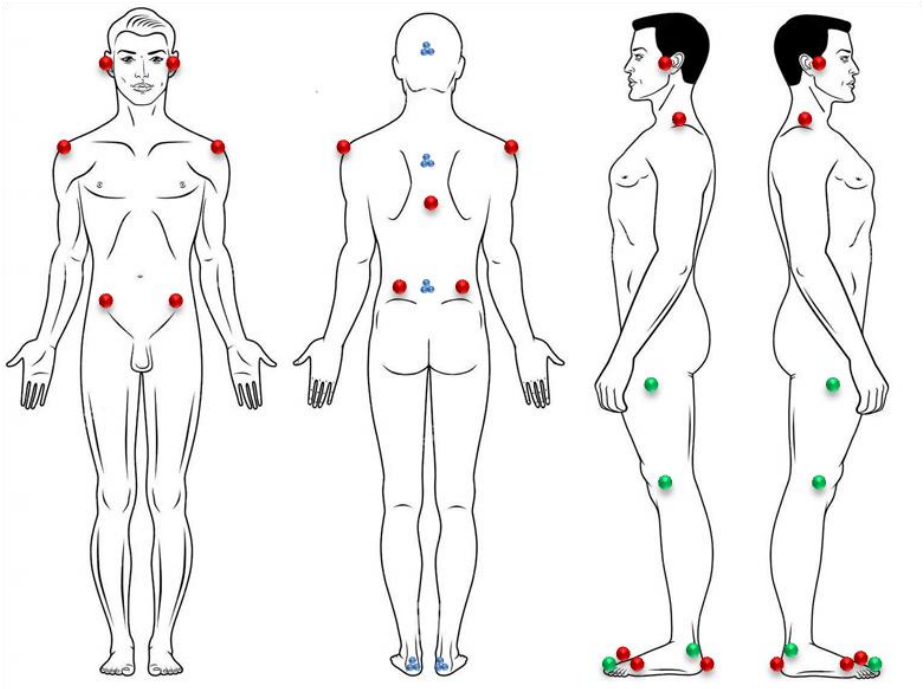

According to the EyeHead integration procedure the frames of reference of the stereo-photogrammetric and of the eye-tracker systems were set reciprocally parallel. The stereo-photogrammetric system frame of reference had the x-axis (anterior-posterior –AP– direction) parallel to the ground and pointing accordingly to the direction of progression, the z-axis (vertical –V– direction) perpendicular to the ground and pointing down and the y-axis (medio-lateral –ML– direction) perpendicular to the xz plane and pointing toward the right (Laboratories Applied Science, 2014). The origin of the stereo-photogrammetric system frame of reference was set on the treadmill, on a position coinciding with the resting upright standing position for the AP and

ML directions (in between the treadmill bars). The eye-tracker frame of reference had its origin at the centre of the calibration grid (Figure 3.4).

Figure 3.4 Schematic representation of the experimental set-up with the detail of the position and orientation of the technical reference frames of the optoelectronic system and of the wearable eye-tracker system. The stereo-photogrammetric system reference frame had the x-axis (anterior-posterior –AP– direction) parallel to the ground and pointing accordingly to the direction of progression, the z-axis (vertical –V– direction) perpendicular to the ground and pointing down and the y-axis (medio-lateral –ML– direction) perpendicular to the xz plane and pointing toward the right. The eye-tracker reference frame had its origin coinciding with the centre of the calibration grid and was parallel to the stereo-photogrammetric system reference frame.

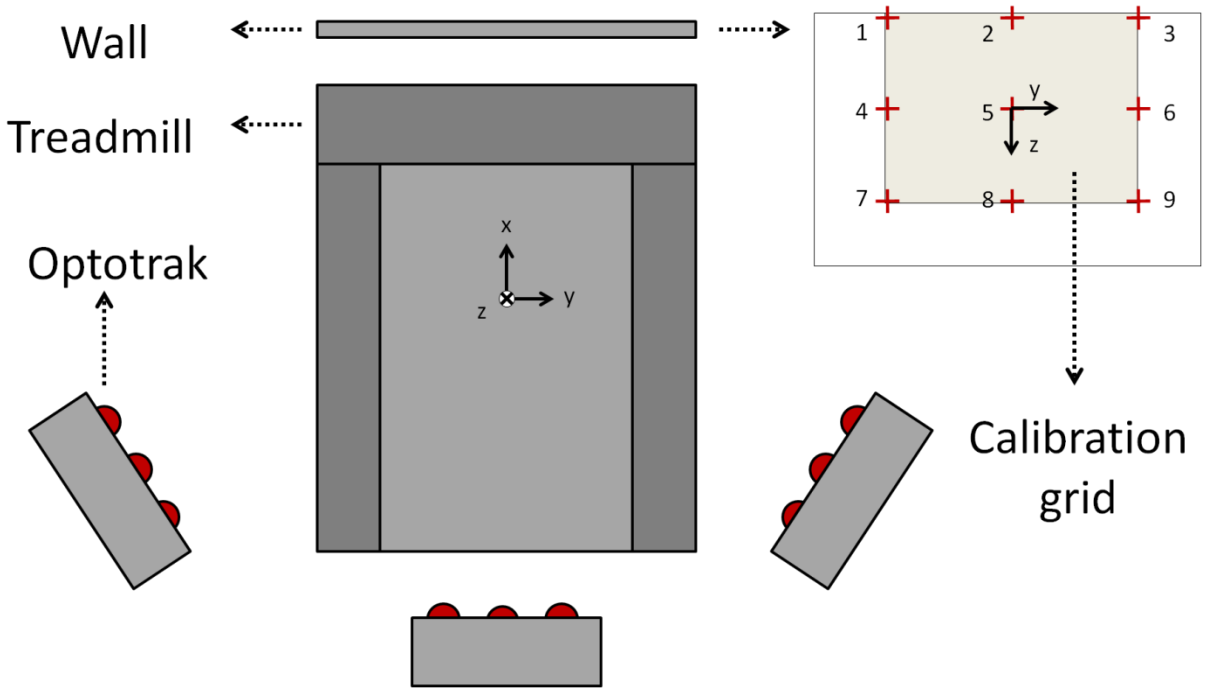

Experimental protocol

First, an anatomical calibration of the bony landmarks relatively to the position of the clusters of markers was performed: left and right ears, left and right shoulders, T10, left and right ASIS and PSIS, left and right 1st and 5th metatarsals and heels (Figure 3.3). The subject had to stand upright in the center of the acquisition volume of the stereo-photogrammetric system looking

towards the screen. The operator pointed out the body landmarks with the stereo-photogrammetric system wand and linked them to the cluster of markers. A static data collection was performed prior the start of the experimental protocol.

The *PoG* was then calibrated over the calibration grid with the subject upright standing on the treadmill. The subject had to look at each point of the screen and in the meanwhile the operator had to click over the same spot over the scene camera image. The calibration was then validated over the calibration grid and repeated if necessary. The accuracy and precision of the *PoG* measurements over the calibration grid was recorded to be used in the data processing.

During the entire acquisition protocol, the subject had to walk on the treadmill while navigating the VR environment. The VR environment was moving constantly toward the subjects in according to the motion of the markers placed on the feet of the participants (Figure 3.3). In this way the motion of the VR world occurred only if the motion of the feet of the subjects was detected. The translation speed of the VR scene was set at a subject-specific a priori chosen comfortable speed. Before the start of the acquisition protocol the subject was made walking on the treadmill and the speed was adjusted until an optimal comfortable speed was reached.

In this study a trial was defined as the elapse of time starting with the entrance of one obstacle in the scene and ending with the disappearance of the same obstacle.

Acquisition protocol

The acquisition protocol involved a training and evaluation session.

The training session consisted of 20 trials during which the participant was presented with the avatar shoes and with no distractors. The subject was instructed on how to successfully negotiate the obstacles being aware of a second experimental session during which the avatar shoes would not be available anymore.

In the evaluation session, the participant had to step over the obstacles with no avatar shoes. The transparency of the avatar shoes was set to the highest level in order to avoid any distraction from the motion of the avatar shoes on the visual behavior of the subjects. Nevertheless, the motion of the subject within the virtual scene was the same as in the training condition. On a subset of the trials of the evaluation session the subject was presented with visual distractors trying to challenge his/her performance. The same amount of distractors with a starting position

on the left side of the road and on the right side of the road was proposed. The evaluation session presented 48 trials (24 distractors and 24 control trials).

The recording of the stereo-photogrammetric, eye-tracker and VR systems were started by two different operators through a countdown.

The entire acquisition protocol lasted about ten minutes. Between the two experimental sessions the calibration of the gaze was checked and repeated if necessary. Between the two experimental sessions, the participant could rest if necessary.

Data analysis

Pre-processing

The kinematics and the visual behavior data were imported and processed in Matlab (The MathWorks Inc., Natick, MA, USA). The synchronization of the recordings of the eye-tracker, the stereo-photogrammetric system and the timestamp of the VR was performed manually through the alignment of the markers of the head coordinates streamed from the stereo-photogrammetric system to the eye-tracker and the VR systems (Figure 3.5).

Kinematics

Digital markers were reconstructed by mean of the information gathered through the original anatomical calibration (Cappello, Cappozzo, La Palombara, Lucchetti, & Leardini, 1997). Prior the computation of the relevant spatio-temporal parameters, the kinematics data were filtered through a zero-phase second order Butterworth filter ($\omega_n = 0.12$) (Roithner R. Schwameder, 2000).

Gaze

The gaze data was de-blinked (pupil diameter equal to zero) and filtered through a simple velocity filter. A velocity over 1000 deg/s was considered as not compatible with physiological eye movements and therefore the relative frames were discarded from the signal (Holmqvist et al., 2011). The missing parts of the gaze signal were linearly interpolated. Missing values instances lasting more than 40 ms were flagged and discarded from the analysis.

Figure 3.5 Representation of the steps followed in order to align the signals gathered from the stereo-photogrammetric system (NDI), the eye-tracker (ASL) and the VR (VZRD) systems. The head coordinates were streamed from the stereo-photogrammetric system to the other two systems. Therefore the same signal was saved in the output of the three systems with a different time-stamp proper of the specific device. The operator pointed out a point for each signal (a) and computed a delay factor to be used in order to align the time-stamp of the three systems (b) and therefore to get a synchronization between the recordings.

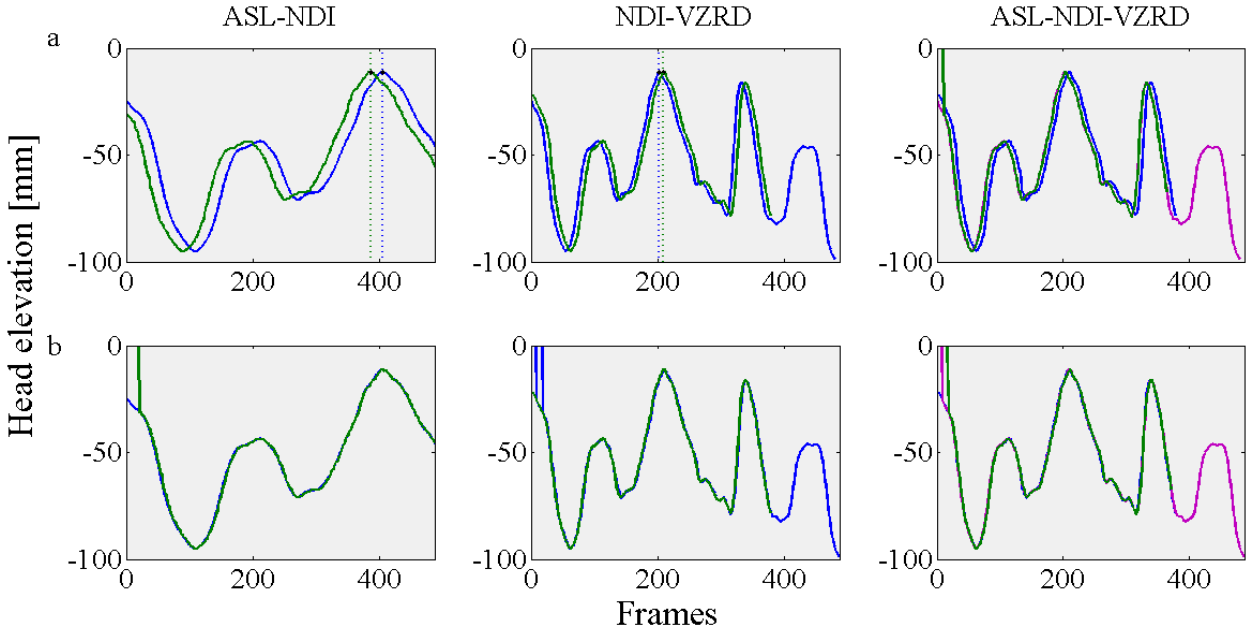

Data processing

Kinematics

The head, upper trunk and pelvis frames of reference were defined (Cappozzo, Catani, Della Croce, & Leardini, 1995). The head, upper trunk and pelvis rotations and translations were then computed with respect to the static frames of reference.

The angles of the joints were computed:

a) The left and right hip flexion-extention angle was computed as the angle between the projection of the vector lying on the thigh in the frontal plan of the pelvis frame of reference and the vertical axis of the pelvis.

b) The left and right hip ab-/adduction angle was computed as the angle between the projection of the vector lying on the thigh in the sagittal plan of the pelvis frame of reference and the vertical axis of the pelvis.

c) The left and right knee flexion-extention angle was computed as the angle between the vector lying on the thigh and the vector lying on the tibia.

d) The left and right ankle plantar-dorsiflexion angle was computed as the angle between the long axis of the feet and the vector lying on the tibia.

For each trial of the evaluation session, toe-offs and heel-strikes events were detected through a velocity-based algorithm validated for treadmill walking (Zeni, Richards, & Higginson, 2008). The gait was then segmented into steps and strides.

The leading foot was defined as the foot with the maximum AP coordinate at the time of the obstacle passing. For the leading foot the obstacle clearance (*CL*) of the foot over the obstacle and delay of the maximum V peak with respect to the clearance index (ΔP) were computed. A description of the computation of the previously reported parameters is reported:

1. The clearance index (CL_i) was identified as the time with the minimum vertical heel-obstacle distance when the obstacle and the foot had the same AP coordinates (Figure 3.6-a).

2. The maximum peak index (P_i) was identified as the time with the maximum V heel coordinates in the obstacle crossing step cycle (Figure 3.6-b).

3. The obstacle clearance (CL) was defined as the V heel-obstacle distance at CL_i.

4. The delay of the maximum peak (ΔP) was defined as the absolute value of the difference between CL_i and P_i.

Figure 3.6 A schematic representation of the steps followed to compute the CL and ΔP parameters. In black the trailing (dotted) and leading (solid) feet AP (a) and V (b) coordinates are reported, along with the AP and V coordinates of the obstacle (red) in the virtual scene. The toe-offs (TO) and heel-strikes (HS) of the leading foot are reported. The leading foot was the more advanced foot in the AP direction during the obstacle crossing. The clearance index (CL_i) was identified as the time with the minimum vertical heel-obstacle distance when the obstacle and the foot had the same AP coordinates (a). The maximum peak index (P_i) of the leading foot was identified as the time with the maximum heel V coordinates during the obstacle crossing (a). Afterwards the obstacle clearance (CL) was defined as the V heel-obstacle distance at CL_i and the delay of the maximum peak (ΔP) was defined as the absolute value of the difference between CL_i and P_i (b).

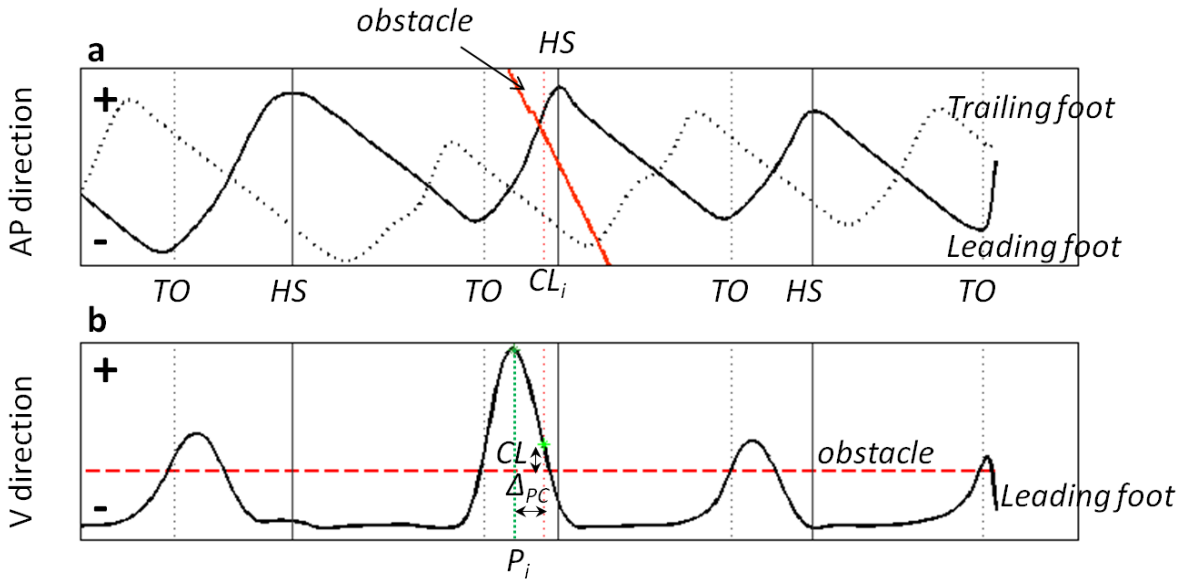

The unsuccessful rate was computed as the number of the unsuccessful trials over the total number of trials for each condition of the evaluation session. The total unsuccessful rate for the trials with distractors was also computed.

Gaze

Region of interests were drawn around the positions of the obstacles and distractors on the screen accordingly to the accuracy and precision of the measurements of the eye-tracker (Holmqvist et al., 2011; Serchi, Peruzzi, Cereatti, & Della Croce, 2016; Stuart, Lord, Hill, & Rochester, 2016). A margin equal to the sum of the precision and the accuracy values was added to the size of the elements on the 2D scene (Holmqvist et al., 2011). A gaze hit was assigned to a region of interest if the coordinates of the gaze were within the defined region of interest. If the regions of interest overlapped, the distance between the gaze coordinate and the center of the areas of interest was computed and the hit of the gaze was assigned to the region of interest having the closest center. For both the obstacle and the distractor, a cognitive delay of 80 ms with respect to their appearance was considered. Moreover, *PoG* hitting instances less than 150 ms were considered as not cognitively relevant and discarded (Holmqvist et al., 2011) (Figure 3.7).

Figure 3.7 Example of the *PoG* hit assignment to the regions of interest defined around the obstacle and the distractor during a trial. The horizontal (dotted lines) and vertical (solid line) coordinates of the gaze (blue), obstacle (green) and distractor (yellow) with respect to the calibration grid frame of reference are reported. The assignment of the *PoG* to the regions of interest of the obstacle and of the distractor is reported in black and in red respectively.

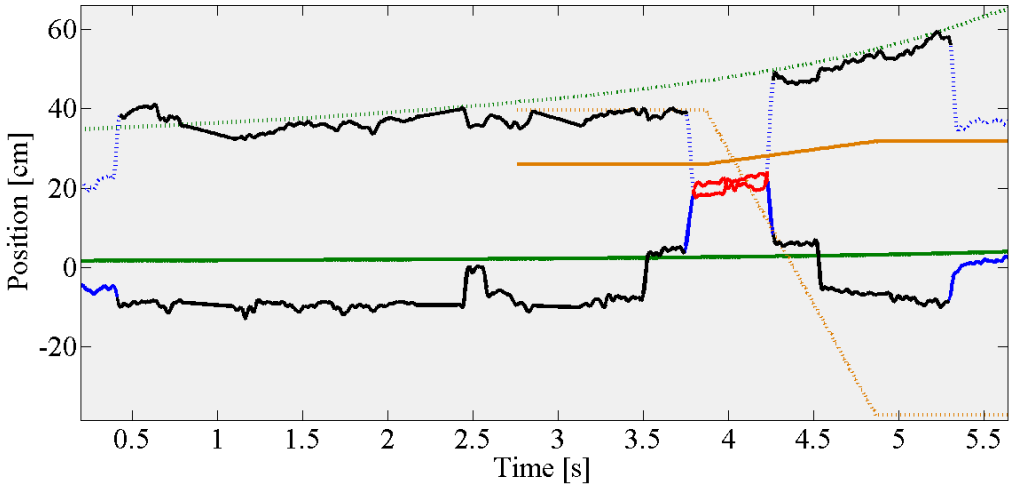

The *PoG* hit percentage over the obstacle region of interest was assessed over the total obstacle presentation time. The horizontal and vertical variability of the gaze over the screen was computed as the standard deviation of the y-, z- coordinates of the *PoG* on the screen during the obstacle presentation time.

Statistical analysis

For both the younger and older adults, a statistical analysis was performed aiming at:

a. Assessing the effect of the distractors on the kinematics parameters with respect to the trials with no distractors: on the failure rate of the task, on the *CL* and on the ΔP parameters. The hypothesis was that the presence of the distractors would affect the motor performance in terms of an increase in the failure rate of the task, a decrease in the value of the *CL* and an increase in the value of the ΔP with respect to the trials with no distractors.

b. Assessing the effect of the distractors on the gaze parameters with respect to the trials with no distractors: on the percentage of the *PoG* hitting the obstacle, and on the horizontal and vertical variability of the *PoG* on the calibrated plane. The hypothesis was that the distractors would decrease the *PoG* hit over the obstacle and in the meanwhile would decrease the vertical variability of the *PoG* and increase the horizontal variability of the *PoG* on the calibrated plane. The three analyses were performed because on one side the obstacle hit gives us information on how much the subject is following the obstacle in the scene. On the other hand the detailed information on the visual span of the screen could highlight different strategies in the visual behavior of the subject potentially pointing out an allocation of the attention at points of stimulus different from those fixated.

To compare the performances of the two groups with and with no distractors in the scene, a statistical analysis was performed aiming at:

a. Assessing the differences of the tested groups for the trial with distractors and with no distractors in terms of the kinematics parameters. The older adults were hypothesized to have a generally worse performance than the young adults (higher global failure rate) and specifically in the presence of distractors (higher failure rate with distractors). Moreover we hypothesized smaller values of *CL* and ΔP parameter for the older adults than the young

adults with distractors in the scene.

b. Assessing the differences of the tested groups for the trial with distractors and with no distractors in terms of the gaze parameters. The older adults were hypothesized to have a generally different visual exploration strategy with respect to their younger counterpart. In the specific we hypothesized that they would fixate more than the young adults the obstacle and that, in the presence of distractors, they would have a greater variability of the horizontal *PoG* and a decreased vertical variability of the *PoG*.

Data were investigated for normality and then analyzed trough a Wilcoxon-two-sample-test procedures for non parametric distribution (SAS University edition, α=0.05).

Results

An example of computation of the kinematics (trunk and pelvis V, AP and ML rotations, hip ab-adduction and flexion-extention angles, knees flexion-extention angles and ankles plantar-dorsiflexion angles) for a successful and an unsuccessful trial for one old and one young adult is reported in Figure 3.8 - 3.11. In the same figure the heel elevation and the hit of the *PoG* over the regions of interest of the obstacle and of the distractor are reported.

Figure 3.8 Kinematics and visual behavior output computation for a successful trial performed by one of the participant belonging to the young adults group. From the top to the bottom the trunk and pelvis rotation angles (AP: black; ML: gray and V: red), the left (green) and right (blue) angles of the joints (hip flexion-extention, hip ab-adduction, knee flexion-extention and ankle plantar-dorsiflexion), the elevation of the left (green) and right (blue) heels and the *PoG* hit over the areas of interest defined in the scene are reported. The vertical lines stand for the left (green) and right (blue) heel-strikes (plain line) and toe-offs (dotted lines). A vertical dashed line is reported in correspondence to the clearance time stamp of the leading foot (the color of the line corresponds to the leading foot side). Green and red stars are reported over the signal if at the specific time of the trial the heel quote was above or under the height of the obstacle. The *PoG* hit is reported in blue if no assignment occurred, in black if the assignment of the hit was for the obstacle area of interest and in red if it was for the distractor area of interest.

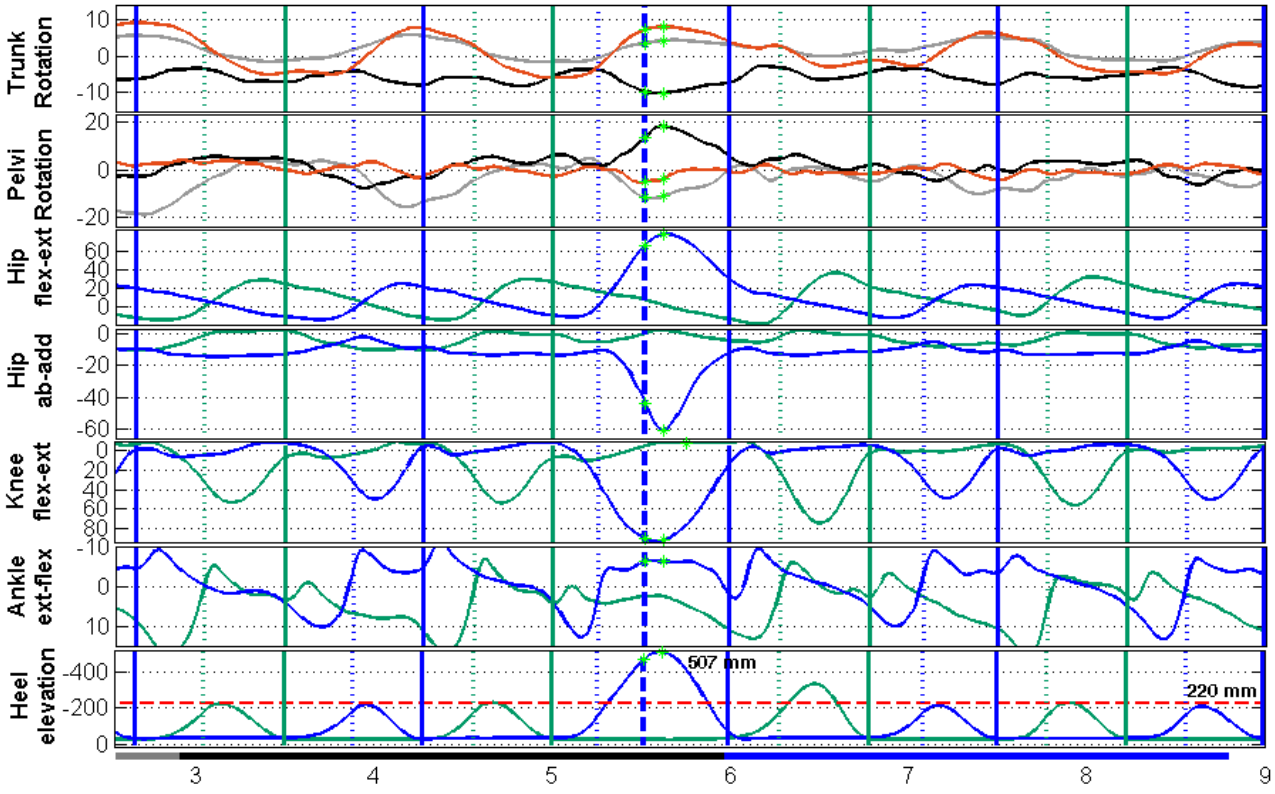

Figure 3.9 Kinematics and visual behavior output computation for an unsuccessful trial performed by one of the participant belonging to the young adults group. From the top to the bottom the trunk and pelvis rotation angles (AP: black; ML: gray and V: red), the left (green) and right (blue) angles of the joints (hip flexion-extention, hip ab-adduction, knee flexion-extention and ankle plantar-dorsiflexion), the elevation of the left (green) and right (blue) heels and the *PoG* hit over the areas of interest defined in the scene are reported. The vertical lines stand for the left (green) and right (blue) heel-strikes (plain line) and toe-offs (dotted lines). A vertical dashed line is reported in correspondence to the clearance time stamp of the leading foot (the color of the line corresponds to the leading foot side). Green and red stars are reported over the signal if at the specific time of the trial the heel quote was above or under the height of the obstacle. The *PoG* hit is reported in blue if no assignment occurred, in black if the assignment of the hit was for the obstacle area of interest and in red if it was for the distractor area of interest.

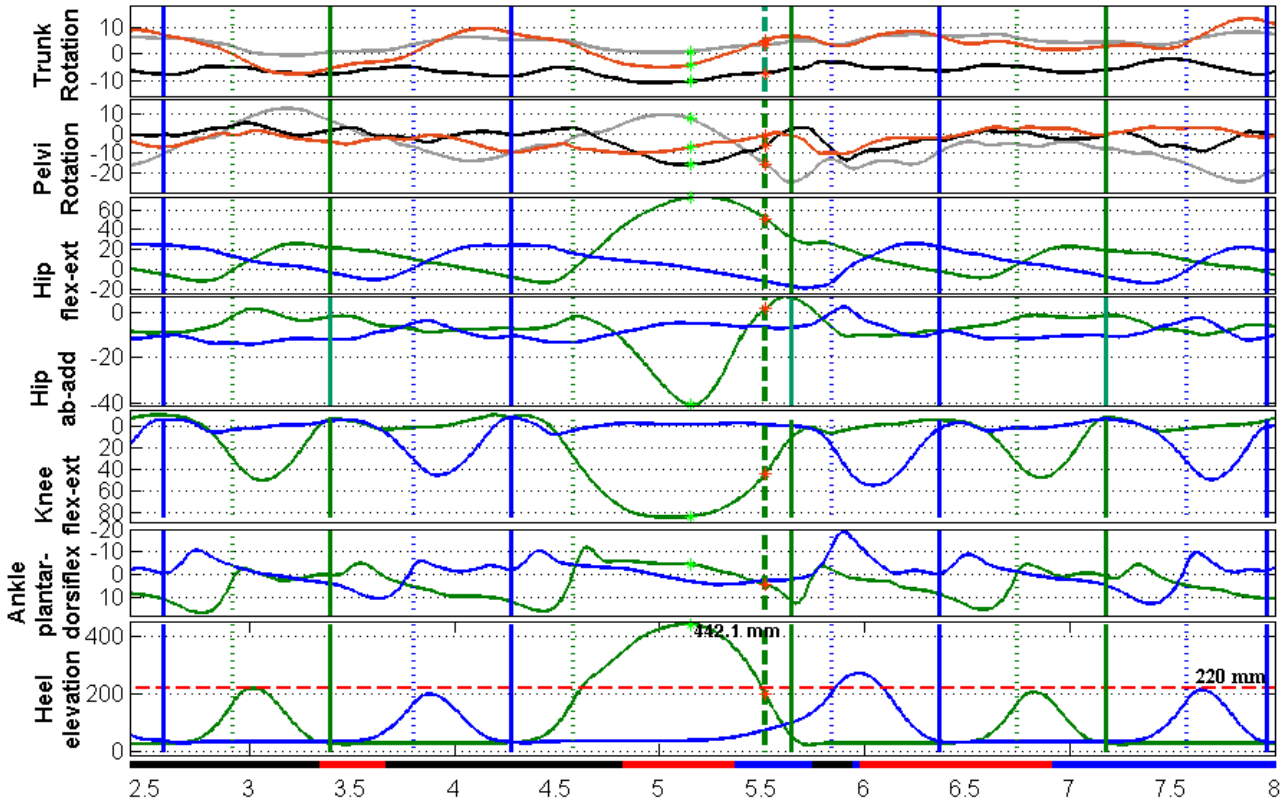

Figure 3.10 Kinematics and visual behavior output computation for a successful trial performed by one of the participant belonging to the older adults group. From the top to the bottom the trunk and pelvis rotation angles (AP: black; ML: gray and V: red), the left (green) and right (blue) angles of the joints (hip flexion-extention, hip ab-adduction, knee flexion-extention and ankle plantar-dorsiflexion), the elevation of the left (green) and right (blue) heels and the *PoG* hit over the areas of interest defined in the scene are reported. The vertical lines stand for the left (green) and right (blue) heel-strikes (plain line) and toe-offs (dotted lines). A vertical dashed line is reported in correspondence to the clearance time stamp of the leading foot (the color of the line corresponds to the leading foot side). Green and red stars are reported over the signal if at the specific time of the trial the heel quote was above or under the height of the obstacle. The *PoG* hit is reported in blue if no assignment occurred, in black if the assignment of the hit was for the obstacle area of interest and in red if it was for the distractor area of interest.

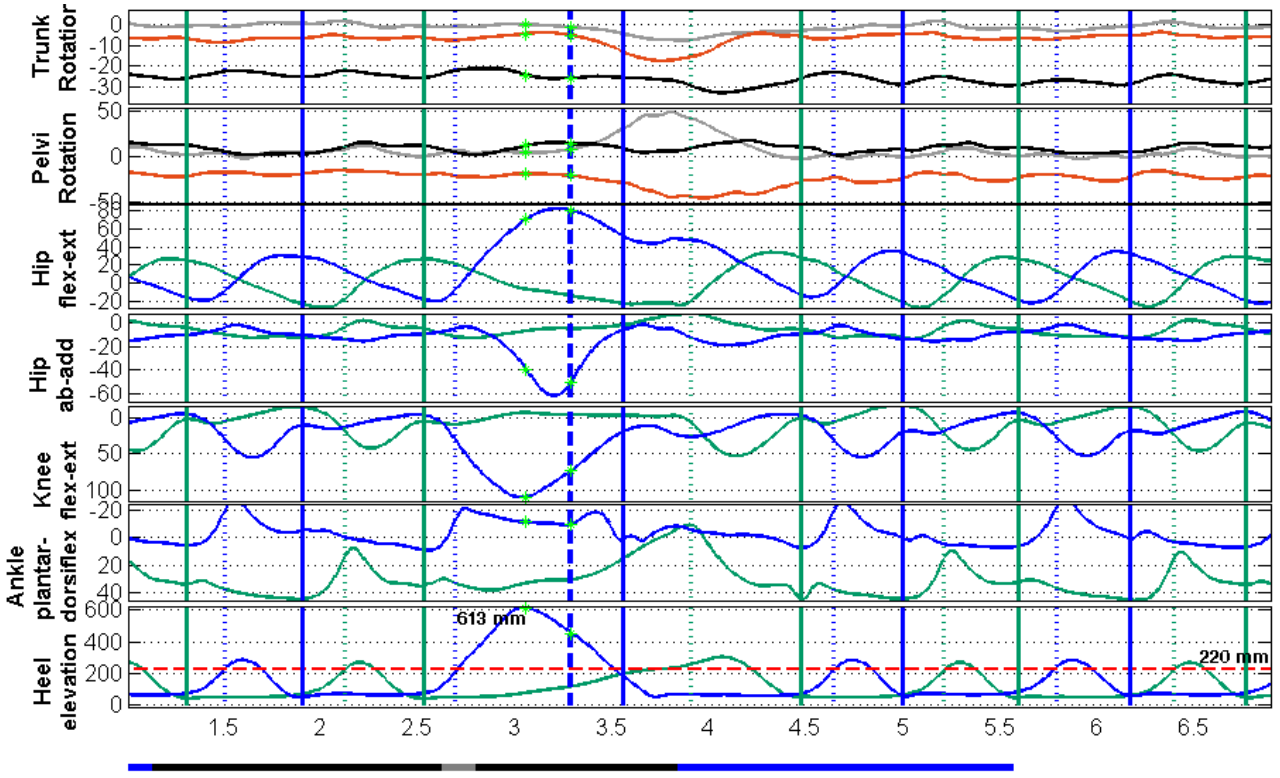

Figure 3.11 Kinematics and visual behavior output computation for an unsuccessful trial performed by one of the participant belonging to the older adults group. From the top to the bottom the trunk and pelvis rotation angles (AP: black; ML: gray and V: red), the left (green) and right (blue) angles of the joints (hip flexion-extention, hip ab-adduction, knee flexion-extention and ankle plantar-dorsiflexion), the elevation of the left (green) and right (blue) heels and the *PoG* hit over the areas of interest defined in the scene are reported. The vertical lines stand for the left (green) and right (blue) heel-strikes (plain line) and toe-offs (dotted lines). A vertical dashed line is reported in correspondence to the clearance time stamp of the leading foot (the color of the line corresponds to the leading foot side). Green and red stars are reported over the signal if at the specific time of the trial the heel quote was above or under the height of the obstacle. The *PoG* hit is reported in blue if no assignment occurred, in black if the assignment of the hit was for the obstacle area of interest and in red if it was for the distractor area of interest.

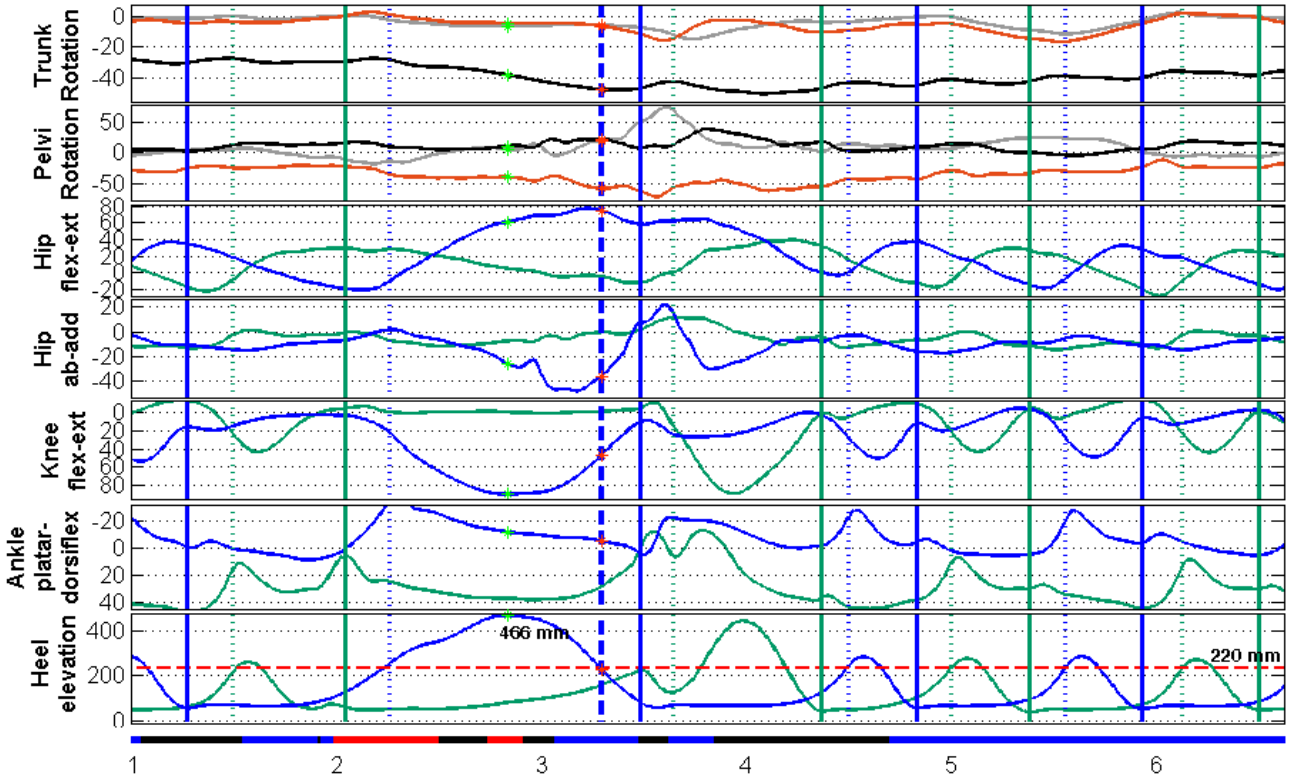

For the older and young adults, the overall failure percentage rate and the failure percentage rate for the trials with and with no distractors are reported in terms of mean and standard deviation in Table 3.2 and in terms of mean and standard error values in Figure 3.12.

Table 3.2 Mean and standard deviation values of the failure rates of the young (**YA**) and older adults (**OA**) during the evaluation session. The values are reported divided by trials with distractors (**Dis**), trials with no distractors (**NoDis**) and global unsuccessful rate (**Total**).

%	**Dis**	**NoDis**	**Total**
YA	28±9	29±22	34±12
OA	43±23	30±23	39±22

Figure 3.12 Mean and standard error of the values of failure rate of the young (**Young**) and older (**Old**) adults for the trials of the evaluation session. The values are reported divided by the trials with (**Dis**) and with no (**NoDis**) distractors and global unsuccessful rate (**All**).

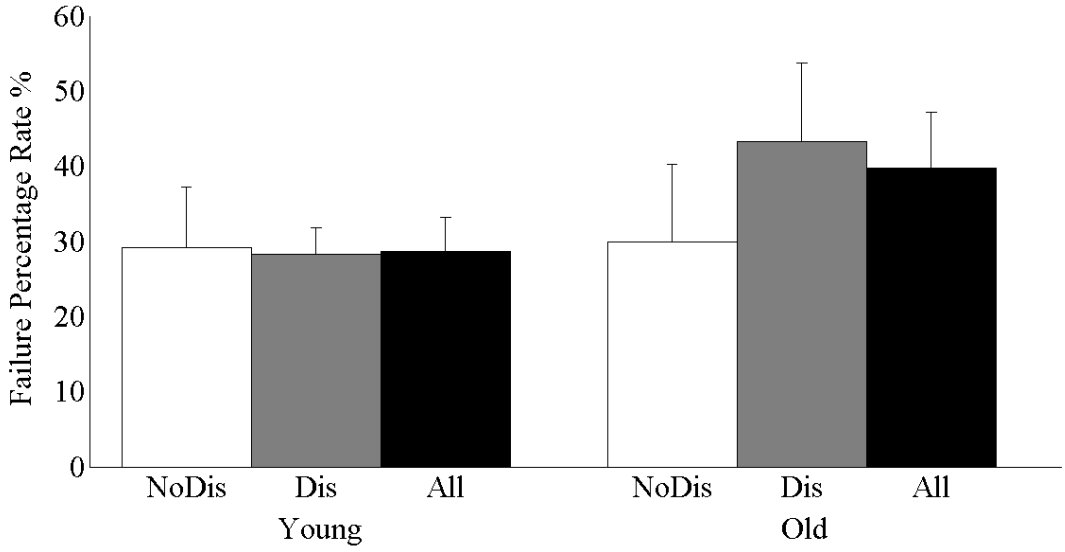

No significant differences were found between the conditions with and with no distractors for both of the groups. The groups did not differ significantly in terms of percentages of failure both for the global unsuccessful rate and for the failure rates with and with no distractors. Therefore the null hypotheses cannot be rejected.

For the successful trials, the *CL* and *ΔP* are reported in Table 3.3 in terms of mean and standard deviations values and in terms of mean and standard error values in Figure 3.13 for both groups divided by the trials with and with no distractors.

Table 3.3 Mean and standard deviation values of the *CL* and *ΔP* parameters achieved by the young (**YA**) and the older (**OA**) adults for the successful trials occurred during the evaluation session. The values are reported divided by trials with (**Dis**) and with no (**NoDis**) distractors.

	***CL* [mm]**		***ΔP* [ms]**	
	Dis	NoDis	Dis	NoDis
YA	164±118	169±107	132±99	129±89
OA	190±117	186±119	139±135	148±98

Figure 3.13 Mean and standard error values of the *CL* (a) and *ΔP* (b) parameters achieved by the young (**Young**) and the older (**Old**) adults for the successful trials occurred during the evaluation session. The values are reported divided by trials with (**Dis**) and with no distractors (**NoDis**).

a)

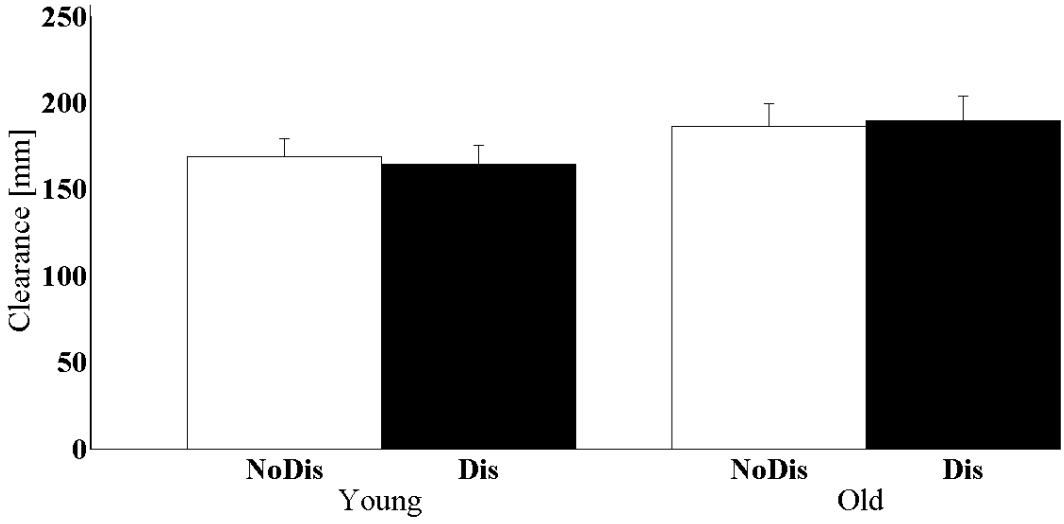

b)

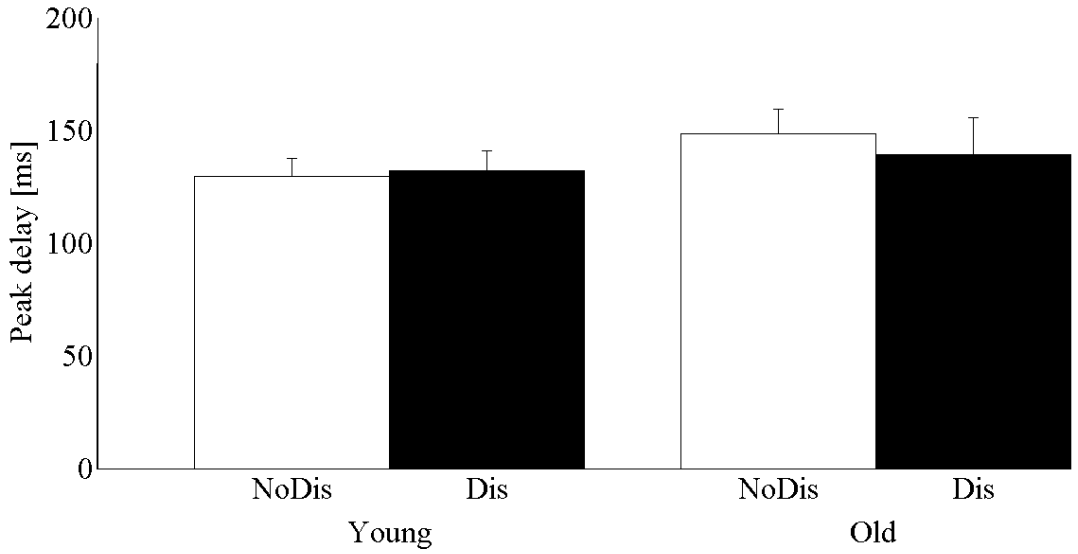

No significant differences were found between the conditions with and with no distractors for the *CL* and for the *ΔP* values for both of the groups. The groups did not differ significantly in terms of the *CL* and for the *ΔP* values in the trials with and with no distractors. Therefore the null hypotheses cannot be rejected.

For the successful trials, the mean and standard deviation values of the obstacle *PoG* hit percentage are reported in Table 3.4 in terms of mean and standard deviation values and in terms of mean and standard error values in Figure 3.14 for both groups divided by trials with and with no distractors.

Table 3.4 Mean and standard deviation of the obstacle gaze hit percentages of young (**YA**) and older (**OA**) adults for the successful trials occurred during the evaluation session. The values are reported divided by trials with (**Dis**) and with no distractors (**NoDis**).

	Dis %	**NoDis %**
YA	79±21	82±19
OA	88±11	89±11

Figure 3.14 Mean and standard error of the obstacle gaze hit percentages of young (**Young**) and older (**Old**) adults for the successful trials occurred during the evaluation session. The values are reported divided by trials with (**Dis**) and with no distractors (**NoDis**). The significant differences are reported.

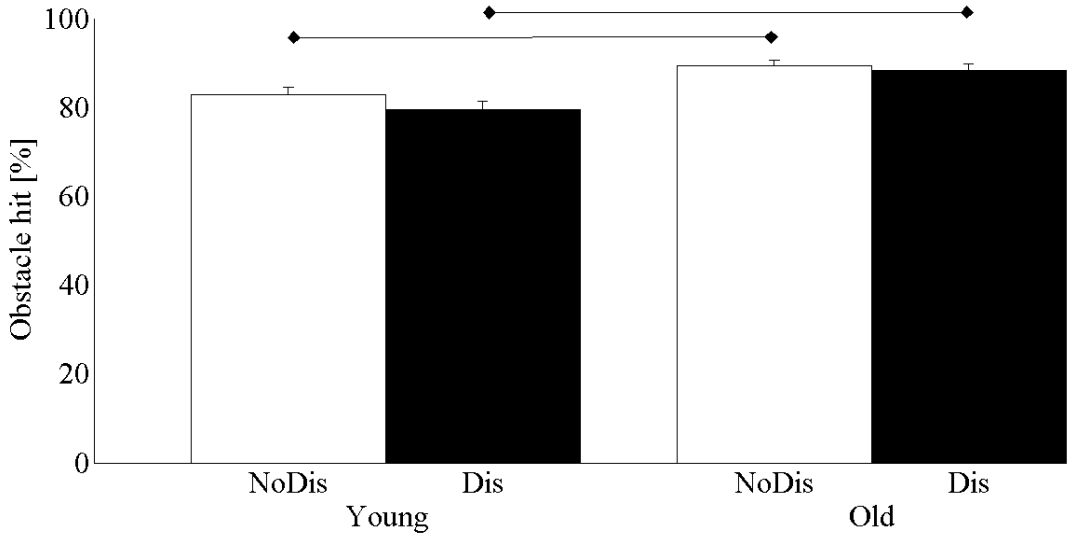

No significant differences were found between the conditions with and with no distractors for the *PoG* hit percentage values for both of the groups. The percentage of *PoG* hitting the obstacle was significantly greater for the older adults than for the young adults either when a distractor was present in the scene ($z=2.3414$, $p=0.0096$) and when no distractors were in the scene ($z=2.8419$, $p=0.0022$).

For the successful trials, the horizontal and vertical variability of the gaze are reported in Table 3.5 in terms of mean and standard deviation values and in terms of mean and standard error values in Figure 3.15 for both groups divided by trials with and with no distractors.

The horizontal variability of the *PoG* over the calibrated plan was significantly greater for the older adults in the conditions with distractors than in those with no distractors ($z = 4.0776$, $p < 0.0001$). The young adults did not show any significant difference in the horizontal variability of the *PoG* between the trials with and with no distractors. The horizontal variability of the *PoG* was not significantly different for the young and the older adults for the trials with distractors, whereas it was significantly different for the trials with no distractors ($z = -3.1439$, $p = 0.0008$). The vertical variability of the *PoG* over the calibrated plan was significantly greater for the young

adults in the trials with no distractors than in those with distractors ($z = -2.5843$, $p = 0.0049$). The older adults did not show any significant difference in the vertical variability if the *PoG* achieved in the trials with distractors with respect to those with no distractors. The vertical variability of the *PoG* over the calibrated plane was greater for the older adults than for the young adults in the trials with distractors ($z = 4.1303$, $p < 0.0001$), while the vertical variability of the groups did not differ significantly in the trials with no distractors.

Table 3.5 Mean and standard deviation values of the horizontal (***horGaze***) and vertical (***verGaze***) variability of the gaze of the young (**YA**) and older (**OA**) adults for the successful trials occurred during the evaluation session. The values are reported divided by trials with (**Dis**) and with no (**NoDis**) distractors.

	***horGaze* [mm]**		***vertGaze* [mm]**	
	Dis	NoDis	Dis	NoDis
YA	58±49	50±34	109±49	113±30
OA	68±53	35±20	122±26	115±19

Figure 3.15 Mean and standard error values of the horizontal (a: **Horz Gaze**) and vertical variability (b: **Vert Gaze**) of the *PoG* of the young (**Young**) and older (**Old**) adults for the successful trials occurred during the evaluation session. The values are reported divided by trials with (**Dis**) and with no (**NoDis**) distractors. The significant differences are reported.

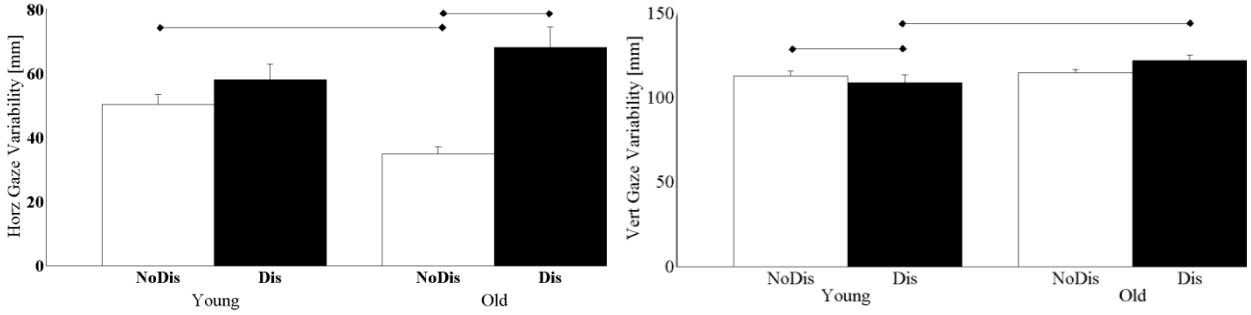

Discussion

This study aimed at assessing the influence of visual distractors on the visuo-motor strategies of young and older adults in virtual reality based obstacle negotiation tasks. To this end an interactive virtual reality environment was purposely depicted. Young and older adults had to navigate the virtual reality environment trying not to collide with obstacles lying on the walking path while both their gaze and kinematics were tracked. On a subset of the obstacle crossing trials visual distractors were administered trying to challenge the performance of the participants. To assess the motor interaction with the obstacle within the evaluation session, the analysis assessed the failure rate, the clearance of the foot over the obstacle and the delay of the maximum elevation of the leading foot with respect to the crossing time. In terms of gaze, the analysis assessed how the visual span of the scene occurred by analyzing the percentage of the point of gaze falling within a region of interest defined around the obstacle and the horizontal and vertical variability of the point of gaze over the scene. The obstacle was considered to be the main attentive demanding object on the scene. A hit of the gaze on the region of interest defined around it could point out a following of the obstacle, but the attention is not always headed toward the object we are looking at. For this reason the horizontal and vertical variability of the coordinates of the point of gaze were also assessed. Since the dynamic of the obstacle was always purely vertical in the 2D plane (projection of the virtual environment on the screen) and that of the distractor only purely horizontal, a decrease or an increase of the visual span along such directions could point out differences in the allocation of the attention on the scene.

The kinematics and the visual parameters, except for the failure rates, were computed only for the successful trials. In fact, for the unsuccessful trials when a collision with the obstacle occurred, the subject received a visual feedback in terms of a shaking of the image. Such a virtual feedback could possibly distort the visuo-motor behavior of the subject and therefore the unsuccessful trials were not considered for the analysis.

Both the older and young adults were able to perform the tasks. Even if not significantly different, the failure rate worsened for the older adults with respect to the young adults and in particular in the trials with distractors. The clearance of the leading foot over the obstacle and the timing of the foot with respect to the obstacle seem not to be influenced by the distractors presence and were not different between the young and the older adults.

The visual behavior assessment highlighted that in this study the young and the older adults significantly differed in the way they looked at the visual scene. In particular, the older adults showed a significantly increased focus on the area of interest of the obstacle with respect to their younger counterpart both with and with no distractors in the scene. The horizontal variability of the point of gaze was increased in the trials with distractors compared to those with no distractors for the older adults. The younger adults showed an increased horizontal variability of the gaze than the older adults for the trials with no distractors, while the two groups were not different in the trials with distractors. The young adults showed the vertical variability of the gaze significantly decreased in the trials with distractors with respect to those with no distractors. The older adults had a vertical variability of the point of gaze not different in the trials with distractors with respect to those with no distractors. For the trials with distractors the young adults showed significantly lower vertical variability of the gaze if compared to the older adults.

In contrast with the literature, this study did not show a worsening in the motor performances when visual distractors were in the scene (Lo & Chou, 2015; Lo, van Donkelaar, & Chou, 2015) neither in the young adults nor in the older adults. This difference is probably due either to the type of experimental set-up used (treadmill) or to the kind of distractors proposed in this study. The use of a treadmill allowing only for a constant speed could have in fact had an effect on the motor strategies of the subjects while crossing the obstacle. First, part of the trials (unsuccessful trials) was excluded from the analysis because for those the computation of the clearance and the delay of the maximum elevation of the leading foot with respect to the crossing time was not possible. Second, the use of a treadmill at constant speed imposed to the subject to accommodate consequentially their motor strategy over the obstacle. Therefore possible significant results in terms of the kinematics could have been distorted and masked. Another possible explanation of the absence of significant results in terms of the kinematics parameters could be in the type of visual distractors adopted in this study. In the literature, studies proposed visual-cognitive distractors adding a greater difficulty to the navigation task (Lo et al., 2015). In this study the distractors were chosen to be elements in the back of the scene crossing the road as if they were realistic (deers). This choice was made not to reduce the safety of the older adults walking on the treadmill and to simulate a realistic situation. Nevertheless, the use of more challenging and

cognitive involving distractors could have had a more pronounced effect on the avoidance strategy.

From the visual behavior point of view, this study showed that the younger adults differ from the older adults in the way they explore the scene. The older adults seem generally more focused on the obstacle when it is the only element of the scene, while when distractors appear they show a deviation of the gaze along the direction where the distractors are. The young adults instead show a more variable behavior no matter which condition they are facing. A possible explanation of the disparity in the visual behavior between the older and young adults is that the older adults are able to focus on the obstacle but are unable to suppress the shift of their attention even to unchallenging distractors. On the other side a more variable visual behavior of the young adults could point out that this population is more ready to unexpected changes from the scene.

The study of how distractors interfere with the visuo-motor strategies during obstacle crossing is important mainly for the elderly. This study tried both to propose a new way to address this type of studies and to get insights in the visuo-motor strategies adopted during treadmill and virtual reality based obstacle crossing tasks.

The results got through this investigation are promising and let for sure space to further improvements. Future implementations should increase the number of participants and try to overcome the experimental set-up limits highlighted by this pilot study. For instance, the experimental set-up could be improved with a treadmill not at constant speed and the naturalistic distractors could be enriched of detail the subject has to refer to the operator.

Conclusion

This study first highlights the visuo-motor strategy of young and older adults in a set-up similar to those recently used in the rehabilitation of gait (Mirelman et al., 2006). This and further investigations are important to better address the rehabilitation intervention of gait that could start always to include also the training of the visual strategy. These first results are promising and point out that this kind of test, once standardized for the clinics, could be easily used for the diagnosis and the intervention on neuro-motor diseases and the improvement of the coordination between eyes and body movement.

References

Applied Science Laboratories (2014a). EyeHead Integration Manual for use with Eye-Trac 7 Head Mounted Optics.

Applied Science Laboratories (2014b). Eye Tracker Systems Manual ASL EYE-TRAC 7 Head Mounted Optics.

Beurskens, R., & Bock, O. (2012). Age-related Deficits of dual-task walking: A review. *Neural Plasticity*, 2012. http://doi.org/10.1155/2012/131608.

Beurskens, R., & Bock, O. (2013). Does the walking task matter? Influence of different walking conditions on dual-task performances in young and older persons. *Human Movement Science*, 32(6), 1456–1466. http://doi.org/10.1016/j.humov.2013.07.013.

Brown, L. a, McKenzie, N. C., & Doan, J. B. (2005). Age-dependent differences in the attentional demands of obstacle negotiation. *The Journals of Gerontology. Series A: Biological Sciences and Medical Sciences*, 60(7), 924–927. http://doi.org/10.1093/gerona /60.7.924.

Cappello, A., Cappozzo, A., La Palombara, P. F., Lucchetti, L., & Leardini, A. (1997). Multiple anatomical landmark calibration for optimal bone pose estimation. Human Movement Science, 16(2–3), 259–274. http://doi.org/10.1016/S0167-9457(96)00055-3.

Cappozzo, A., Catani, F., Della Croce, U., & Leardini, A. (1995). Position and orientation in space of bones during movement: Anatomical frame definition and determination. Clinical Biomechanics, 10(4), 171–178. http://doi.org/10.1016/0268-0033(95)91394-T.

Chapman, G. J., & Hollands, M. A. (2006). Evidence for a link between changes to gaze behaviour and risk of falling in older adults during adaptive locomotion. *Gait & Posture*, 24, 288–94. http://doi.org/10.1016/j.gaitpost.2005.10.002.

Chapman, G. J., & Hollands, M. A. (2007). Evidence that older adult fallers prioritise the planning of future stepping actions over the accurate execution of ongoing steps during complex locomotor tasks. *Gait & Posture*, 26, 59–67. http://doi.org/10.1016/j.gaitpost. 2006.07.010.

Chapman, G. J., & Hollands, M. A. (2010). Age-related differences in visual sampling requirements during adaptive locomotion. *Experimental Brain Research*, 201(3), 467–478. http://doi.org/10.1007/s00221-009-2058-0.

Cheng, T.-J., Yang, B., Holloway, C., & Tyler, N. (2016). Effect of environmental factors on how older pedestrians detect an upcoming step, 1–11.

Franz, J. R., Francis, C. a., Allen, M. S., O'Connor, S. M., & Thelen, D. G. (2015). Advanced age brings a greater reliance on visual feedback to maintain balance during walking. *Human*

Movement Science, 40, 381–392. http://doi.org/10.1016/j.humov.2015.01.012.

Harley, C., Wilkie, R. M., & Wann, J. P. (2009). Stepping over obstacles: Attention demands and aging. *Gait & Posture*, 29(3), 428–432. http://doi.org/10.1016/j.gaitpost.2008.10.063.

Healey, M. K., Campbell, K. L., & Hasher, L. (2008). Chapter 22 Cognitive aging and increased distractibility: Costs and potential benefits. *Progress in Brain Research* (Vol. 169). Elsevier. http://doi.org/10.1016/S0079-6123(07)00022-2.

Holmqvist, K., Nyström, M., Andersson, R., Dewhurst, R., Jarodzka, H., & Van de Weijer, J. (2011). Eye Tracking: A comprehensive guide to methods and measures. *OXFORD University*.

Lo, O.-Y., & Chou, L.-S. (2015). Effects of Different Visual Attention Tasks on Obstacle Crossing in Healthy Young Adults. *Biomedical Engineering: Applications, Basis and Communications*, 27(6), 1550059. http://doi.org/10.4015/S1016237215500593.

Lo, O.-Y., van Donkelaar, P., & Chou, L.-S. (2015). Distracting visuospatial attention while approaching an obstacle reduces the toe-obstacle clearance. *Experimental Brain Research*, 233(4), 1137–1144. http://doi.org/10.1007/s00221-014-4189-1.

Marigold, D. S., & Patla, A. E. (2007). Gaze fixation patterns for negotiating complex ground terrain. Neuroscience, 144(1), 302–313. http://doi.org/10.1016/j.neuroscience.2006.09.006.

Mevorach, C., Spaniol, M. M., Soden, M., & Galea, J. M. (2016). Age-dependent distractor suppression across the vision and motor domain. *Journal of Vision*, 16(11), 27. http://doi.org/10.1167/16.11.27.

Mirelman, A., Rochester, L., Maidan, I., Din, S. Del, Alcock, L., Nieuwhof, F., Rikkert, M. O., Bloem, B. R., Pelosin, E., Avanzino, L., Abbruzzese, G., Dockx, K., Bekkers, E., Giladi, N., Nieuwboer, A., and Hausdorff, J. M., (2006). Addition of a non-immersive virtual reality component to treadmill training to reduce fall risk in older adults (V-TIME): a randomised controlled trial. *The Lancet*, 0(0), 807–824. http://doi.org/10.1016/s0140-6736(16)31325-3.

Northen Digital (2010). First Principles User Guide.

Patla, A. E. (1997). Understanding the roles of vision in the control of human locomotion. *Gait & Posture*, 5(1), 54–69. http://doi.org/10.1016/S0966-6362(96)01109-5

Patla, A. E., Adkin, A., Martin, C., Holden, R., & Prentice, S. (1996). Characteristics of voluntary visual sampling of the environment for safe locomotion over different terrains. *Experimental Brain Research. Experimentelle Hirnforschung. Experimentation Cerebrale*, 112(3), 513–522. http://doi.org/10.1007/BF00227957

Patla, A. E., & Vickers, J. N. (2003). How far ahead do we look when required to step on specific locations in the travel path during locomotion?. *Experimental Brain Research*, 148(1), 133–

138. http://doi.org/10.1007/s00221-002-1246-y.

Roithner, R., Schwameder, H., & Müller, E. (2000). Determination of optimal filter parameters for filtering kinematic walking data using butterworth low pass filter. *Proceedings of the 18th International Symposium on Biomechanics in Sports*, 982.

Serchi, V., Peruzzi, A., Cereatti, A., & Della Croce, U. (2016). Use of a Remote Eye-Tracker for the Analysis of Gaze during Treadmill Walking and Visual Stimuli Exposition, *BioMed research international, Hindawii*.

Stuart, S., Lord, S., Hill, E., & Rochester, L. (2016). Gait in Parkinson's disease: A visuo-cognitive challenge. *Neuroscience & Biobehavioral Reviews*, 62, 76–88. http://doi.org/ 10.1016/j.neubiorev.2016.01.002.

WorldViz LLC. WorldViz 5 Documentation. Retrieved from http://docs.worldviz.com/vizard.

Zeni, J. a., Richards, J. G., & Higginson, J. S. (2008). Two simple methods for determining gait events during treadmill and overground walking using kinematic data. *Gait & Posture*, 27(4), 710–714. http://doi.org/10.1016/j.gaitpost.2007.07.007.

Chapter 4

Conclusions and future perspectives

4.1 General results and main contributions

The research presented in this thesis consisted in the assessment of the visuo-motor strategies of young and older adults during obstacles crossing in a projected virtual reality environment with the presence of visual distractors. A set-up allowing for such an assessment with a completely remote eye-tracking system was full characterized for future applications in gait rehabilitation protocols. The main results and contributions of this work are summarized in the following sections.

4.1.2 Validation study: "Use of a Remote Eye-Tracker for the Analysis of Gaze during Treadmill Walking and Visual Stimuli Exposition"

In this part of the thesis project the investigation of the combined visuo-motor strategies during obstacles crossing was addressed by proposing a new laboratory-based experimental set-up (virtual reality, treadmill, stereo-photogrammetric system and eye-tracking). From the scientific literature it is evident that gait in complex locomotor tasks is visually influenced (Chapman & Hollands, 2010) and that a rehabilitation of the gaze combined with the already implemented intervention to enhance the gait could be effective (Reed-Jones et al., 2012; Young & Hollands, 2010). Unobtrusive or mini-intrusive technology is to prefer to intrusive one in order not to change the normal behavior of the subject being tested. Therefore, in this thesis the use of a remote eye-tracker is proposed to be integrated to the already existing gait rehabilitation protocols (Mirelman et al., 2013). Recently, the remote eye-tracking technology has been improved in order to track the gaze also in the presence of the head moving in a certain workspace in front of the infrared sensor. Nevertheless, the remote eye-tracking technology is usually used for application not requiring the subject to move (analysis of the participants sat on a chair while reading or internet surfing) or, in the case of clinical applications, the head motion is

restrained by mean of chinrests or bite-bars. A characterization of the performances of this technology in the presence of the motion of the head related to walking is still lacking in the literature (Niehorster et al., 2017). Therefore, this work aimed at validating the reliability of the use of the remote eye-tracking technology during walking in order to supply the characterization of this kind of device for applications like the rehabilitation of the gait (Serchi, Cereatti, Federighi, Rufa, & Della Croce, 2013; Serchi, Peruzzi, Cereatti, & Della Croce, 2014a, 2014b, 2014c, 2014d; Serchi et al., 2016). An experimental set-up recently proposed for the rehabilitation of the gait with the use of the virtual reality (Mirelman et al., 2013; Peruzzi et al., 2016) was integrated with a recent model of commercial remote eye-tracker, the Tobii TX300 (Tobii Technology AB, 2010). The experimental set-up implied the use of a treadmill and of a virtual reality scene projected on a large surface in front of the treadmill. In this way the gait was confined within a limited region in front of the remote eye-tracker and the stimuli presented onto the screen forced the head to be headed toward the screen, and the eyes facing the sensitive elements of the remote eye-tracker. In order to full validate the tested remote eye-tracker for treadmill walking, the study assessed the robustness of the tracking, the accuracy and the precision of the gathered measures at different distances from the eye-tracker, with different rotation of the head and for different gaze angles sustained by the stimuli on the screen. Walking motion was also assessed in order both to verify if the motion of the head during walking was included in the allowable tracking box of the remote eye-tracker, and to compare the accuracy and precision of the point of gaze measurements gathered during walking with those obtained during the static conditions.

The outcomes of this study helped in understanding better the performances of the tested remote eye-tracker during walking and demonstrated that as long as the head remains within the working space of the remote eye-tracker, the gaze measurements gathered from the device are well comparable to those got for the static conditions.

This part of the thesis fosters the feasibility of the use of the tested remote eye-tracker for gaze analysis during walking in virtual reality based applications. The authors want to highlight that the validation of the eye-tracking technology for the specific application and population being analyzed is important in order to get feasible results for the specific eye-tracking investigation.

4.1.3 Assessment of the visuo-motor strategies in the presence of visual distractors

In the scientific literature, studies tried to assess the effect of visual-attentional distractors on the motor strategies while crossing obstacles. These studies implied the administration of visuo-cognitive distractors to young adults during obstacle crossing tasks in a physical setting prepared in the laboratory (Lo & Chou, 2015; Lo et al., 2015). The outcomes of such studies showed that presenting a visuo-attentional distractor prior the obstacle crossing phase reduces the toe-off clearance over the obstacle (Lo et al., 2015). Older adults are known to be more prone than the young adults to be distracted (Healey, Campbell, & Hasher, 2008; Mevorach, Spaniol, Soden, & Galea, 2016). Recently proposed set-ups for the enhancement of the gait in populations prone to falling include the administration of obstacle crossing tasks on a treadmill with a projected virtual reality (Mirelman et al., 2013). The integration of the monitoring and training of the gaze together with the training of the gait could be a great add-on for the enhancement of the performances of the patients undertaking the rehabilitation treatment (Reed-Jones et al., 2012; Young & Hollands, 2010). The virtual scenes commonly projected in the gait rehabilitation set-ups include urban or rural walking environments with visual distractors (Mirelman et al., 2013; Peruzzi et al., 2016). In this contest, the visuo-motor behavior of young and older adults if distractors are presented has not been assessed yet. A better knowledge of how people manage to coordinate their gaze and their gait over obstacles in such a set-up and of how older and younger adults differentiate themselves could be a great add-on to the literature and to the current design of the rehabilitation protocols. Therefore this part of the thesis aimed at assessing the characteristics of both young and older adults in terms of visuo-motor behavior during obstacles crossing with distractors in a projected virtual reality environment, in order to supply the literature with practical guidelines on the behavior of the tested population and, particularly, on how the elderly manage the task with their "*over-distractible*" characteristic (Serchi, Cereatti, Cinelli, & Della Croce, *in preparation*, 2015; Serchi, Cereatti, Della Croce, & Cinelli, 2015). A custom virtual reality environment was depicted in order to test healthy young and older adults when stepping over obstacles while visual distractors tried to challenge their performance. Both populations were tested after a training session and with the administration of a visual feedback suggesting a fall in the case of unsuccessful obstacle avoidances. The outcomes gathered from this study represent a first attempt of assessment of the visual strategies of both old and young

adults during obstacles crossing in a virtual reality environment (Serchi et al., *in preparation*; Serchi, Cereatti, Cinelli, et al., 2015; Serchi, Cereatti, Della Croce, et al., 2015). Through this study we showed that the tested populations show different patterns in the visual strategies when facing this kind of task. In the specific, young adults appeared to have a more stable way of scanning the visual scene no matter what condition they were exposed to (distractors or no distractors). On the contrary the older adults had a variable scanning strategy when the obstacle was the only element of the scene with respect to the condition in which also a distractor was present in the scene. Moreover, when a distractor was present in the scene, the scanning of the older adults was not significantly different from that of the younger adults in the same condition. This suggests that the younger adults generally scan more the scene when compared to the older ones, and that the older adults appeared to be less flexible to allocate their attention. This study first highlights the visuo-motor strategy of young and older adults in a set-up similar to those recently used in the rehabilitation of gait (Mirelman et al., 2013). Specifically, this study showed that it is possible to distinguish the two tested population in a task as the one proposed (Serchi et al., *in preparation*; Serchi, Cereatti, Cinelli, et al., 2015; Serchi, Cereatti, Della Croce, et al., 2015). This study is a first necessary step both for the future integration of the gaze monitoring in the gait rehabilitation interventions, and to improve our knowledge of the differences that exist between the older and the young adults. This kind of task could be useful both to rehabilitate and to classify the visuo-motor behavior of the tested people in order to identify those particularly exposed to the risk of falling and to monitor the rehabilitation intervention. This and further investigations are important to address better the gait rehabilitation interventions.

4.2 Future perspectives and clinical applications

The research presented in this thesis showed possible solutions for the combined rehabilitation of the gait and gaze and showed that through investigations like that presented, it is possible to highlight differences between the visual strategies of the populations being investigated. The study presented in this thesis could be improved by changing the type of visual distractors and treadmill and by providing more challenging distractions in order to get more meaningful kinematics and visual parameters. These first preliminary results show the great potential of this kind of assessment, and as future improvement the author suggests the testing of a greater

number of subjects characterized by different levels of neurological impairment. Moreover, once standardized for the clinics, this kind of assessment could be easily used for the diagnosis and for the intervention against neuro-motor diseases and the improvement of the coordination between eyes and body movement.

References

Chapman, G. J., & Hollands, M. A. (2010). Age-related differences in visual sampling requirements during adaptive locomotion. *Experimental Brain Research*, 201(3), 467–478. http://doi.org/10.1007/s00221-009-2058-0.

Healey, M. K., Campbell, K. L., & Hasher, L. (2008). Chapter 22 Cognitive aging and increased distractibility: Costs and potential benefits. *Progress in Brain Research* (Vol. 169). Elsevier. http://doi.org/10.1016/S0079-6123(07)00022-2.

Lo, O.-Y., van Donkelaar, P., & Chou, L.-S. (2015). Distracting visuospatial attention while approaching an obstacle reduces the toe-obstacle clearance. *Experimental Brain Research*, *233*(4), 1137–1144. http://doi.org/10.1007/s00221-014-4189-1.

Lo, O.-Y., & Chou, L.-S. (2015). Effects of Different Visual Attention Tasks on Obstacle Crossing in Healthy Young Adults. *Biomedical Engineering: Applications, Basis and Communications*, *27*(6), 1550059. http://doi.org/10.4015/S1016237215500593.

Mevorach, C., Spaniol, M. M., Soden, M., & Galea, J. M. (2016). Age-dependent distractor suppression across the vision and motor domain. *Journal of Vision*, *16*(11), 27. http://doi.org/10.1167/16.11.27.

Niehorster, D. C., Cornelissen, T. H. W., Holmqvist, K., Hooge, I. T. C., & Hessels, R. S. (2017). What to expect from your remote eye-tracker when participants are unrestrained. *Behav Res Methods.* http://doi.org/10.3758/s13428-017-0863-0.

Mirelman, A., Rochester, L., Reelick, M., Nieuwhof, F., Pelosin, E., Abbruzzese, G., Hausdorff, J. M. (2013). V-TIME: a treadmill training program augmented by virtual reality to decrease fall risk in older adults: study design of a randomized controlled trial. *BMC Neurology*, 13(1), 15. http://doi.org/10.1186/1471-2377-13-15.

Tobii Technology AB. (2010). *Tobii TX300 Eye Tracker*.

Peruzzi, A., Cereatti, A., Della Croce, U., & Mirelman, A. (2016). Effects of a virtual reality and treadmill training on gait of subjects with multiple sclerosis: a pilot study. *Multiple Sclerosis and Related Disorders*, *5*(NOVEMBER), 91–96. http://doi.org/10.1016/j.msard.2015.11.002.

Reed-Jones, R. J., Dorgo, S., Hitchings, M. K., & Bader, J. O. (2012). Vision and agility training in community dwelling older adults: Incorporating visual training into programs for fall prevention. *Gait & Posture*, 35(4), 585–589. http://doi.org/10.1016/j.gaitpost.2011.11.029.

Serchi, V., Cereatti, A., Federighi, P., Rufa, A., & Della Croce, U. (2013). An experimental setup for the combined analysis of gaze and gait. In *23th National Congress of SIAMOC*.

Serchi, V., Peruzzi, A., Cereatti, A., & Della Croce, U. (2014). Performance of a remote eye-tracker in measuring gaze during walking. In *20th IMEKO TC4 International Symposium Benevento*.

Serchi, V., Peruzzi, A., Cereatti, A., & Della Croce, U. (2014). Tracking gaze while walking on a treadmill: spatial accuracy and limits of use of a stationary remote eye-tracker. In *36th Annual International Conference of the IEEE Engineering in Medicine and Biology Society*.

Serchi, V., Peruzzi, A., Cereatti, A., & Della Croce, U. (2014). Tracking gaze while walking on a treadmill: limits of use of stationary remote eye-tracker. In *4th Conference Gruppo Nazionale di Bioingegneria (GNB).*

Serchi, V., Peruzzi, A., Cereatti, A., & Della Croce, U. (2014). Validation of a remote eye-tracker: application to gait analysis. In *25th SIAMOC-23th ESMAC*.

Serchi, V., Peruzzi, A., Cereatti, A., & Della Croce, U. (2016). Use of a remote eye-tracker for the analysis of gaze during treadmill walking and visual stimuli exposition. *BioMed Research International*. http://doi.org/10.1155/2016/2696723.

Serchi, V., Cereatti, A., Cinelli, M. E., & Della Croce, U. (2015). Gaze strategies while negotiating obstacles in a virtual environment with distractors. In *Gait & Posture* (Vol. 42, p. S3). http://doi.org/10.1016/j.gaitpost.2015.07.018.

Serchi, V., Cereatti, A., Della Croce, U., & Cinelli, M. E. (2015). Gaze strategies during obstacle negotiation in presence of distractors: a virtual reality assessment of young and older adult populations. In *OBC - Ontario Biomechanics Conference*.

Serchi, V., Cereatti, A., Cinelli, M. E., & Della Croce, U. (*in preparation*). Assessment of the distractors effect on vision and gait strategies during obstacle crossing: a virtual reality assessment. *In Preparation*.

Young, W. R., & Hollands, M. A. (2010). Can telling older adults where to look reduce falls? Evidence for a causal link between inappropriate visual sampling and suboptimal stepping performance. Experimental Brain Research, 204(1), 103–113. http://doi.org/10.1007/s00221-010-2300-9.

Annex 1

Figure A1.1 The head *RoTs* (green) and *RoMs* (magenta) along the V^{rET} (+, up; -, down) direction. The median values of the minimum and maximal limits of the *RoTs* and of the *RoMs* across the subjects are reported (vertical bars).

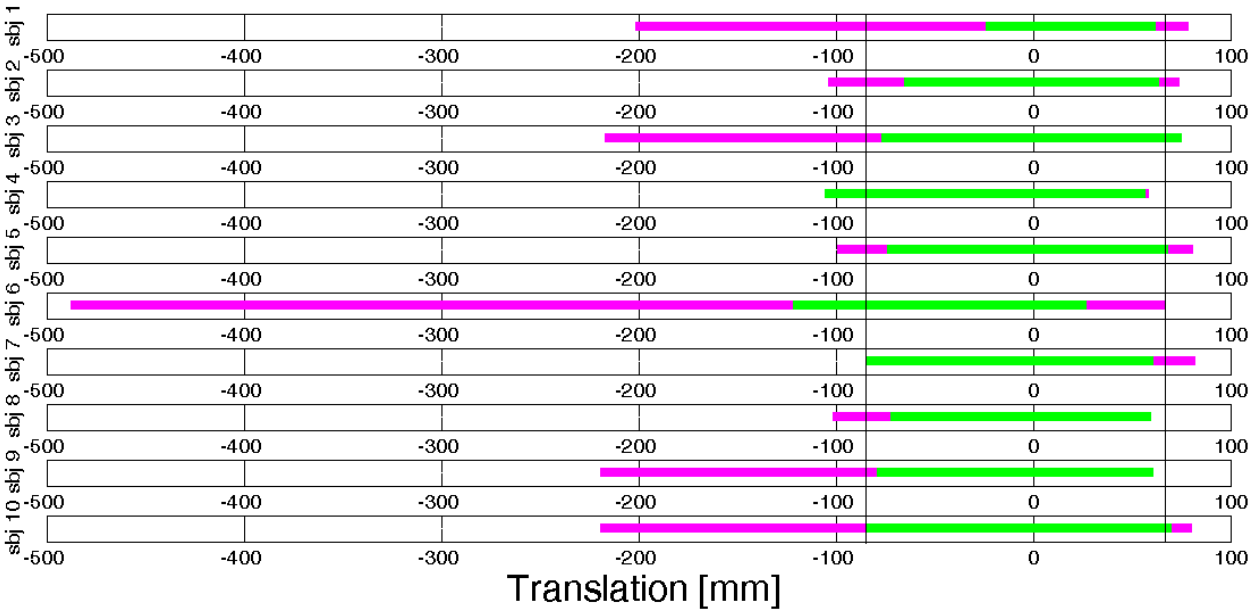

Figure A1.2 The head *RoTs* (green) and *RoMs* (magenta) along the ML^{rET} (-, left; +, right) direction. The median values of the minimum and maximal limits of the *RoTs* and of the *RoMs* across the subjects are reported (vertical bars).

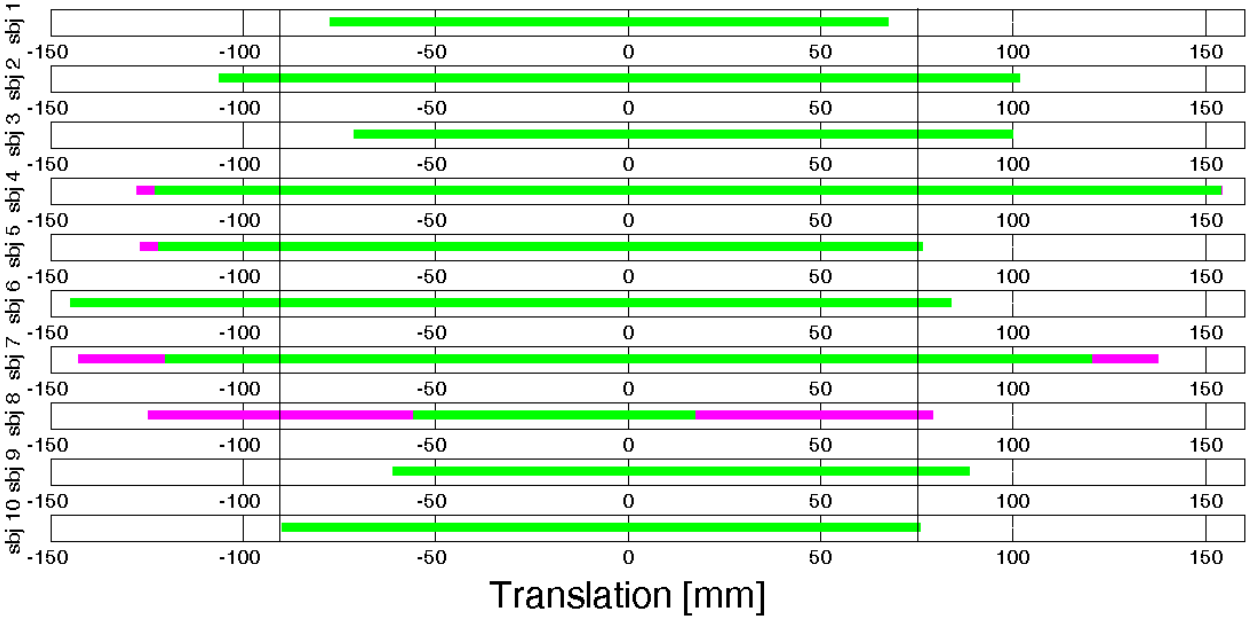

Figure A1.3 The head *RoTs* (green) and *RoMs* (magenta) along the AP^{rET} direction. The median values of the minimum and maximal limits of the *RoTs* and of the *RoMs* across the subjects are reported (vertical bars).

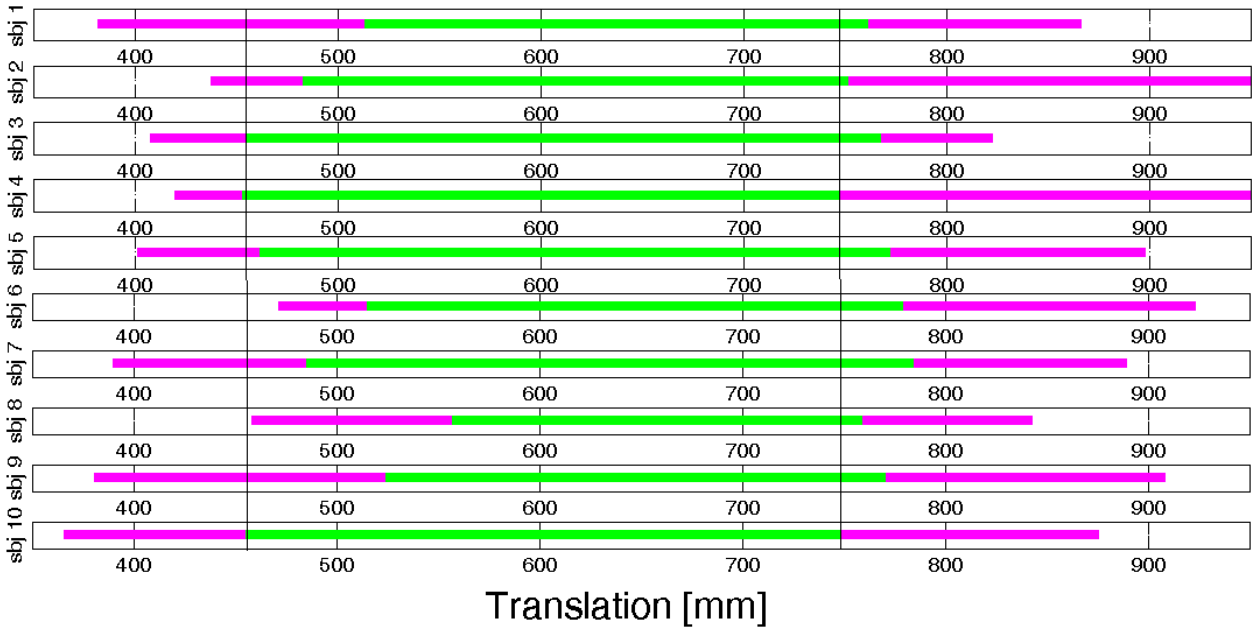

Figure A1.4 The head *RoTs* (green) and *RoMs* (magenta) around the V^{H} direction (-, down; +, up). The median values of the minimum and maximal limits of the *RoTs* and of the *RoMs* across the subjects are reported (vertical bars).

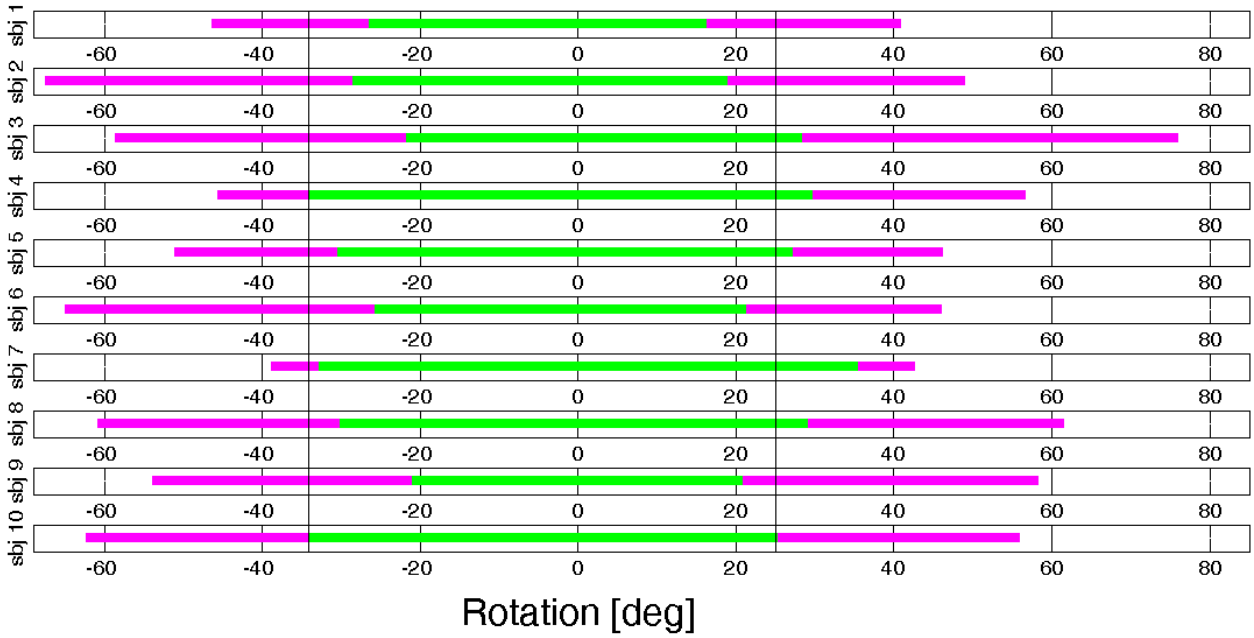

Figure A1.4 The head *RoTs* (green) and *RoMs* (magenta) around the ML^H direction (-, left; +, right). The median values of the minimum and maximal limits of the *RoTs* and of the *RoMs* across the subjects are reported (vertical bars).

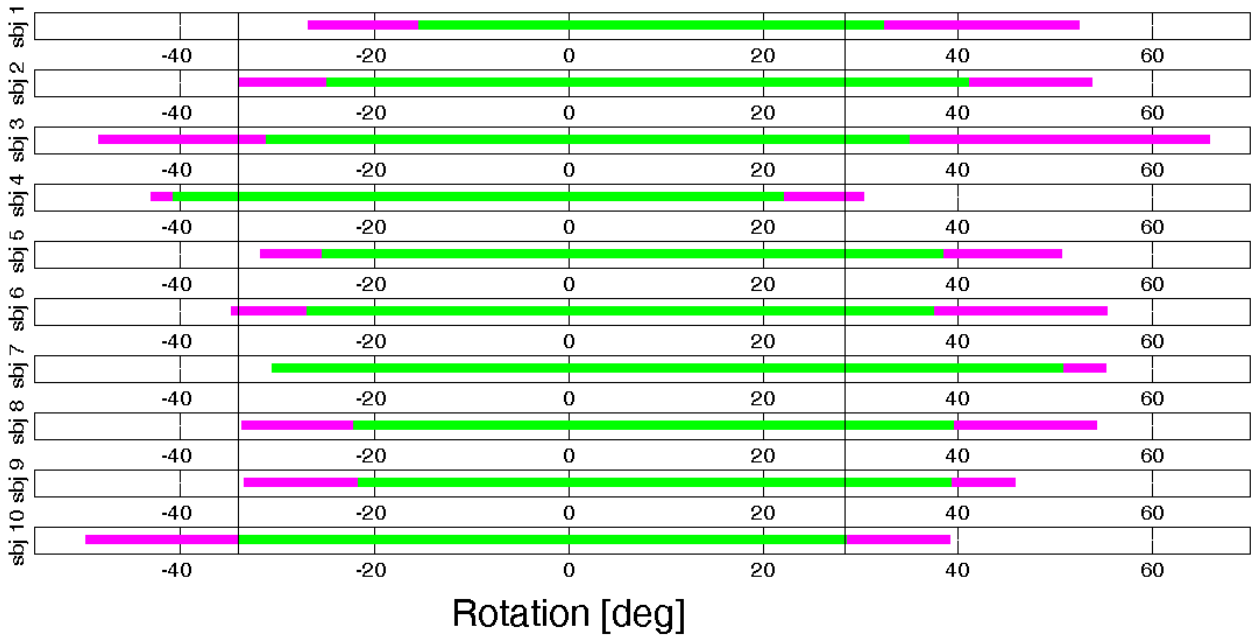

Annex 2

Figure A2.1 A graphical representation of ε_i and δ_i values for subject 1 found for each dot-target location during the trials *st550* (blue), *st650* (green), *st750* (red). Each dot-target location on the image is a black dot. The circles center positions (colored dots) reflect the accuracy of the *PoG* measurements (ε_i) while their radius reflects the precision of the *PoG* measurements (small radius, $\delta_i < 4$ mm; average radius, 4 mm$< \delta_i <$ 8 mm; large radius, $\delta_i > 8$ mm).

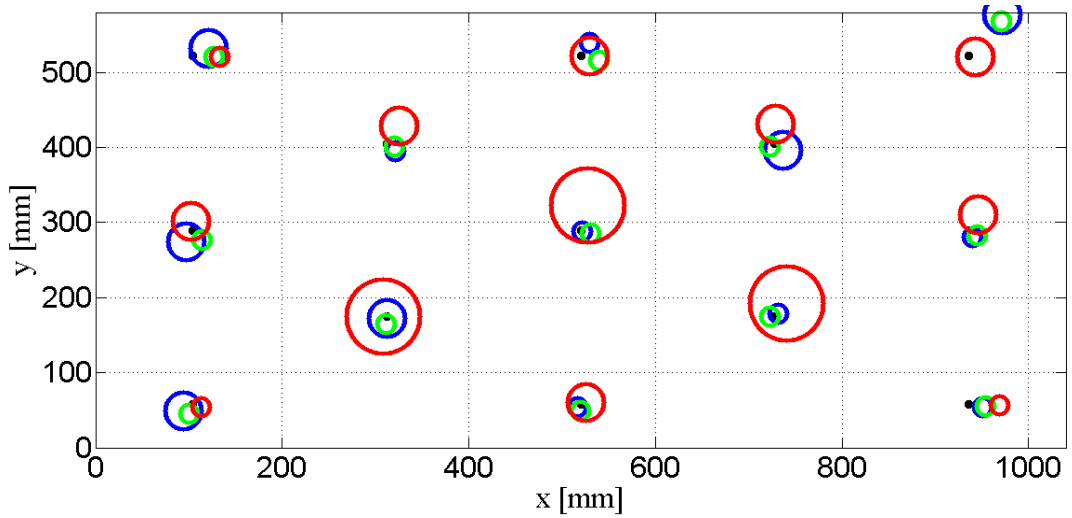

Figure A2.2 A graphical representation of ε_i and δ_i values for subject 2 found for each dot-target location during the trials *st550* (blue), *st650* (green), *st750* (red). Each dot-target location on the image is a black dot. The circles center positions (colored dots) reflect the accuracy of the *PoG* measurements (ε_i) while their radius reflects the precision of the *PoG* measurements (small radius, $\delta_i < 4$ mm; average radius, 4 mm$< \delta_i <$ 8 mm; large radius, $\delta_i > 8$ mm).

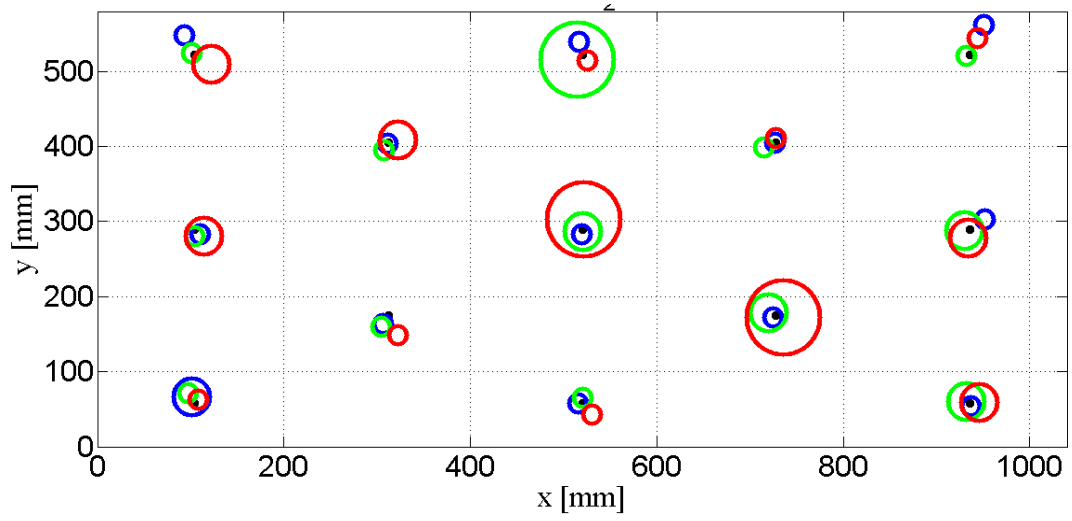

Figure A2.3 A graphical representation of ε_i and δ_i values for subject 3 found for each dot-target location during the trials *st550* (blue), *st650* (green), *st750* (red). Each dot-target location on the image is a black dot. The circles center positions (colored dots) reflect the accuracy of the *PoG* measurements (ε_i) while their radius reflects the precision of the *PoG* measurements (small radius, $\delta_i < 4$ mm; average radius, 4 mm$< \delta_i <$ 8 mm; large radius, $\delta_i > 8$ mm).

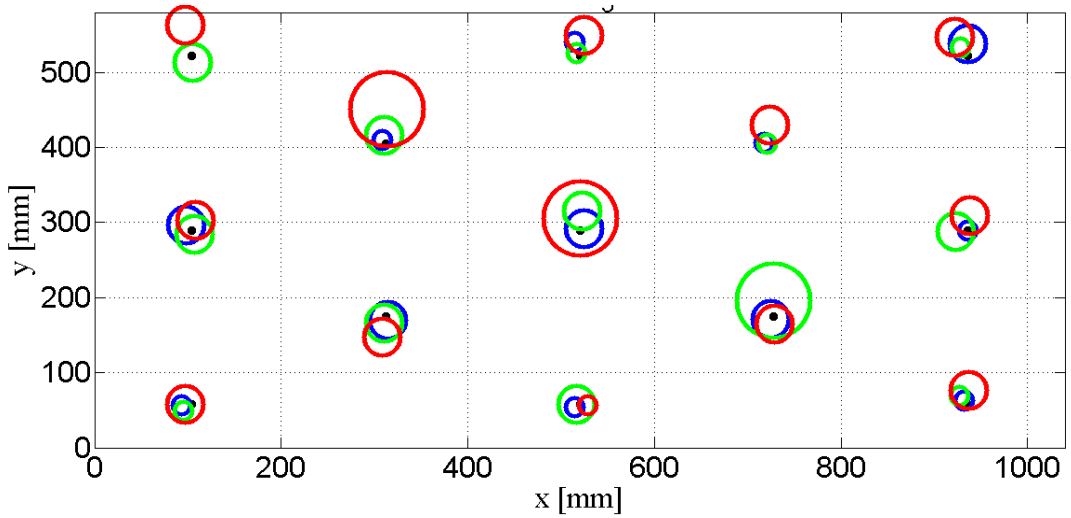

Figure A2.4 A graphical representation of ε_i and δ_i values for subject 4 found for each dot-target location during the trials *st550* (blue), *st650* (green), *st750* (red). Each dot-target location on the image is a black dot. The circles center positions (colored dots) reflect the accuracy of the *PoG* measurements (ε_i) while their radius reflects the precision of the *PoG* measurements (small radius, $\delta_i < 4$ mm; average radius, 4 mm$< \delta_i <$ 8 mm; large radius, $\delta_i > 8$ mm).

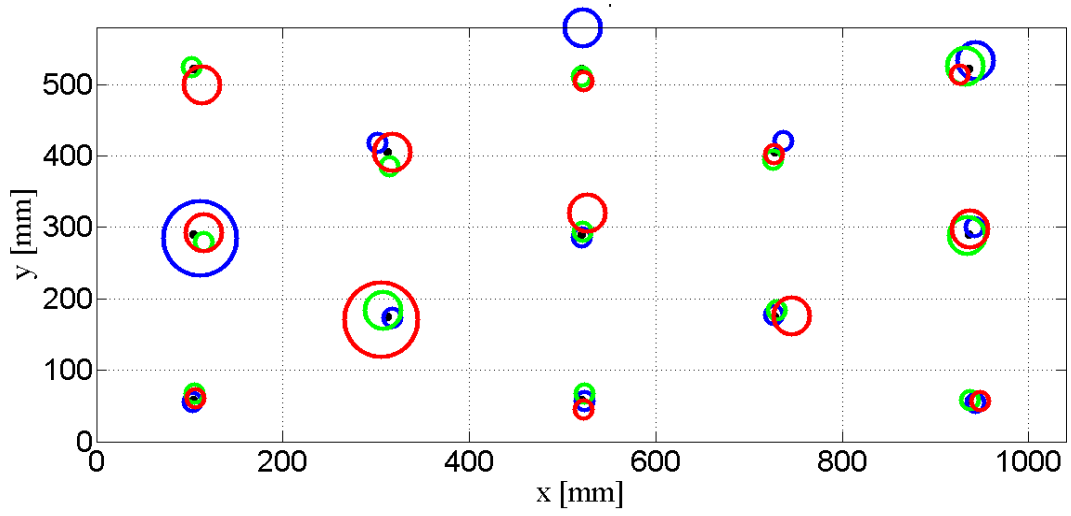

Figure A2.5 A graphical representation of ε_i and δ_i values for subject 5 found for each dot-target location during the trials *st550* (blue), *st650* (green), *st750* (red). Each dot-target location on the image is a black dot. The circles center positions (colored dots) reflect the accuracy of the *PoG* measurements (ε_i) while their radius reflects the precision of the *PoG* measurements (small radius, $\delta_i < 4$ mm; average radius, 4 mm$< \delta_i <$ 8 mm; large radius, $\delta_i > 8$ mm).

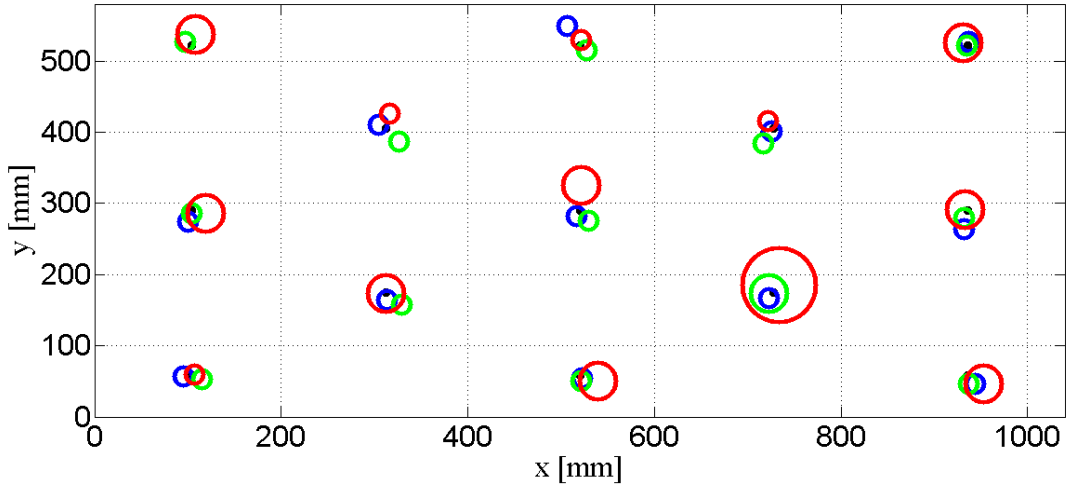

Figure A2.6 A graphical representation of ε_i and δ_i values for subject 6 found for each dot-target location during the trials *st550* (blue), *st650* (green), *st750* (red). Each dot-target location on the image is a black dot. The circles center positions (colored dots) reflect the accuracy of the *PoG* measurements (ε_i) while their radius reflects the precision of the *PoG* measurements (small radius, $\delta_i < 4$ mm; average radius, 4 mm$< \delta_i <$ 8 mm; large radius, $\delta_i > 8$ mm).

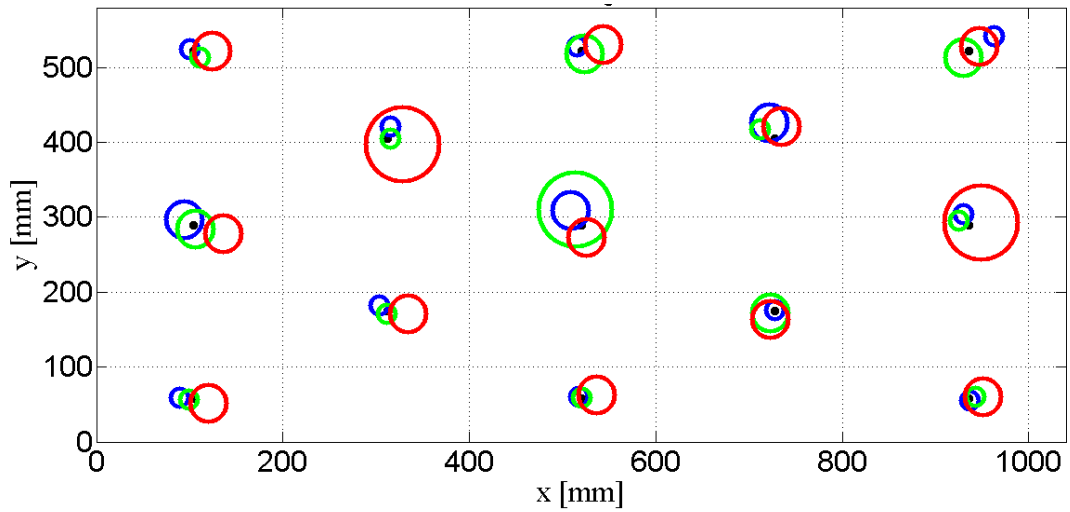

Figure A2.7 A graphical representation of ε_i and δ_i values for subject 7 found for each dot-target location during the trials *st550* (blue), *st650* (green), *st750* (red). Each dot-target location on the image is a black dot. The circles center positions (colored dots) reflect the accuracy of the *PoG* measurements (ε_i) while their radius reflects the precision of the *PoG* measurements (small radius, $\delta_i < 4$ mm; average radius, 4 mm$< \delta_i <$ 8 mm; large radius, $\delta_i > 8$ mm).

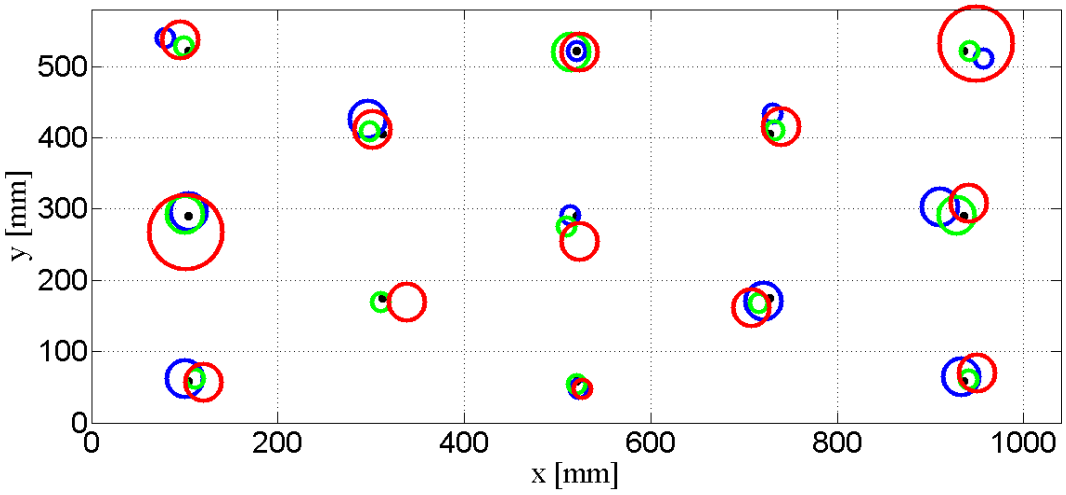

Figure A2.8 A graphical representation of ε_i and δ_i values for subject 8 found for each dot-target location during the trials *st550* (blue), *st650* (green), *st750* (red). Each dot-target location on the image is a black dot. The circles center positions (colored dots) reflect the accuracy of the *PoG* measurements (ε_i) while their radius reflects the precision of the *PoG* measurements (small radius, $\delta_i < 4$ mm; average radius, 4 mm$< \delta_i <$ 8 mm; large radius, $\delta_i > 8$ mm).

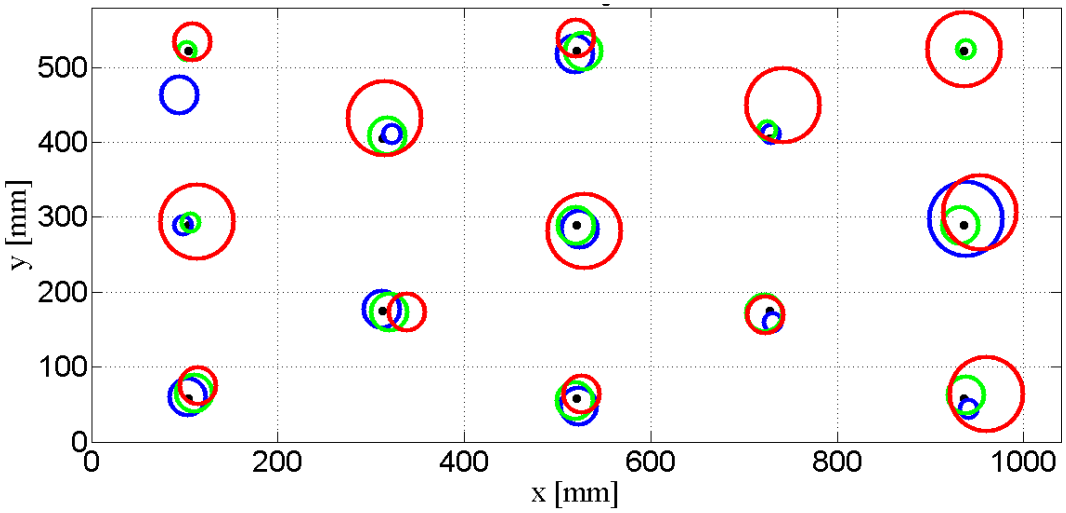

Figure A2.9 A graphical representation of ε_i and δ_i values for subject 9 found for each dot-target location during the trials *st550* (blue), *st650* (green), *st750* (red). Each dot-target location on the image is a black dot. The circles center positions (colored dots) reflect the accuracy of the *PoG* measurements (ε_i) while their radius reflects the precision of the *PoG* measurements (small radius, $\delta_i < 4$ mm; average radius, 4 mm$< \delta_i <$ 8 mm; large radius, $\delta_i > 8$ mm).

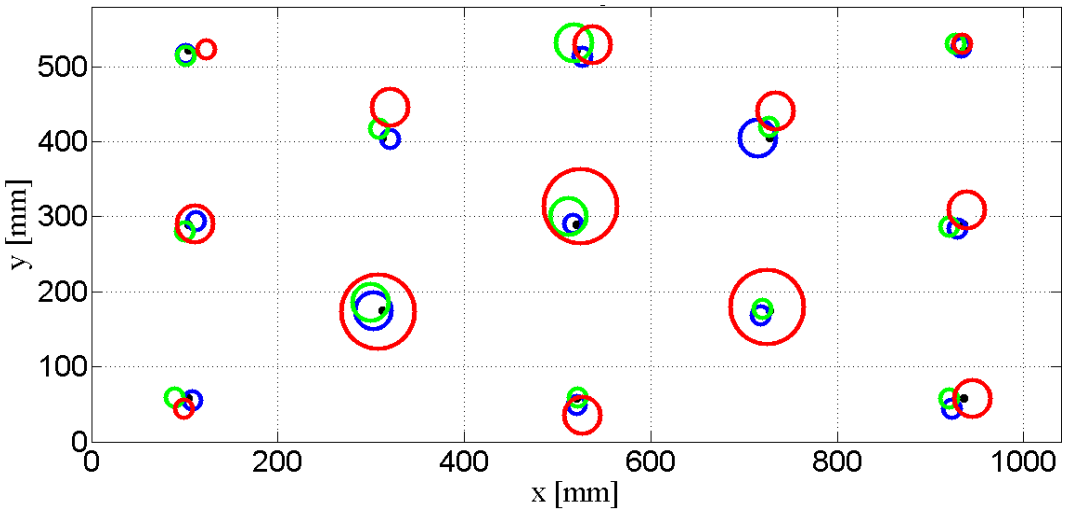

Figure A2.10 A graphical representation of ε_i and δ_i values for subject 10 found for each dot-target location during the trials *st550* (blue), *st650* (green), *st750* (red). Each dot-target location on the image is a black dot. The circles center positions (colored dots) reflect the accuracy of the *PoG* measurements (ε_i) while their radius reflects the precision of the *PoG* measurements (small radius, $\delta_i < 4$ mm; average radius, 4 mm$< \delta_i <$ 8 mm; large radius, $\delta_i > 8$ mm).

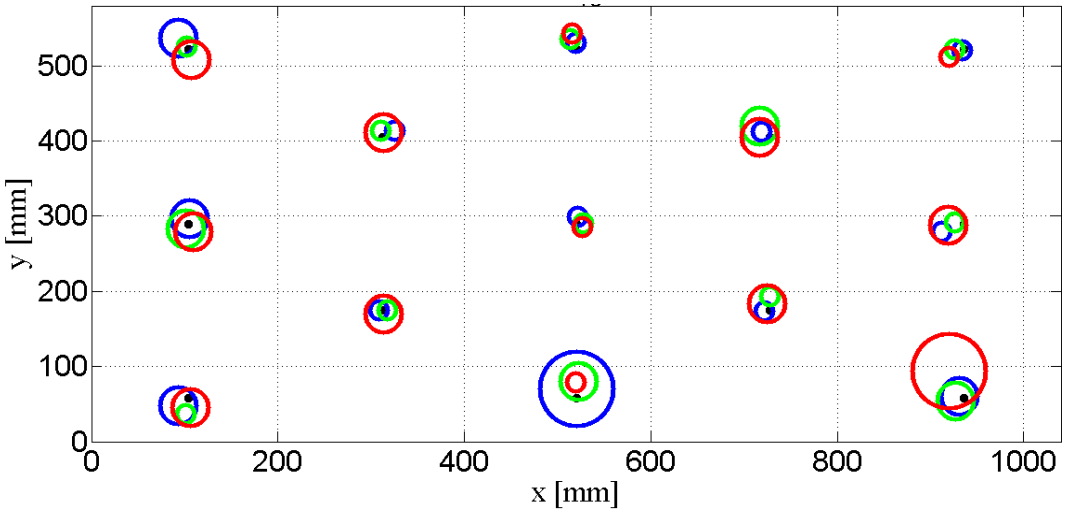

Annex 3

Figure A3.1 A graphical representation of ε_i and δ_i values for subject 1 found for each dot-target location during the trials *wslow* (magenta) and *walkfast* (light blue). Each dot-target location on the image is a black dot. The circles center positions (colored dots) reflect the accuracy of the *PoG* measurements (ε_i) while their radius reflects the precision of the *PoG* measurements (small radius, δ_i < 4 mm; average radius, 4 mm< δ_i < 8 mm; large radius, δ_i > 8 mm).

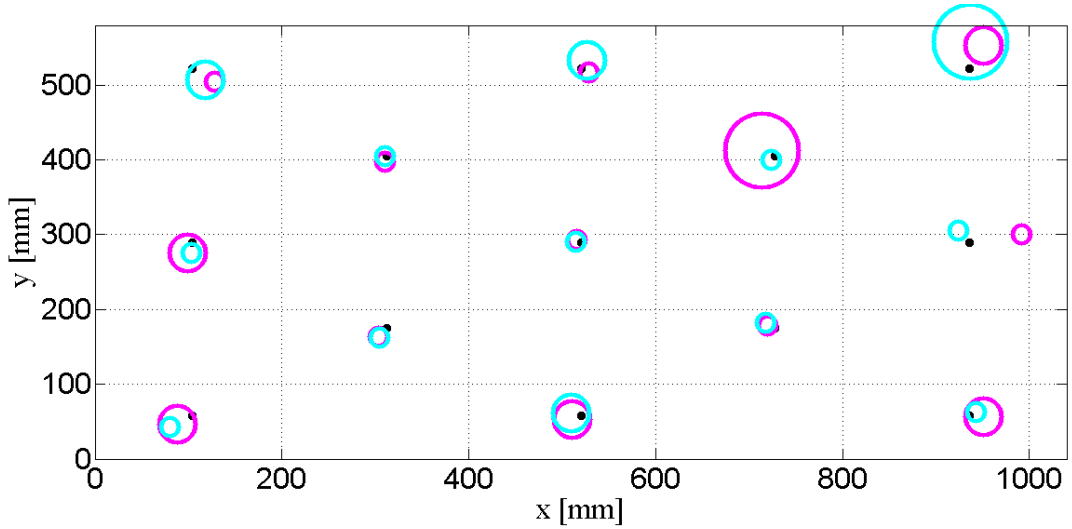

Figure A3.2 A graphical representation of ε_i and δ_i values for subject 2 found for each dot-target location during the trials *wslow* (magenta) and *walkfast* (light blue). Each dot-target location on the image is a black dot. The circles center positions (colored dots) reflect the accuracy of the *PoG* measurements (ε_i) while their radius reflects the precision of the *PoG* measurements (small radius, δ_i < 4 mm; average radius, 4 mm< δ_i < 8 mm; large radius, δ_i > 8 mm).

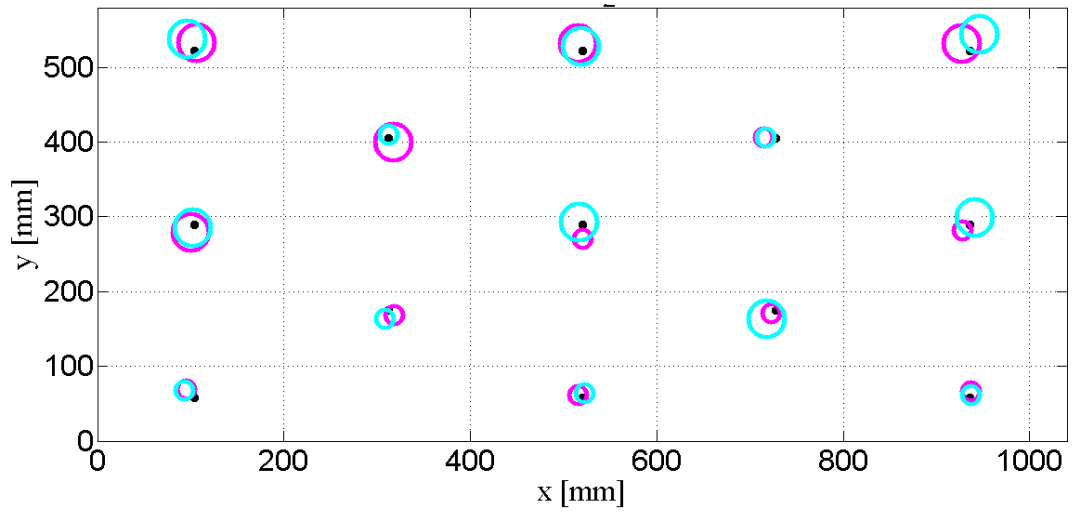

Figure A3.3 A graphical representation of ε_i and δ_i values for subject 3 found for each dot-target location during the trials *wslow* (magenta) and *walkfast* (light blue). Each dot-target location on the image is a black dot. The circles center positions (colored dots) reflect the accuracy of the *PoG* measurements (ε_i) while their radius reflects the precision of the *PoG* measurements (small radius, $\delta_i < 4$ mm; average radius, 4 mm$< \delta_i <$ 8 mm; large radius, $\delta_i > 8$ mm).

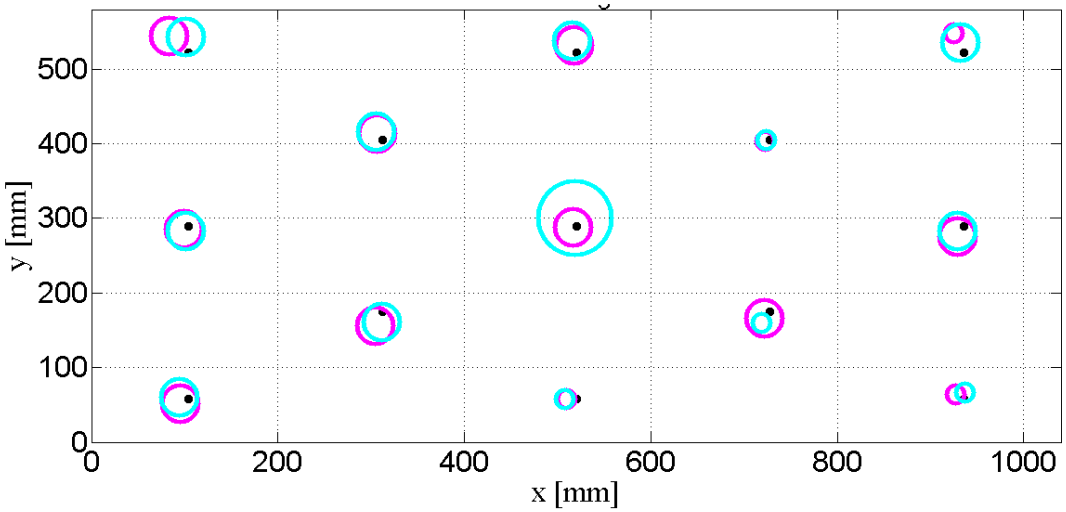

Figure A3.4 A graphical representation of ε_i and δ_i values for subject 4 found for each dot-target location during the trials *wslow* (magenta) and *walkfast* (light blue). Each dot-target location on the image is a black dot. The circles center positions (colored dots) reflect the accuracy of the *PoG* measurements (ε_i) while their radius reflects the precision of the *PoG* measurements (small radius, $\delta_i < 4$ mm; average radius, 4 mm$< \delta_i <$ 8 mm; large radius, $\delta_i > 8$ mm).

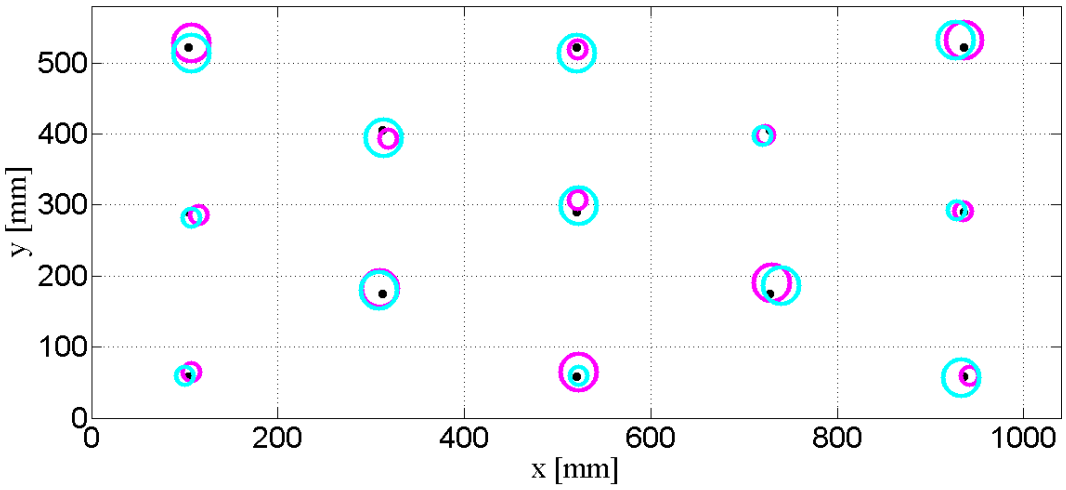

Figure A3.5 A graphical representation of ε_i and δ_i values for subject 5 found for each dot-target location during the trials *wslow* (magenta) and *walkfast* (light blue). Each dot-target location on the image is a black dot. The circles center positions (colored dots) reflect the accuracy of the *PoG* measurements (ε_i) while their radius reflects the precision of the *PoG* measurements (small radius, $\delta_i < 4$ mm; average radius, 4 mm$< \delta_i <$ 8 mm; large radius, $\delta_i > 8$ mm).

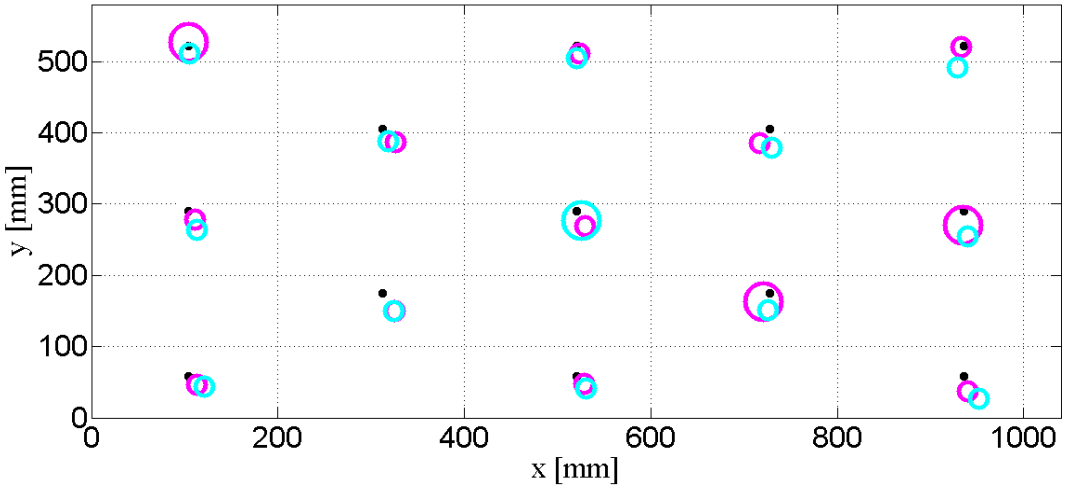

Figure A3.6 A graphical representation of ε_i and δ_i values for subject 6 found for each dot-target location during the trials *wslow* (magenta) and *walkfast* (light blue). Each dot-target location on the image is a black dot. The circles center positions (colored dots) reflect the accuracy of the *PoG* measurements (ε_i) while their radius reflects the precision of the *PoG* measurements (small radius, $\delta_i < 4$ mm; average radius, 4 mm$< \delta_i <$ 8 mm; large radius, $\delta_i > 8$ mm).

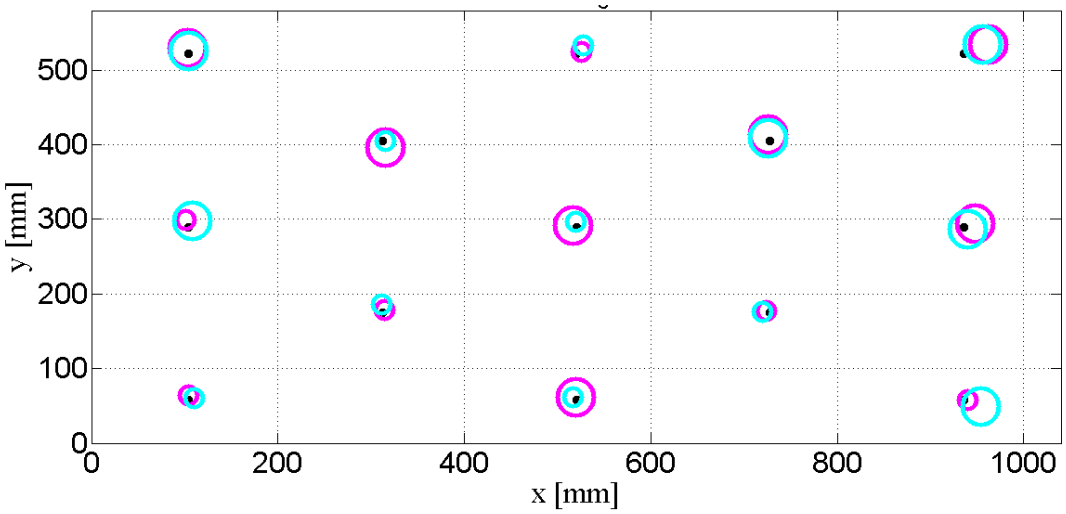

Figure A3.7 A graphical representation of ε_i and δ_i values for subject 7 found for each dot-target location during the trials *wslow* (magenta) and *walkfast* (light blue). Each dot-target location on the image is a black dot. The circles center positions (colored dots) reflect the accuracy of the *PoG* measurements (ε_i) while their radius reflects the precision of the *PoG* measurements (small radius, $\delta_i < 4$ mm; average radius, 4 mm$< \delta_i <$ 8 mm; large radius, $\delta_i > 8$ mm).

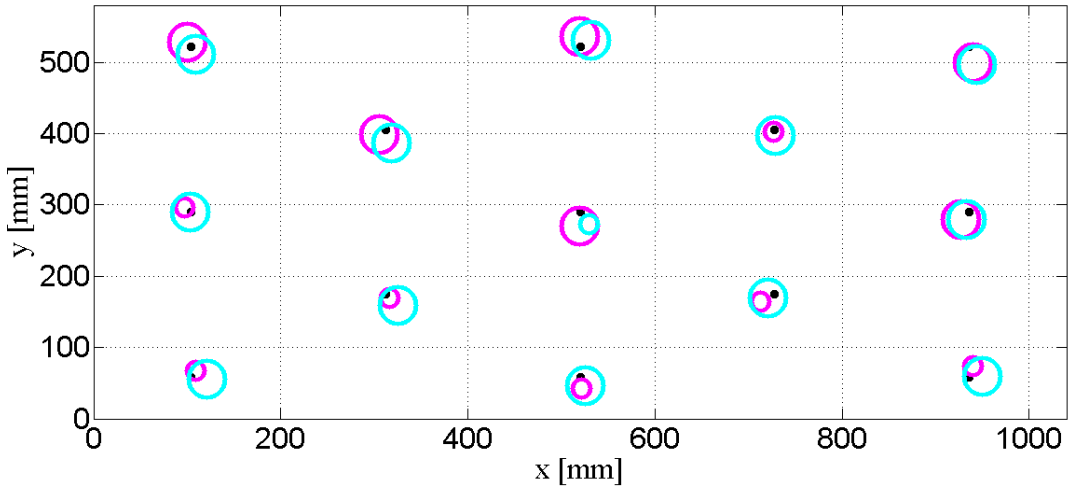

Figure A3.8 A graphical representation of ε_i and δ_i values for subject 8 found for each dot-target location during the trials *wslow* (magenta) and *walkfast* (light blue). Each dot-target location on the image is a black dot. The circles center positions (colored dots) reflect the accuracy of the *PoG* measurements (ε_i) while their radius reflects the precision of the *PoG* measurements (small radius, $\delta_i < 4$ mm; average radius, 4 mm$< \delta_i <$ 8 mm; large radius, $\delta_i > 8$ mm).

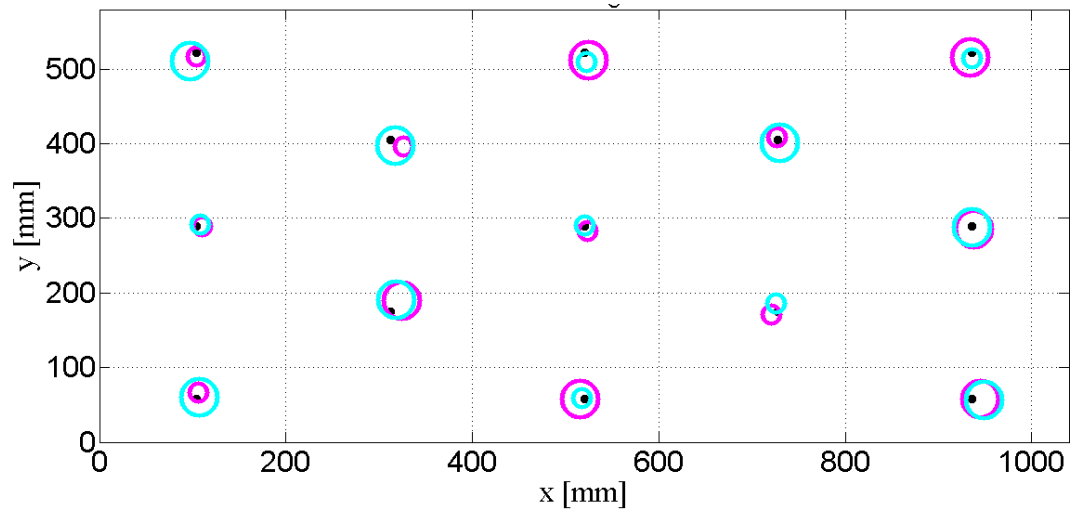

Figure A3.9 A graphical representation of ε_i and δ_i values for subject 9 found for each dot-target location during the trials *wslow* (magenta) and *walkfast* (light blue). Each dot-target location on

the image is a black dot. The circles center positions (colored dots) reflect the accuracy of the *PoG* measurements (ε_i) while their radius reflects the precision of the *PoG* measurements (small radius, δ_i < 4 mm; average radius, 4 mm< δ_i < 8 mm; large radius, δ_i > 8 mm).

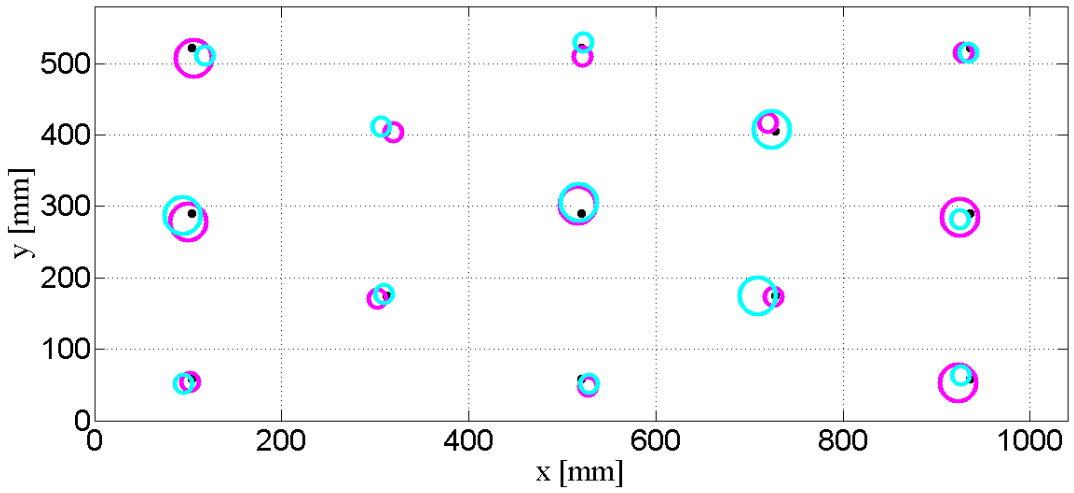

Figure A3.10 A graphical representation of ε_i and δ_i values for subject 10 found for each dot-target location during the trials *wslow* (magenta) and *walkfast* (light blue). Each dot-target location on the image is a black dot. The circles center positions (colored dots) reflect the accuracy of the *PoG* measurements (ε_i) while their radius reflects the precision of the *PoG* measurements (small radius, δ_i < 4 mm; average radius, 4 mm< δ_i < 8 mm; large radius, δ_i > 8 mm).

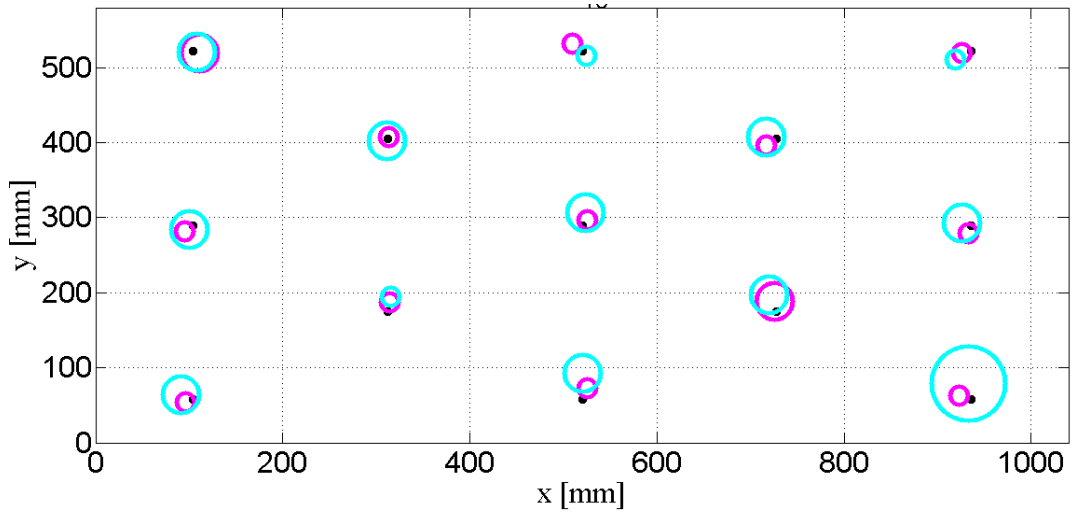

Annex 4

PARTICIPANTS NEEDED FOR RESEARCH IN THE AREA OF MOTOR CONTROL

ASSESSING THE GAZE STRATEGY DURING OBSTACLE NEGOTIATION IN PRESENCE OF DISTRACTORS IN A VIRTUAL REALITY ENVIRONMENT

You are invited in this study which aims at assessing how people negotiate obstacles in the presence of distractors and where their gaze is directed during a walking task in a virtual reality environment.

Your participation would involve 1 session of approximately 60 minutes. This study will include a walking on a treadmill while looking at a virtual reality environment.

For more information about this study, or volunteer for this study, please contact:

Valeria Serchi

at

E-mail: vserchi@wlu.ca

The Research Ethics Board at Wilfrid Laurier University has reviewed and approved this project

Annex 5

WILFRID LAURIER UNIVERSITY - INFORMED CONSENT STATEMENT

Gaze strategies during obstacle negotiation in presence of distractors: a virtual reality assessment of young and older adult populations

Valeria Serchi[*], Michael Cinelli[*]

[*]Wilfrid Laurier University

You are invited to participate in a research study. The aim of this work is to assess how people negotiate obstacles in the presence of distractors and where their gaze is directed during a walking task in a virtual reality environment.

INFORMATION

You will be asked to walk on the treadmill while looking at a virtual reality environment projected in front of you onto a wall (2 m by 2 m). The virtual reality environment will virtually reproduce a country road environment. The virtual reality is interactive and you will be able to progress along the street while you are walking on the treadmill. Along the road you will find virtual obstacles and you should do your best to step over them avoiding a collision. The treadmill will move at a constant rate and set at a speed that you feel comfortable. During the tasks your point of gaze on the virtual reality scene will be recorded as well as the movement of your body on the treadmill. You will be instrumented with four rigid bodies on your body segments (head, trunk and ankles) and with a wearable eye-tracker. The experimenters will help you in wearing the instrumentation to make sure its correct position. The experimenters will take written notes about the execution of the task (your comments about the task or any interference to the acquisition which may help for the data interpretation). From such recordings you will not be identifiable. The analysis will require about an hour.

This study enrolls about 30 people with normal or corrected to normal sight and no neuro-motor deficits which may prevent them from comfortable walking on a treadmill.

_____

Place your initials to confirm you have read and understand the above information

RISKS

The risks of the study are similar to those experienced while walking on a treadmill with a slight added risk by having the participants step over virtual objects. The use of a virtual object will significantly decrease the risk of falls. As well you will be instrumented with an emergency shut off cord that will stop the treadmill if you move too far away from the front of the treadmill.

BENEFITS

The outcomes of this study may help in the understanding of the gaze strategy adopted by subjects (young and older adults) in their all day life. Such insights can help in the design of rehabilitation protocols to prevent the risk of fall, which is a goal of the researchers and a benefit to the participants and the research community.

CONFIDENTIALITY

Ms. Valeria Serchi and Dr. Cinelli or one of the graduate students from the lab will collect data from you. The experimenter will collect some general information (as: age, name and surname) to generate an alphanumeric code to which associate data collected from you. Therefore, from the collected recordings and notes you will not be identifiable. Your name will never compare anywhere in our study so that your anonymity will be safeguarded. Data will be protected through password to avoid any steal or loss during and after the study.

CONTACT

If you have questions at any time about the study or the procedures, (or you experience adverse effects as a result of participating in this study) you may contact the researchers Valeria Serchi (e-mail: vserchi@wlu.ca) or Michael Cinelli (e-mail: mcinelli@wlu.ca).

This project has been reviewed and approved by the University Research Ethics Board. If you feel you have not been treated according to the descriptions in this form, or your rights as a participant in research have been violated during the course of this project, you may contact Dr. Robert Basso, Chair, University Research Ethics Board, Wilfrid Laurier University, (519) 884-1970, extension 5225 or rbasso@wlu.ca

_____

_

Place your initials to confirm you have

read and understand the above information

PARTICIPATION

Your participation in this study is voluntary; you may decline to participate without penalty. If you decide to participate, you may withdraw from the study at any time without penalty and without loss of benefits to which you are otherwise entitled. If you withdraw from the study, every attempt will be made to remove your data from the study, and have it destroyed. You have the right to omit any question(s)/procedure(s) you choose.

FEEDBACK AND PUBLICATION

Results will be presented in the ISPGR congress and any publication will be accessible from the laboratory home page.

CONSENT

I have read and understand the above information. I have received a copy of this form. I agree to participate in this study.

Participant's signature _____ Date _____

Investigator's signature _____ Date _____